PROPERTIES OF SINGLE FIBERS IN GLOBAL EXTRAOCULAR MUSCLE OF THE CANE TOAD, *Bufo marinus*

A thesis

submitted in partial fulfilment

of the requirements for the Degree

of

Doctor of Philosophy in Biological Sciences

at the

University of Waikato

by

ELIZABETH HOPE HALSEY

The
University
of Waikato
Te Whare Wānanga
o Waikato

1999

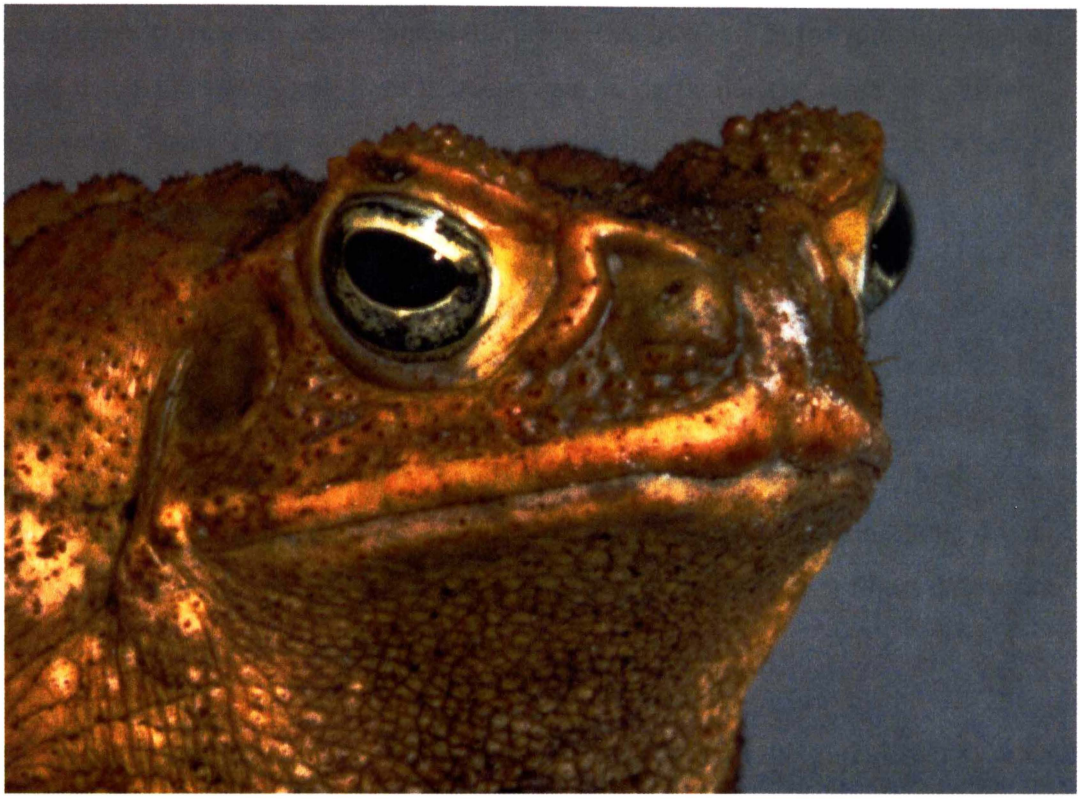

The cane toad, *Bufo marinus*.

ABSTRACT

Very limited information exists on the contractile physiology of the specialized muscle fibers that make up vertebrate extraocular muscle (EOM). This study was undertaken to measure some contractile properties of fibers in the global region of EOM using the cane toad, *Bufo marinus,* and in particular the tonic or multiply-innervated fibers (MIFs). Fiber types were characterized using a number of methods.

Tonic and twitch fibers were identified in EOM using transmission electron microscopy. Tonic fibers lacked an M-line, had sparse sarcoplasmic reticulum (SR), few mitochondria and a thick Z-line. Some twitch fibers showed the presence of lipid stores and abundant mitochondria, whereas others were distinguished more by well developed SR. In transverse section, tonic fibers showed a *felderstruktur* pattern of fused myofibrils and the twitch fibers displayed a *fibrillenstruktur* pattern of well-delineated myofibrils.

The distribution and diameter of tonic and twitch fibers in the global region were characterized using histochemistry. Transverse sections stained for mATPase, α-GPDH and NADH-TR activity revealed the presence of at least three different fiber types in global EOM of *Bufo marinus.* Tonic fibers showed little or no activity for all three enzymes and were distributed randomly within the global region where they made up about 20% of the fibers. Tonic fibers always occurred at lower frequencies than twitch fibers at all diameter ranges analysed. Two further types of fiber were characterized by their histochemical appearance as twitch light and twitch dark.

Force-pCa relationships were determined for chemically skinned single fibers by recording peak isometric force at maximal and submaximal calcium activation. Fibers were found to differ in their force response to initial and maximal calcium activation. Force-pCa data were fitted to Hill plots and Hill coefficients, n_1 and n_2, obtained for responses at high and low calcium concentrations, respectively. This information together with diameter and appearance (clear versus dark) also

allowed fibers to be divided into three groups. Tonic fibers developed tension slowly and had significantly lower maximum normalized tension and n_2 values than twitch light fibers. Twitch dark and twitch light fibers developed tension rapidly in response to initial and maximal calcium activation and had similar n_2 values. However, twitch dark fibers had a significantly lower maximum normalized tension than twitch light fibers. The pCa_{50} values did not differ between the three groups of fibers. Fiber classifications were corroborated by single fiber transmission electron microscopy (TEM). SDS-PAGE followed by silver staining was used to resolve the MLC components of single fibers for which force-pCa relationships were known. Both twitch light and twitch dark fibers had three myosin light chains, each having the same electrophoretic mobility as the light chains from the fast-twitch rabbit psoas muscle. The tonic fibers were found to lack the low molecular weight light chain, myosin light chain three (MLC3), and the regulatory light chain (MLC2) of these fibers showed reduced mobility compared to that of the twitch fibers.

The finding that tonic fibers responded in a different manner to initial and maximal calcium activation from twitch fibers can be used by others to aid in their identification. The significantly different responses of twitch and tonic fibers to maximal and submaximal calcium activation highlight the extent to which these fiber types differ. Additional work using single fibers will undoubtedly reveal further differences in the composition and functioning of contractile proteins in EOM fibers.

ACKNOWLEDGEMENTS

During the course of this research there was no-one else involved in single fiber experimental work at the university or nearby. Thus, my supervisor, Dr Nick Ling, played a key role in teaching me the techniques used and his advice was invaluable. Further, he was the only one able to assist in T-clipping fibers when it got too much for my back. I'd like to thank him for his willing assistance, his valuable suggestions, comments and discussions during the write-up stage, and for always sharing a laugh.

The varied nature of the work undertaken took me out of my cost center lab for at least half the duration of the thesis, and into the labs of others. Much gratitude goes to Kerry Allen, not only for allowing me to take up space and use facilities in her lab over several years, but also for her teaching and trouble-shooting support. Many thanks to Dr Ray Cursons and Raewyn Towers for also giving me space in their lab, their advice and support during the gel electrophoresis stage of this work. Off campus, Dave Wild, formerly of Meat Industry Research Institute of NZ, welcomed me into his lab, taught me how to process samples for TEM and developed all the electron micrographs.

Steve Hardy was always there to help with electronic matters and saved the day on more than one occasion by attending at a moments notice. Craig Harper was a computer support person in every sense of the word "support". To Graeme and Jack of the store, I did appreciate your understanding that sometimes students do just need something NOW! Thank you Vivienne for helping me with a couple of (fiddley) figures, and Lisa and Mary for your willingness to help with anything, anytime.

I enjoyed the comradeship of many fellow students over the years - too many to mention but special thanks to Lissa McKinney who was always there to listen and support. I'd like to thank Mom for her encouragement across the miles. Finally, I would like to thank Kevin Collier for his continual support, both academic and emotional, throughout this work.

TABLE OF CONTENTS

Title Page i
Frontis Piece ii
Abstract iii
Acknowledgements v
Table of Contents vi
List of Figures ix
List of Tables xi
List of Appendices xii
List of Abbreviations xiii

Chapter 1: INTRODUCTION

1.1 Vertebrate Skeletal Muscle: Fiber Classification and Properties 1
1.2 Extraocular Muscle 5
1.3 Why Study EOM? 8
1.4 Terminology Used in this Thesis 9
1.5 Aim and Outline of this Work 10

Chapter 2: ULTRASTRUCTURAL COMPARISON OF TONIC AND TWITCH FIBERS IN EOM

2.1 Introduction 13
2.2 Materials and Methods 15
2.2.1 Use and Care of Cane Toads 15
2.2.2 Preparation of EOMs for TEM 16
2.3 Results 17
2.4 Discussion 24

Chapter 3: HISTOCHEMICAL PROPERTIES, DIAMETER, FREQUENCY AND DISTRIBUTION OF TONIC AND TWITCH FIBERS IN GLOBAL EOM

3.1 Introduction 29
3.2 Materials and Methods 33
3.2.1 Use and Care of Cane Toads 33
3.2.2 Preparation of Toad Extraocular Muscles for Histochemical Analysis 34
3.2.3 Histochemical Staining Procedures 34
3.2.3.1 Myosin ATPase Activity 35
3.2.3.2 NADH Tetrazolium Reductase Activity 35
3.2.2.3 α-Glycerophosphate Dehydrogenase Activity 36
3.2.4 Measurement of Fiber Diameter in the Global Region of Toad Inferior Rectus 36
3.3 Results 37
3.4 Discussion 44

Chapter 4: CONTRACTILE PROPERTIES OF SINGLE PERMEABILIZED FIBERS FROM GLOBAL EOM

4.1 Introduction 49
4.2 Materials and Methods 55
4.2.1 Use and Care of Cane Toads 55
4.2.2 TEM of Single Muscle Fibers 55
4.2.3 Single Fiber Contractile Activation Experiments 58
4.2.3.1 Experimental Solutions 58
4.2.3.2 Muscle Preparation 59
4.2.3.3 Experimental Protocol 60
4.3 Results 67
4.3.1 Ultrastructure of 'Light' and 'Dark' Fibers 67
4.3.2 Maximim Force Responses 70

4.3.3 Maximum Normalized Tension 72
4.3.4 Force-pCa Curves 73
4.3.5 Decline in Maximal Tension 73
4.3.6 Hill Coefficients 76
4.3.7 Sensitivity to Ca^{2+}: pCa_{50} 78
4.3.8 Ca^{2+} Threshold of Activation: pCa_{10} 79
4.4 Discussion 81
4.4.1 Appearance 81
4.4.2 Maximum Force Responses and Decline in Maximum Force 83
4.4.3 Maximum Normalized Tension 84
4.4.4 Force-pCa Relationships 86
4.4.5 Problems Encountered 89
4.4.6 Summary 90

Chapter 5: MYOSIN LIGHT CHAIN PROFILES OF SINGLE FIBERS FROM GLOBAL EOM

5.1 Introduction 92
5.2 Materials and Methods 99
5.2.1 Extraction and Purification of Myosin Light Chains 99
5.2.2 Preparation of Whole EOM Extract 101
5.2.3 SDS-PAGE of Single Fiber Proteins 101
5.3 Results 106
5.4 Discussion 110

Chapter 6: CONCLUSION 114

References 118
Appendices 130

LIST OF FIGURES

Figure 2.1 Ultrastructure of tonic fiber from EOM of *Bufo marinus* 18
Figure 2.2 Ultrastructure of twitch fibers from EOM of *Bufo marinus*... 20
Figure 2.3 Longitudinal sections showing ultrastructure of fiber types found in *Bufo marinus* EOM 21
Figure 2.4 Types of neuromuscular junctions observed in *Bufo marinus* EOM 23

Figure 3.1 Representative transverse sections of *Bufo marinus* medial rectus muscle stained with (a) NADH-TR and (b) α-GPDH 38
Figure 3.2 Serial transverse sections showing the global regions of the inferior oblique muscle of *Bufo marinus* stained for (a) mATPase, (b) α-GPDH and (c) NADH-TR 40
Figure 3.3 Serial transverse sections from the global region of *Bufo marinus* superior rectus muscle stained with (a) α-GPDH and (b) mATPase 42
Figure 3.4 Frequency of twitch and tonic fibers as defined by mATPase staining in the global region of *Bufo marinus* inferior rectus muscle 43

Figure 4.1 Assembly of embedding mould for TEM of single fibers 57
Figure 4.2 T-clip and inferior rectus muscle of *Bufo marinus* 62
Figure 4.3 Fixing fiber ends 62
Figure 4.4 Single fiber experimental apparatus 64
Figure 4.5 Representative micrographs of 'dark' and 'clear' fibers 68
Figure 4.6 Representative force responses obtained upon initial and maximal Ca^{2+}-activation for twitch dark, twitch light and tonic fibers 71
Figure 4.7 Time to 90% maximum force for twitch dark, twitch light and tonic fibers 71

Figure 4.8 Maximum normalized tension, P_o, for twitch dark, twitch light and tonic fibers 72

Figure 4.9 Force-pCa curves for twitch dark, twitch light and tonic fibers 74

Figure 4.10 Decline in maximum tension with pCa index 75

Figure 4.11 Decline in maximum tension versus Hill coefficients, n_1 and n_2, for twitch light and tonic fibers 75

Figure 4.12 Hill coefficients, n_1 and n_2, obtained for EOM fiber types 76

Figure 4.13 pCa_{50} values for twitch dark, twitch light and tonic fibers 78

Figure 4.14 pCa_{10} values for twitch dark, twitch light and tonic fibers 79

Figure 5.1 Schematic diagram showing MLC profile of EOM as found in five studies 97

Figure 5.2 Purification of low molecular weight components of toad EOM myosin by anion exchange chromatography on a Mono-Q column 107

Figure 5.3 SDS-PAGE of rabbit and toad myosin light chains, myofibrillar proteins and standards 108

Figure 5.4 Representative densitometric scan of gel obtained from a toad EOM tonic and twitch light fiber 109

LIST OF TABLES

Table 1.1 Some characteristics of fibers that make up adult mammalian limb skeletal muscle 2

Table 1.2 Some properties of the six EOM fiber types 8

Table 3.1 Histochemical profiles of mammalian EOM fiber types..... 32

Table 4.1 Solutions used for skinning EOMs 60

Table 4.2 Comparison of Hill coefficients obtained by two methods.... 77

Table 4.3 Summary of tension-pCa relationships for tonic, twitch light and twitch dark fiber populations of EOM..... 80

Table 5.1 Composition of stacking and separating gels 103

Table 5.2 Silver staining procedure..... 104

Table 5.3 Standards that were routinely used in the gels..... 105

LIST OF APPENDICES

Appendix A: *IPLab Spectrum* script to determine fiber diameter 130

Appendix B: Solutions used in single fiber contractile experiments 131

Appendix C: Program used on the Liquid Chromatography Controller of the FPLC apparatus 133

LIST OF ABBREVIATIONS

ADP	adenosine 5'-diphosphate
ATP	adenosine 5'-triphosphate
BSA	bovine serum albumin
CA	carbonic anhydrase
EGTA	ethylene glycol-(β-aminoethylether)-N,N,N',N'-tetra-acetic acid
EOM	extraocular muscle
FPLC	Fast Protein Liquid Chromatography
IS	ionic strength
kDa	kiloDalton
Lys	lysozyme
mATPase	myosin adenosine triphosphatase
men-α-GPDH	menadione-α-glycerophosphate dehydrogenase
MHC	myosin heavy chain
MIF	multiply innervated fiber
MLC	myosin light chain
MW	molecular weight
Myo	myoglobin
n_1	Hill coefficient at high calcium concentrations
n_2	Hill coefficient at low calcium concentrations
NADH	nicotinamide adenine dinucleotide
NADH-TR	nicotinamide adenine dinucleotide – tetrazolium reductase
P_o	peak tension (maximum force normalized for cross-sectional area)

P_r	ratio of peak tension at submaximal $[Ca^{2+}]$ to peak tension at maximal $[Ca^{2+}]$
PAGE	polyacrylamide gel electrophoresis
pCa_{10}	free $[Ca^{2+}]$ eliciting one-tenth maximal activation
pCa_{50}	free $[Ca^{2+}]$ eliciting one-half maximal activation
SDH	succinate deyhydrogenase
SDS	sodium dodecyl sulphate
SE	standard error
SIF	singly innervated fiber
SR	sarcoplasmic reticulum
TEM	transmission electron microscopy
Tm	tropomyosin
Tn	troponin
Tryp	trypsinogen
V_{max}	maximum shortening velocity
α-GPDH	α-glycerophosphate dehydrogenase

CHAPTER 1: INTRODUCTION

1.1 Vertebrate Skeletal Muscle: Fiber Classification and Properties

Vertebrate limb skeletal muscle is composed of a heterogeneous population of cells or fibers that have been classified into fiber types using a variety of approaches. These methods include ultrastructural analysis, histochemical fiber typing, biochemical and immunohistochemical analyses, measurement of physiological properties and determination of myofibrillar protein composition. The first histochemical method used to classify fibers was based on the myosin adenosine triphosphatase (mATPase) activity of fibers (Padykula & Herman 1955). This technique initially identified two fiber types: type I and type II (Engel 1962). It was not long before the link between fiber histochemistry and contractile properties became apparant. Barany (1967) showed that the ATPase activity of myosin correlated with the speed of muscle shortening. Muscles with a fast shortening time exhibited type II staining whereas slow fibers exhibited type I staining. Different types of fibers have also been distinguished on the basis of histochemical reactions for enzymes of aerobic and anaerobic metabolism (Padykula & Gauthier 1967, Gauthier 1969). When these metabolic enzyme-based techniques were combined with mATPase methodology, three major fiber types were identified in the muscles of guinea pig and rabbit. The terminology given to these fiber types is still widely used today: slow-twitch oxidative (SO), fast-twitch oxidative glycolytic (FOG) and fast-twitch glycolytic (FG) (Barnard *et al.* 1971, Peter *et al.* 1972).

Other investigations of histochemical fiber-typing using the mATPase technique found that fast and slow myosins have different alkaline and acid stabilities (Sreter *et al.* 1966, Seidel 1967). More detailed analysis using this technique led to the delineation of fast fiber subtypes and these were termed types IIA, IIB, and IIC (Brooke & Kaiser 1970). The four main fiber types found in limb skeletal muscle are summarized in Table 1.1. They are all singly innervated and are able to propagate an action potential.

Table 1.1: Some characteristics of fibers that make up adult mammalian limb skeletal muscle. (From Spencer & Porter 1988 and Pette & Staron 1990).

Fiber type	I Slow twitch oxidative	IIA Fast twitch oxidative glycolytic	IIB Fast twitch glycolytic	IIC Fast intermediate
Ultrastructure				
Z-line	Wide	Wide	Narrow	Narrow
Mitochondria	Many, small	Many, large	Few, small	Moderate, small
SR; T-tubules	Elaborate, narrow	Elaborate, narrow	Compact, broad, parallel	Moderate, small
Histochemistry*				
mATPase (pH 9.4)	Low	High	High	High
NADH-TR	High	Intermediate - high	Low	Intermediate
Men-α -GPDH	Low	High	High	Intermediate
Physiological properties				
Twitch contraction time	Slow	Intermediate	Fast	Fast
Twitch tension	Very low	Low	High	Intermediate
Relative fatigue resistance	Very resistant	Moderately resistant	Sensitive	Intermediate
MHC profile	I	IIa	IIb	IIa > I

* Staining intensity

As previously mentioned, early studies showed a link between the contractile properties of a given muscle and its mATPase activity. These studies focused on contractile speed (V_{max} and force-velocity relationship) to classify muscle as slow

or fast (Barany 1967, Close 1972). However, additional elements of the muscle fiber, apart from the mATPase, may contribute to its functional properties. For example, time-course studies of low-frequency stimulation of fast-twitch muscle have found that changes in Ca^{2+} sequestration, Ca^{2+}-ATPase activity and the composition of the sarcoplasmic reticulum (SR) correlate with fast- to slow-twitch muscle transitions (Pette 1989, Simoneau *et al.* 1989). With the advent of skinned fiber preparations, in which the sarcolemma, SR and T-tubules are made permeable, the role of myofibrillar proteins alone could be investigated. Through these studies it has been found that the force-pCa relationship is different for fast- and slow-twitch muscle fibers (Reiser *et al.* 1985, Greaser *et al.* 1988). The complexity of skeletal muscle is seen most clearly upon analysis of the myofibrillar protein composition of individual muscle fibers (Bottinelli *et al.* 1991, Galler *et al.* 1994). Thus, studies have now progressed to measuring contractile properties of single permeabilized muscle fibers followed by determination of the protein isoform composition of these same fibers.

In addition to the four fiber types listed in Table 1.1, there exists a slow-tonic fiber present in extraocular muscle (EOM) of mammals and lower vertebrates, and also in limb skeletal muscle of lower vertebrates. The structure, pattern of innervation and mechanical properties of this muscle-type have been extensively reviewed by Morgan and Proske (1984). Since slow-tonic fibers were first discovered in the Amphibia and the greatest amount of detailed information exists for this group, amphibian slow-tonic fibers are often considered as the slow fiber 'prototype'. In the Amphibia, most limb and trunk muscles, in addition to the eye muscles, contain slow-tonic fibers. Using the frog, Kuffler and Vaughan Williams (1953) were the first to describe the physiological properties of slow-tonic skeletal muscle. The

physiological characteristics of slow-tonic muscle are as follows (Morgan & Proske 1984):

- They are unable to twitch; i.e. the sarcolemma is not capable of propagating an action potential but responds to direct and indirect (nerve) stimulation with a graded depolarization.
- They have a slow and graded isotonic shortening speed.
- They have the ability to develop a maintained contracture in depolarizing solutions (high external $[K^+]$).

Morphologically, slow-tonic fibers are characterized by having the following features:

- They have multiple nerve endings distributed along the length of the fiber. Studying a frog hindlimb muscle, Luff and Proske (1979) found that the combined tension developed upon stimulating two slow motor units was less than the sum of the tension produced by stimulating each motor unit separately. This implied that slow fibers received terminals from both motor units giving them 'polyneuronal' innervation.
- Their neuromuscular junctions are of the *en grappe* type; i.e. small junctional areas are not raised from the fiber surface and post-junctional folds are fewer and less deep than in twitch fibers.
- Their myofibrils are large, irregular in shape and mostly confluent at the A band level. In addition, the SR is sparse and so does not completely surround the myofibrils which diffuse into one another, sometimes forming a ribbon-like appearance. This produces the characteristic *felderstruktur* appearance in

cross section under the light microscope and TEM. This is in contrast to the discrete cylindrical myofibrils found in fast twitch muscle fibers, called *fibrillenstruktur* (Uehara *et al.* 1976).

- They have a wider Z-line than that seen in twitch fibers.
- The M-line is often absent.

1.2 Extraocular Muscle

In all vertebrates there are six EOMs: (i) the superior rectus elevates the eye and turns it medially, (ii) the inferior rectus depresses the eye and turns it medially, (iii) the medial and (iv) lateral recti turn the eye toward the midline and laterally, respectively, (v) the superior oblique depresses the eye and turns it laterally, and (vi) the inferior oblique elevates the eye and turns it laterally. In addition to these six muscles there are three accessory EOMs. The levator palpebrae superioris and orbicularis oculi are involved in blinking and eyelid movement and do not share the same fiber make-up as the six principal EOMs (Porter *et al.* 1989). The retractor bulbi retracts the eye, by reflex, into the orbit following corneal stimulation and is present in amphibia, reptiles and lower mammals (Cords 1924).

Together these muscles move the eye in a wide variety of movement patterns. There are five distinct eye movement systems that exert their diverse roles through the EOMs via the oculomotor, trochlear or abducens nerves. Optokinetic and vestibulo-ocular movements produce eye position changes that compensate for head/body movements thereby preventing blur. Vergence movements bring the eyes together to focus on a single point and combine with pursuit movements

which allow slowly moving targets to be tracked. Saccadic movements, which are small, rapid and jerky, allow rapid reorientation to new sensory targets (Porter *et al.* 1995). The EOMs can also affect our ability to see clearly (Bates 1920, Benjamin 1974) and many cases of defective vision are actually the result of strain upon the EOMs which in time causes the eyeball to change shape.

Reflecting their unusual organization and complex fiber make-up, EOMs have been termed a skeletal muscle allotype (Hoh *et al.* 1989). Other allotypes include masticatory muscles, and perhaps middle ear and laryngeal muscles. The following points highlight the unique features of EOMs:

- They are organised into two distinct regions: the orbital (outer) layer and the global (inner) layer.
- They are composed of six types of muscle fibers.
- They have multiply-innervated fibers (MIFs) which do not propagate action potentials.
- They have fibers (in the orbital region) that change in diameter as well as morphologically along their length.
- They are among the smallest, fastest and most fatigue resistant skeletal muscles.

Kato (1938) was the first to observe the layered arrangement of each EOM in which the layer facing the orbital bone (orbital layer) is composed mainly of small diameter fibers and the inner region (global layer) contains a mixture of small to large diameter fibers. Following this, Siebech and Kruger (1955) concluded that

EOM twitch fibers were characterized by a *fibrillenstruktur* pattern whereas myofibrils of slow fibers show a *felderstruktur* pattern. As for limb skeletal muscle, the myofibrils of the former are regularly spaced and well delineated, being encircled with SR, whereas in the latter the myofibrils appear to fuse into one another due to the scarcity of SR. Ultrastructural and histochemical studies carried out in the 1960s through to early 1980s (see Spencer & Porter 1988 for review), revealed that EOMs are composed of six fiber types and that two of these fiber populations are multiply innervated. Using an immunohistochemical technique, Pierobon Bormioli *et al.* (1979) showed that MIFs in human EOMs labelled with a fluorescent antiserum that specifically stains the multiply innervated slow fibers of birds and amphibians. Also around this time, the electrical and contractile properties of EOM were being investigated (see Chiarandini & Davidowitz 1979 for review) and it was discovered that the global-MIFs use a non-twitch or tonic mode of contraction and are activated focally at each neuromuscular junction in the absence of propogated action potentials (Chiarandini & Stefani 1979). In more recent times, motoneuron recording techniques and electromyography have been used to examine EOMs and their motor units (Shall & Goldberg 1992, 1995, Goldberg & Shall 1997). Together these diverse studies have defined several key properties of the six EOM fiber types (Table 1.2).

Table 1.2: Some properties of the six EOM fiber types (from Porter *et al.* 1995); for mammals. (int. = intermediate).

EOM region:	Orbital		Global			
Fiber type:	orbital-SIF	orbital-MIF	dark-SIF	int.-SIF	pale-SIF	global-MIF
Properties:						
Mean diameter (μm)	24.8 ± 3.8	19.3 ± 3.2	27.2 ± 4.7	34.5 ± 4.6	46.7 ± 6.2	35.7 ± 4.1
Percentage of layer[a]	80	20	33	25	32	10
Innervation	single	multiple	single	single	single	multiple
Contraction						
Mode	twitch	mixed	twitch	twitch	twitch	non-twitch
Speed	fast	fast/slow	fast	fast	fast	slow
Fatigue resistance[b]	high	variable	high	intermediate	low	high
Recruitment order[c]	first	third	second	fifth	six	fourth

[a] by fiber number
[b] estimates based on fiber morphology (Spencer & Porter 1988) and motor unit data of Shall and Goldberg (1992)
[c] based on Robinson (1978)

1.3 Why Study EOM?

The EOMs succumb to many neurogenic and myogenic diseases and are the most common site of surgical intervention in the treatment of strabismus and other ocular motility disorders (Porter *et al.* 1995). A clearer understanding of the fibers that make up EOM would assist in both the pharmacological treatment of these muscles as well as the surgical approach taken. Intriguingly, the EOMs are more susceptible to certain diseases than limb muscle but they are also more resistant to others (see Porter & Baker 1996 for review). EOMs are sometimes exclusively involved in the autoimmune disorder myasthenia gravis (Kaminiski *et al.* 1990). This has been attributed to differences in acetylcholine receptor types expressed in

extraocular versus other skeletal muscle types but may also be related to their normally high activation rates. EOMs are also preferentially involved in the thyroid disease, Graves opthalmopathy, while other skeletal muscles are spared, although this appears to be due to changes in orbital fibroblasts rather than a direct effect on the EOM fibers themselves (Porter *et al.* 1995, Porter & Baker 1996). The involvement of the EOMs in disease states coupled with the increasing awareness that EOMs play a powerful role in our ability (or inability) to see clearly (Quackenbush 1997) highlights the importance of studying these still poorly understood muscles. Furthermore, since EOMs are among the most phylogenetically conserved of all skeletal muscles (Webster & Webster 1974), new information regarding their functioning, even in Amphibia, may be of significance to human oculomotor research. Finally, it is worthwhile studying the contractile properties of tonic fibers simply because so little information is available on this fiber type in skeletal muscle in general, and no information of this nature exists for tonic fibers in EOM.

1.4 Terminology Used in this Thesis

The terminology used for EOM fiber types has changed considerably over the years as more and more information has been gained about them. Initially the presence of slow and fast fibers was emphasized with Hess (1961a & b) using the 'slow' and 'fast' terminology to structurally distinguish between EOM fibers. The terms *'felderstruktur'* and *'fibrillenstruktur'* were also used after Hess (1961a) linked these patterns with slow and fast fibers, respectively. Later, Mayr (1971) used fiber appearance after Sudan Black B staining and differences in the amount

of granula (mitochondria) seen by phase contrast microscopy in combination with diameter (*vis* large pale, intermediate, small dark and clear) to distinguish fiber types. Harker (1972) termed the fibers found in sheep EOM 'large A', 'intermediate C', 'small C', central core G and peripheral G' based on diameter, type of innervation and layer location. Finally Pachter (1982) developed a naming system utilizing phase contrast appearance (colour/granulation), innervation (single versus multiple) and layer (global versus orbital): global pale SIF, global intermediate SIF, global dark or red SIF, global MIF, orbital SIF and orbital MIF. This terminology is used in this thesis when individual fiber types are distinguished. However, when the global-MIFs are simply distinguished from the global-SIFs (dark-, pale- and intermediate-SIFs) then the terms 'tonic' and 'twitch' are used, respectively.

1.5 Aim and Outline of this Work

Very little is known about the contractile properties of single EOM fibers with only two studies in this area (Lynch *et al.* 1994, Campbell 1997). These studies both looked at Ca^{2+} and Sr^{2+}-activated isometric contractile properties of single fibers from EOMs of the rabbit and are described in Chapter 4. This lack of attention may be due in part to the fiber composition of these muscles which is quite different to that of the more extensively studied limb and trunk skeletal muscles. There are also methodological difficulties in working with EOM. For example, the greater amount of connective tissue in these muscles (Asmussen & Gaunitz 1981, Campbell 1997) makes fiber dissection more difficult. The location of these muscles within the bony orbit, and their relatively small size, add to the

challenge. With regard to the tonic fibers, the difficulty in identifying them during dissection and their less obvious signs of damage (Morgan & Proske 1984) make them difficult to work with.

The aim of this research was to measure contractile properties of single demembranated tonic fibers from EOM. MIFs from the global region were chosen rather than those from the orbital region since the former do not have the morphological changes along their length that have been found in orbital MIFs (Chiarandini & Davidowitz 1979, Davidowitz *et al.* 1982, Pachter 1984,) and also because these fibers run the length of the muscle (Mayr *et al.* 1975).

Before the contractile properties of tonic fibers could be measured, some preliminary questions needed answering. The existence of tonic fibers in cane toad EOM first needed to be confirmed. This was accomplished by looking for tonic fiber ultrastructure in sections prepared for TEM. This approach also allowed morphological comparison to be made between tonic and twitch fibers. The results of this study are presented in Chapter 2.

Since tonic fibers were being targeted for contractile activation studies, it was then necessary to focus on properties of the tonic fibers that could be used to assist their selection from the EOM. In order to maximize chances of obtaining a tonic fiber from the global region of EOM, the frequency, diameter and distribution of tonic fibers, relative to the twitch fibers, was investigated using histochemical techniques. Three histochemical stains were used to identify the tonic fibers and characterize the twitch fiber types in global EOM. Image analysis was used to measure fiber diameters and so obtain the frequency of tonic and twitch fibers

within a particular size range. The information gained from this work is presented in Chapter 3.

Although the information gained in Chapter 3 helped to increase the likelihood of selecting a tonic fiber from the EOM, it did not lead to a reliable method of doing so. A non-invasive, reliable technique was sought to distinguish the tonic fibers from the twitch fibers once a fiber was freed from the muscle. The fibers had to be distinguished in a way that did not alter the protein filaments because of their central role in the Ca^{2+}-activated tension response. To this end, fiber appearance under the stereomicroscope was investigated by subjectively identifying the fiber as 'dark' or 'clear' and then confirming the fiber-type (twitch or tonic) by single fiber TEM. The calcium activation response to maximal and submaximal [Ca^{2+}] was obtained for fibers that differed in appearance and spanned a wide diameter range. Fibers were grouped according to their initial maximal force responses, diameter and appearance. The tension-pCa data obtained for fibers was used to calculate Hill coefficients, pCa_{50} and activation threshold values for the fiber populations. Chapter 4 presents this work on contractile properties of single twitch and tonic fibers.

In order to confirm the fiber groupings made in Chapter 4, myosin light chain (MLC) profiles were obtained for individual fibers for which calcium activation responses were known. Chapter 5 presents the results from this work utilizing techniques in protein purification and SDS-PAGE.

CHAPTER 2: ULTRASTRUCTURAL COMPARISON OF TONIC AND TWITCH FIBERS IN EOM

2.1 Introduction

Hess (1961a) was the first to describe the ultrastructure of EOM. Using phase contrast and electron microscopes he studied the nerve endings and ultrastructure of guinea pig EOM. In transverse section he found two kinds of fibers. The *fibrillenstruktur* fibers had myofibrils surrounded by SR and aligned in an orderly arrangement with regular spaces between them. In longitudinal sections, the Z-line ran straight across the width of the myofibril. *Felderstruktur* fibers had myofibrils which appeared to join with their neighbours, and they were larger and more irregular in form. The Z-line had a jagged appearance across the width of the myofibril. Using cholinesterase staining he observed two types of nerve endings, *en plaque* and *en grappe*, that never occurred together on the same muscle fiber. *En plaque* endings had interlacing finger-like processes on a compact portion of the muscle fiber and occurred singly on a fiber. The *en grappe* endings were seen as clusters of droplets of stained material and appeared "grape-like". Several of these endings occurred on a single fiber. Furthermore he determined that *en plaque* endings only occurred on *fibrillenstruktur* fibers while *en grappe* endings occurred only on *felderstruktur* fibers. Thus, *felderstruktur* fibers were multiply innervated fibers (MIFs). Hess and Pilar (1963) linked the appearance of *felderstruktur* morphology with fiber physiology. They demonstrated the presence in cat EOM of *felderstruktur* MIFs that were unable to generate action potentials but merely produced a graded tension upon repetitive electrical stimulation. *Fibrillenstruktur* fibers on the other hand, responded with

action potentials that were similar to those recorded in twitch fibers from other muscles.

Since then, there have been a number of ultrastructural studies of EOM including two studies of anuran EOM (Kilarski & Bigaj 1969, Nowogrodzka-Zagorska 1974) and several of mammalian EOM tissue (human: Dietert 1965; monkey: Miller 1967, Pachter, 1982; rat: Mayr 1971; sheep: Harker 1972; cat: Peachy *et al.* 1974, Alvarado & van Horn 1975; mouse: Pachter *et al.* 1976). From these studies came the realization that EOM shows a layered appearance and that it is composed of a much more complex assortment of muscle fiber types than limb skeletal muscle. Most of these studies reported five to six fiber types in EOM. All studies agreed on the presence of multiply innervated fibers in the global layer that displayed many of the morphological characteristics of tonic or 'slow' muscle fibers more commonly found in amphibian and avian limb muscle. This characteristic morphology includes wide Z-lines, sparse SR, large myofibrils and few, small mitochondria (Morgan & Proske 1984). These tonic fibers were first physiologically characterized in frog (Kuffler & Vaughan Williams 1953) and avian skeletal muscles (Ginsborg 1960) as being unable to propagate action potentials, and therefore, unable to twitch.

Early studies reported that neuromuscular junctions of EOM fibers generally fell into two categories. In their extensive review of EOM, Spencer and Porter (1988) describe these previous findings on EOM innervation and neuromuscular junctions. The first type of neuromuscular junction had large *en plaque* endings that were associated with *fibrillenstruktur* fibers. These nerve endings displayed a

motor end plate where the axon terminal lies in a depression of the sarcolemma, which may display varying degrees of post-junctional folding. The second category had *en grappe* endings associated with *felderstruktur* MIFs. These terminals were smaller, more superficial and exhibited little if any subjunctional folding. Subsequent studies, such as Pachter *et al.* (1976), found MIF junctions to vary in complexity, with some having reasonably extensive subjunctional folding, sarcoplasmic extensions and axonal penetration into the sarcolemma.

The purpose of this study was to confirm the presence of tonic fibers in EOM of *Bufo marinus* based on ultrastructural characteristics and to compare the morphology of these fibers with that of the twitch fibers. The ultrastructural characteristics of the fiber types present will complement the information gained regarding their physiological properties.

2.2 Materials and Methods

2.2.1 Use and Care of Cane Toads

Mature, adult cane toads *(Bufo marinus)* from Queensland, Australia were purchased from the Department of Primary Industries, PO Box 1143, Bunderburg, Queensland 4670, Australia. The toads were transported to New Zealand via air freight and maintained on a gravel bed in concrete tanks (600 mm x 600 mm x 450 mm) at a stocking density of a maximum of 28 toads per tank. They were

kept at room temperature with a 12:12 h light-dark cycle, showered with water on a daily basis and fed mealworms three times a week.

Permission from the University of Waikato Animal Ethics Committee on the Welfare of Experimental Animals was obtained for using cane toads in these experiments. Toads were euthanased by a blow to the head followed by pithing of the brain and spinal cord. The individual EOMs were located and identified according to Isomura (1981).

2.2.2 Preparation of EOMs for TEM

Prior to being dissected free, the EOMs were bathed in a cold 2% (w/v) paraformaldehyde, 2% (v/v) glutaraldehyde, 0.1 M sodium cacodylate fixative solution, pH 7.5. Bathing the muscles *in situ* in the fixing buffer was aimed at reducing the likelihood of muscle shortening. After *in situ* fixation for 15 min, the EOMs were excised and placed into a 4% glutaraldehyde, 0.1 M sodium cacodylate, pH 7.5 fixative for 2 to 3 h. Muscles were washed twice for 20 min in 0.1 M sodium cacodylate, 0.1 M sodium chloride buffer, pH 7.5. The muscles were left overnight at room temperature in this buffer and then cut into small rectangular blocks (1 mm x 1 mm x 2 mm) oriented longitudinally to the fiber axis. The cacodylate buffer was replaced with 1% aqueous osmium tetroxide for 1 h. The muscle segments were washed once in water prior to addition of 4 % uranyl acetate for 2 h. After a wash in water, segments were dehydrated for 10 min in each of 75%, 95% and two changes of 100% ethanol. Segments were

infiltrated with 50% Spurr's resin (Spurr 1969) : 50% ethanol twice for 30 min to 1 h, 75% Spurr's : 25% ethanol overnight and 100% Spurr's for 8 h. After a final change of 100% Spurr's resin, the blocks were set in an oven at 70 °C for 24 h. Thin (2 μm) and ultrathin (80 - 100 nm) sections were obtained using an ultramicrotome (OMU3, Reichert). Thin sections were observed under the light microscope after staining with 1% toluidine blue. Ultrathin sections were stained with 4% (w/v) uranyl acetate for 5 min followed by lead citrate (Reynolds 1963) for 5 min. A Phillips EM 400 transmission electron microscope with an accelerating voltage of 80 kV was used to view and photograph sections.

2.3 Results

Fibers matching the appearance of tonic fibers were found in all six EOM. They were identified in longitudinal sections by the absence of M-lines and the presence of thick, and in some instances, wavy Z-lines (Figures 2.1a and b). These fibers showed distinct A/I bands, an absence of T-tubule triads, little sarcoplasmic reticulum (SR) and few mitochondria. They had a sarcomere length range of 1.8 to 2.3 μm. In fibers not showing a clear A/I distinction, sarcomere lengths were less than 2 μm indicating that muscle shortening had occurred. Tonic fibers appeared to have a higher content of glycogen granules than the twitch fibers. In cross-section, myofibrils were indistinct due to the scarcity of SR (Figure 2.1c).

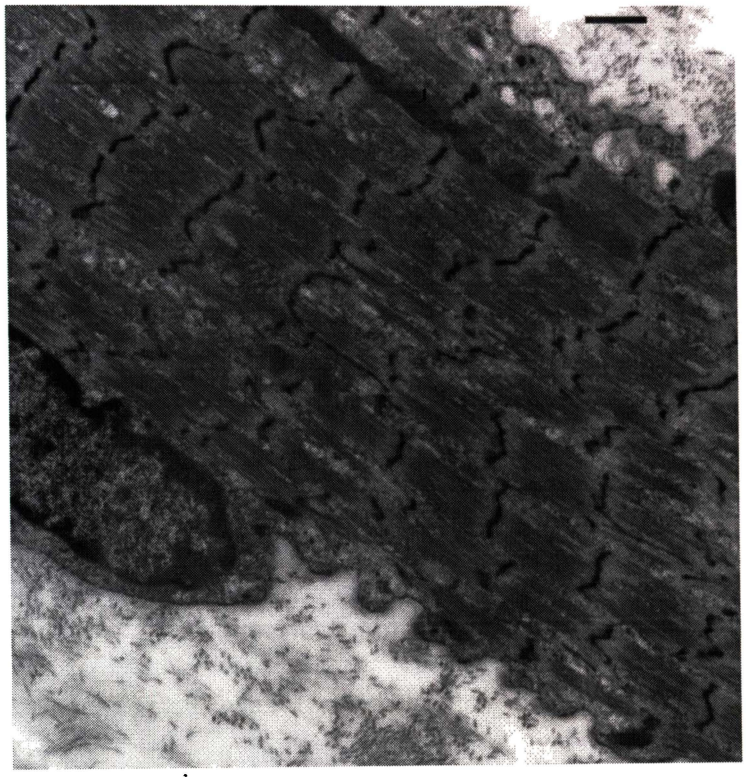

(a)

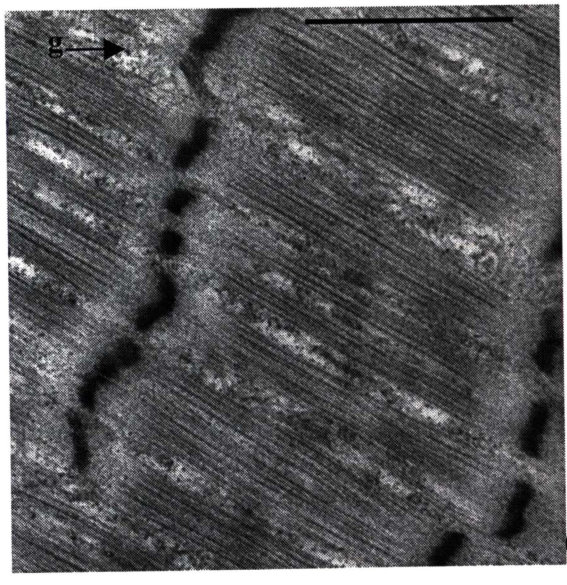

(b)

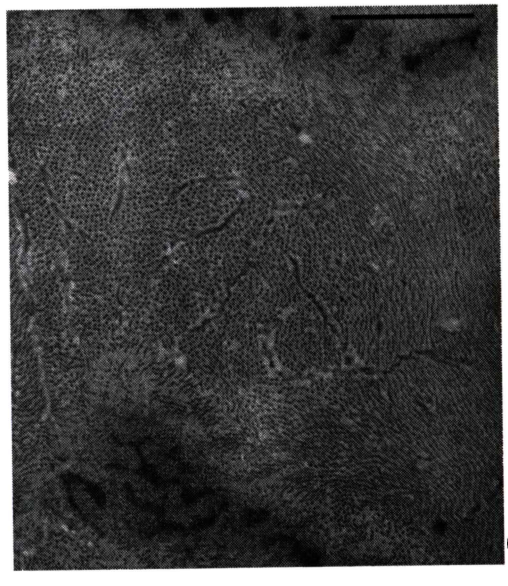

(c)

Figure 2.1: Ultrastructure of a tonic fiber from *Bufo marinus* EOM: (a) longitudinal section showing sparse SR, absence of M-lines and triads as well as thick and wavy Z-lines; (b) high magnification view of sarcomere showing SR and glycogen granules (g); (c) transverse section through tonic fiber showing *felderstruktur* pattern of myofibrils. Scale bars = 1 μm.

In longitudinal section twitch fibers showed straight Z-lines, distinct A/I bands and triads situated at the level of the Z-line (Figures 2.2a and b). Sarcomere lengths ranged from 1.8 to 2.46 μm. Myofibrils showing clear boundaries (*fibrillenstruktur* pattern) formed by SR, were also observed in twitch fibers (Figures 2.2c and d). In some cases, the SR was highly developed showing large diameter longitudinal tubules in transverse section (Figure 2.2c).

The twitch fibers could be subdivided into two types on the basis of appearance in longitudinal sections. One type had numerous mitochondria and lipid droplets (Figures 2.3a and b) and was termed 'twitch dark'. [An equivalent fiber population was identified during single fiber contractile experiments (Chapter 4) as being small in diameter, having a 'dark' appearance under the light microscope and developing tension rapidly in response to maximal calcium activation. The terminology used here is in keeping with the terminology in Chapter 4]. The small, oval mitochondria were usually clustered together and often appeared to be situated just beneath the sarcolemma (Figure 2.3b). The other type of twitch fiber was larger, had fewer mitochondria and no lipid droplets (Figure 2.3a). The mitochondria were usually elongate and arranged longitudinally. This fiber type was termed 'twitch light'. [Again, this terminology was in keeping with the population of fibers, presumed to be the same, that were identified in single fiber experiments (Chapter 4). During these experiments they were identified as having a 'light' appearance under the light microscope and rapid development of tension in response to maximal calcium activation.]

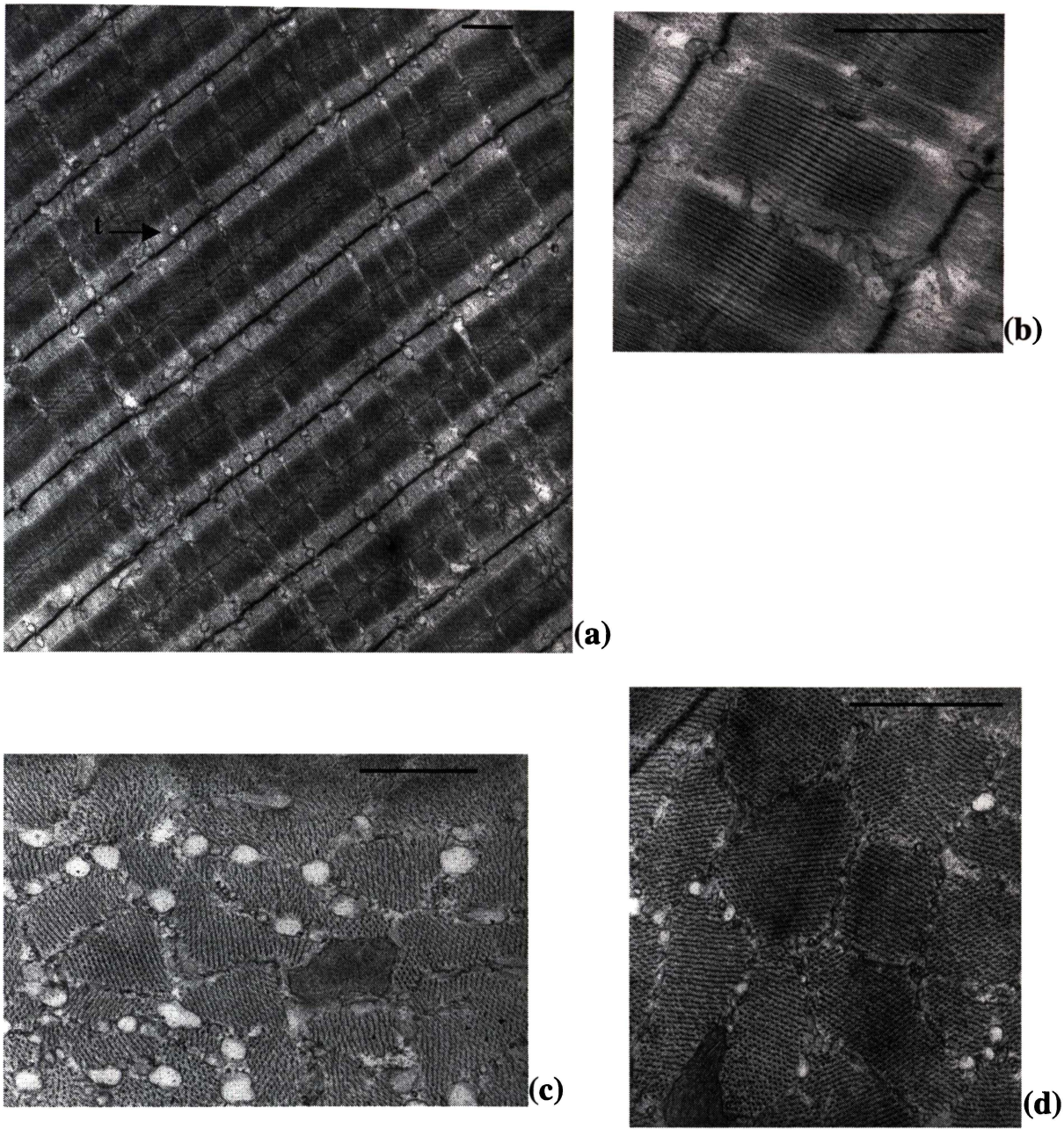

Figure 2.2: Ultrastructure of twitch fibers from *Bufo marinus* EOM: (a) longitudinal section showing distinct A/I bands, triads (t), straight Z-lines and presence of M-lines; (b) longitudinal section of sarcomere showing SR; (c and d) transverse sections showing *fibrillenstruktur* pattern of myofibrils due to well developed SR. Note the highly developed SR in (c). Scale bars = 1 μm.

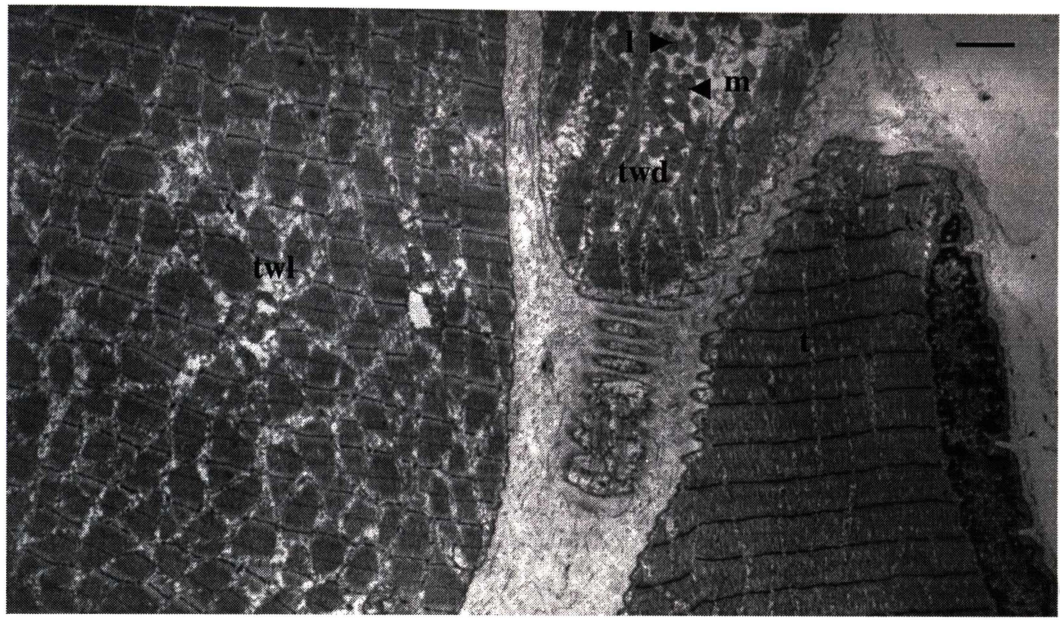

(a)

(b)

Figure 2.3: Longitudinal sections showing ultrastructure of fiber types in *Bufo marinus* EOM: (a) a twitch light (twl) fiber, a twitch dark (twd) fiber showing lipid droplets (l) and numerous mitochondria (m), and a tonic (t) fiber showing few mitochondria; (b) tonic fiber adjacent to a twitch dark fiber. Scale bars = 2 μm.

Three types of neuromuscular junctions were also observed. One type was characterized by a junctional area raised from the fiber surface that showed a high degree of post-junctional folding (Figures 2.4a and b). The junction shown in these figures is clearly associated with a twitch-type fiber. The other two types were much simpler in complexity with one showing limited post-junctional folding (Figure 2.4c) and the other showing axonal penetration into the sarcolemma (Figure 2.4d). Judging by the amount of SR visible, the junctions shown in Figures 2.4c and 2.4d appear to be associated with twitch and tonic fibers, respectively.

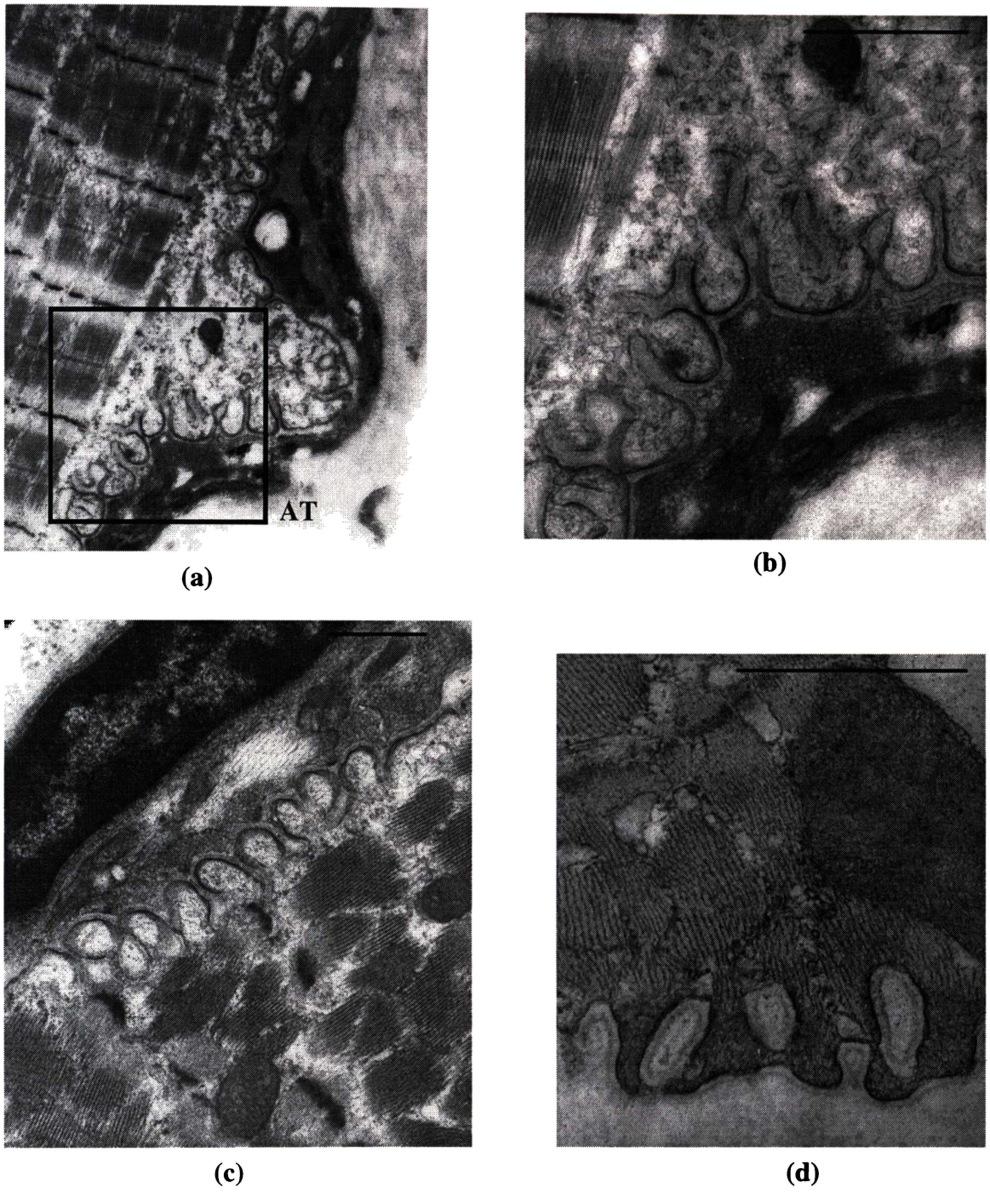

Figure 2.4: Types of neuromuscular junctions observed in *Bufo marinus* EOM: (a) *en plaque* ending on a twitch fiber where the axon terminal (AT) makes synaptic contact with a well developed, raised postsynaptic region; (b) magnified view of region in (a) showing regular deep junctional folds; (c) and (d) two neuromuscular junctions showing no raised plate and decreased junctional folding. Scale bars = 1 μm.

2.4 Discussion

The tonic fiber ultrastructure in cane toad EOM was similar to that described in anuran EOM by Nowogrodzka-Zagovska (1974) in that these fibers had no M-line, a broad Z-line, and a poorly developed SR. Similarly, Kilarski and Bigaj (1969) found that the A-band of tonic fibers of *Rana temporaria* EOM, divided by the less dense H-band, showed no distinct M-line. Also in keeping with the findings of Nowogrodzka-Zagovska (1974) and Pachter (1982) using monkey EOM, tonic fibers showed abundant glycogen granules within the myofibrils themselves.

Although it appears to hold true for Anura, the absence of an M-line cannot always be taken as a characteristic of tonic fibers. Harker (1972) found an M-line to be present in MIFs (tonic fibers) of the central core (global region) of sheep superior rectus, but not in the MIFs of the orbital rim. Similarly, Alvarado and van Horn (1975) found an M-line in global-MIFs of the cat inferior oblique muscle. However, results within Anura tend to be consistent: an M-line was absent in tonic EOM fibers of all five species of Anura (*Bufo bufo* L., *Bufo viridis* Laur., *Hyla arborea* L., *Rana esculenta* L. and *Rana temporaria* L.) studied by Nowogrodzka-Zagorska (1974). Furthermore, the findings for tonic fibers of *Rana temporaria* support those of Kilarski and Bigaj (1969). These results support the conclusion of Cheng-Minoda *et al.* (1968), that the presence or absence of an M-line in tonic fibers may be a species-related property. More reliable criteria for differentiating EOM fiber-types at the TEM level are mitochondrial size and number, myofibril size and delineation, degree of SR or T-tubule development, and Z-line width (Spencer & Porter 1988).

The apparent absence of an M-line in anuran tonic fibers could affect the physiology and structural integrity of the muscle fiber. Several proteins make up the M-line, or M-band region of skeletal muscle, including myomesin, M-protein and the creatine kinase isoenzyme (MM-CK). Although the biological function of myomesin and M-protein is unknown, they may serve to stabilize the thick filament bundles and/or the linking of the M-line to titin, which then serves to connect the myofibrils to the Z-disc (Perriard 1994). This may help to explain why the arrangement of thick and thin filaments in the A-band region of tonic fibers appears less ordered than in twitch fibers. Instead of having the regular spacing of thick filaments, each surrounded hexagonally by six thin filaments, the thick filaments appear more disordered and subsequently, so does the arrangement of thin filaments. *In vitro*, MM-CK phosphorylates the ADP produced by the Ca^{2+} stimulated myofribrillar myosin ATPase (Turner *et al.* 1973). However, only 5 to 7% of the total creatine kinase activity in skeletal muscle is due to the creatine kinase bound to the M-line, thus its absence would not be expected to have a significant effect on muscle function.

The wider Z-line found in tonic fibers may be related to the actin binding proteins present in that fiber type. For example, capping proteins are a family of actin binding proteins that cap the barbed ends of actin filaments thereby preventing the addition and loss of actin subunits. In muscle, the capping protein is called CapZ because it is found at the Z-line where it probably mediates the attachment of the barbed ends of thin filaments to the Z-line (Cooper 1994). The F-actin binding and cross-linking protein, α-actinin, is a major component of the Z-line. Several skeletal muscle isoforms of α-actinin are likely to exist (Critchley 1994). If these

isoforms are fiber-type specific then this too may have an effect on Z-line appearance.

In this study, sarcomere lengths of tonic fibers tended to be shorter than those of twitch fibers. This could be clearly seen in individual electron micrographs showing both tonic and twitch fibers in longitudinal section. However, the results of others studying the morphology of anuran EOM suggest that twitch fibers have a shorter sarcomere length than tonic fibers. Kilarski and Bigaj (1969) found that the tonic fibers of *Rana temporaria* had sarcomeres ranging in length from 2.6 to 2.9 μm while the twitch fibers were 2.3 to 2.4 μm in length. Although Nowogrodzka-Zagorska (1974) did not report sarcomere length findings, measurements of fibers on separate electron micrographs show this trend also. For example, in the toad *Bufo bufo*, white (twitch) and tonic fibers had sarcomere lengths of approximately 2.1 μm and 2.3 μm, respectively. *Bufo viridis* red and pink (both twitch) fibers had sarcomere lengths of approximately 1.8 μm and 2.1 μm, respectively and are thus similar to sarcomere lengths found in twitch fibers of *Bufo marinus.* However, it is difficult to know whether the sarcomere length measurements from these studies are derived from fibers within the same muscle or from fibers within different EOMs. Comparison of sarcomere lengths in fibers of different EOMs may give erroneous results because the sarcomere length of fibers may vary depending on the respective lengths of the antagonistic muscles during fixation. In addition, although studies that have compared sarcomere length in anuran limb skeletal muscle have reported tonic fibers to have slightly longer sarcomeres than twitch fibers (Page 1965, Nasledov & Lebedinskaya 1971), it was also found that the lengths of the thick and thin filaments were no

different from filament lengths in twitch muscle (Page 1965). It follows that the sarcomere spacing for optimum overlap must also be the same and, therefore, that the sarcomere lengths of both fibers must be the same. Furthermore, Page (1965) found that when the two fiber types where stretched to their respective optimum lengths for tension generation, the twitch fiber was longer than the tonic fiber. This implies that the tonic fiber has fewer sarcomeres. This could explain the reports of longer sarcomere length in tonic fibers: if the whole muscle was stretched for fixation, the slow fibers having fewer sarcomeres would give longer sarcomere lengths than the twitch fibers.

The fibers showing abundant SR are probably intermediate- or pale-SIF fibers as these have been shown to have extensive internal membrane systems (Mayr 1971, Alvarado & van Horn 1975, Pachter *et al.* 1976, Pachter 1982). By contrast, the scarcity of SR in tonic fibers in transverse section is striking when compared to some of the twitch fibers and suggests a low Ca^{2+} storing capacity in the former.

The simple *en grappe* neuromuscular junction observed in Figure 2.4d has been documented before by Pachter *et al.* (1976) in mouse superior rectus muscle. These researchers found multiple neuromuscular junctions on global-MIFs that displayed various degrees of complexity. Other types included endings exhibiting moderate post-junctional folding (like that shown in Figure 2.4c), endings showing pronounced extensions of the sarcoplasm to meet the terminal axons and an end-plate-like junction with the associated axon in a synaptic depression. The more complex end-plate shown in Figure 2.4a is probably that of a pale or

intermediate SIF as these have been found to have the most highly developed junction (Pachter *et al.* 1976).

In summary, the presence of tonic fibers in EOM of *Bufo marinus* was confirmed ultrastructurally in this study. Tonic fibers were found to be present in all six EOM. Comparison of these fibers with twitch fibers showed major differences in ultrastructure in both longitudinal and transverse sections. Tonic fibers had wider Z-lines, no M-line, little SR and few mitochondia. The *felderstruktur* appearance of myofibrils was apparent in transverse sections.

In order to assist with the selection of tonic fibers for use in contractile activation studies more information about the prevalence of these fibers is necessary. The following chapter investigates the distribution, diameter and frequency of tonic fibers in global EOM of *Bufo marinus*.

CHAPTER 3: HISTOCHEMICAL PROPERTIES, DIAMETER, FREQUENCY AND DISTRIBUTION OF TONIC AND TWITCH FIBERS IN GLOBAL EOM

3.1 Introduction

Muscle fiber types can be distinguished using a number of histochemcial methods. Histochemical analysis of tissue often involves reacting specific cellular enzymes with chemicals that eventually result in a coloured end-product. The degree of staining is presumably proportional to the quantity of enzyme in the tissue. Two different histochemical approaches allow for the separation of muscle fiber types (Pette & Staron 1990). One method is based on adenosine triphosphatase activity (mATPase) (Padykula & Herman 1955) while the other method uses reference enzymes of anaerobic and aerobic energy metabolism. NADH – tetrazolium reductase (NADH-TR) and succinate dehdydrogenase (SDH) are commonly chosen as reference enzymes for aerobic or oxidative metabolism, while α–glycerophosphate dehydrogenase (α-GPDH) is often chosen as a reference enzyme for the anaerobic glycolytic pathway.

The ATPase activity associated with myosin catalyses the breakdown of ATP to ADP and inorganic phosphate (P_i). The intensity of mATPase staining is presumed to be proportional to the contractile speed of the fiber (Barany 1967). pH has different effects on the ATPase associated with myosin of different fiber types. Alkaline pre-incubations may have no effect or may denature this protein. In EOM it has been found that following a preincubation of pH 9.4, mATPase is

unstable in the global-MIFs. However, mATPase in global SIFs appears to be stable following this alkaline pre-incubation, and cleaves the terminal phosphate from ATP which combines with calcium in the staining solution to form calcium phosphate. This compound is insoluble at alkaline pH and thus is deposited at the site of enzyme activity. When the tissue section is removed from this solution and placed into a solution of cobalt chloride, the cobalt is exchanged for the calcium and cobalt phosphate forms at the sites where calcium phosphate was present. Finally, placement of the tissue in ammonium sulphide results in the formation of black, insoluble cobaltous sulphide, which is the histologically-visible end-product.

In the NADH-TR staining reaction a purple/blue stain is produced that is proportional to the muscle's ability to process NADH. Since NADH-TR activity resides primarily in the mitochondria, the stain is used to indicate the oxidative capacity of a muscle fiber. Tetrazolium reductase removes a proton from the substrate NADH. Nitro-blue tetrazolium (NBT) acts as the electron acceptor and is reduced to the insoluble, colored, formazan product that is deposited at the site of enzyme activity. Thus the myofibrils are unstained, but the intermyofibrillar network, comprising the mitrochondria and SR, is well demonstrated.

The menadione-linked α-GPDH (men-α-GPDH) reaction is used to indicate the amount of glycolytic activity occurring within the individual fibers. α-GPDH is a sarcoplasmic enzyme that converts α-glycerophosphate to dihydroxyacetone phosphate, an intermediate in glycolysis. In this reaction, NBT is reduced and forms a blue/purple colour at the site of α-GPDH activity.

The combination of metabolic enzyme-based and mATPase-based histochemical methods has resulted in the isolation of three main fiber types in the hind-limb muscles of anurans (Putnam & Bennett 1983, Mendiola *et al.* 1991). The nomenclature most commonly used is based on that for mammalian muscle (Peter *et al.* 1972) and is as follows: fast-twitch oxidative glycolytic (FOG), fast-twitch glycolytic (FG) and tonic. The FOG fibers stained darkly for all three stains, FG fibers stained darkly for mATPase and α-GPDH but lightly for oxidative enzymes (e.g. SDH) and tonic fibers stained lightly for all three enzymes.

The histochemical profile of EOM fibers has primarily been studied in species of higher vertebrates such as the mouse, rat, rabbit, sheep, cat and primates (see Porter & Spencer 1988 for review). These studies have brought to light the distinct layers of EOM with the orbital layer generally staining with a higher intensity for oxidative enzymes than the global layer, the reverse being true for glycolytic activity. In addition, six fiber types have been identified in the orbital and global layers using a combination of histochemical stains. Table 3.1 shows the staining pattern for the three enzymes discussed above: mATPase, NADH-TR and α-GPDH.

Table 3.1: Histochemical profiles of mammalian EOM fiber types (adapted from Porter & Spencer 1988). (int. = intermediate)

EOM region:	Orbital		Global			
Fiber type:	SIF	MIF	dark-SIF	int.-SIF	pale-SIF	MIF
Staining protocol:						
Myosin ATPase pH 9.4	+++	+++	+++	+++	+++	+/-
NADH-TR	+++	++	++++	+++	++	+
Men-α-GPDH	++/+++	+	++	+++	++++	+

Staining intensity: ++++ = very high, +++ = high, ++ = intermediate, + = low, +/- = very low

The only study to look at fiber-types in toad (*Bufo bufo* and *Bufo viridis*) EOM (Nowogrodzka-Zagorska 1974) found them to be composed of five fiber types (white, pink thick, red thick, red thin, and tonic). The dark, outer zone (orbital layer) was primarily composed of red and tonic fibers, whereas the light, inner zone (global layer) had mainly white and pink fibers. Light microscope observations were made on approximately 1 μm thick transverse sections of fixed EOM tissue stained with either a methylene blue/azure II mixture or Sudan black B. Fibers were classified according to diameter, number of mitochondria and lipid droplets, and myofibril morphology. White fibers were the largest in diameter with single mitochondria occurring between 'polygonal' shaped myofibrils. Red fibers had small myofibrils and large aggregates of mitochondria and lipid droplets that in some cases occupied over half the cross-sectional area of the fiber. Pink fibers were similar to red fibers but their mean diameter was larger and the aggregates of mitochondria and lipid occurred mainly in deeper parts of the fiber, in addition to being less numerous. Tonic fibers were characterized as

having the smallest diameter, single mitochondria occurring sporadically and poorly visible myofibrils. The white fibers were probably equivalent to the mammalian pale-SIFs, the pink thick fibers to the intermediate-SIFs, the red fibers to the orbital-SIFs and the tonic fibers to the orbital-MIFs.

In this study, myosin ATPase, NADH-TR and men-α-GPDH stains were used to establish the various fiber types in the global region of toad EOM. The aim of this work was to distinguish the tonic fibers from the twitch fibers in the global region so that their diameter, frequency and distribution could be ascertained. This was intended to assist in the isolation of tonic fibers for contractile activation studies presented in the following chapter. The histochemistry and diameter of fibers only in the global region were analysed as the tonic fibers of interest only occur here (global-MIFs).

3.2 Methods and Materials

3.2.1 Use and Care of Cane Toads

For information regarding source, care and ethical use of cane toads, see Chapter 2: Section 2.2.1.

3.2.2 Preparation of Toad Extraocular Muscles for Histochemical Analysis

Following pithing, the eyeball and socket area were bathed in chilled Toad Ringer: 115 mM NaCl, 2.5 mM KCl, 1.8 mM $CaCl_2$, 3 mM Na_2HPO_4, pH 7.1. The EOMs were length clamped with a purpose-built apparatus prior to excision. The excised muscle was plunged into isopentane pre-chilled in liquid nitrogen. Muscles were kept in liquid nitrogen for up to six months prior to sectioning. Serial transverse 10 μm sections were obtained on a cryostat (Reichert-Jung) at –26 °C, picked up on glass microscope slides and processed for histochemical demonstration of mATPase, α-GPDH and NADH-TR. Dried stained sections were mounted on glass slides with DPX mounting medium. Sections were viewed and photographed using a photo-microscope (Polyvar, Reichert) and AGFA Optima 100 ASA colour film. All of the six EOMs were sectioned and stained with the three histochemical stains.

3.2.3 Histochemical Staining Procedures

All chemicals were obtained from Sigma. Distilled water was used to prepare solutions and rinse sections.

3.2.3.1 Myosin ATPase Activity (Brooke & Kaiser 1970)

Sections were stained in Coplin jars at room temperature using the following protocol:

1) pre-incubated in an alkali solution containing 0.18 M $CaCl_2$, 1.0 M AMPD (2-amino-2-methyl-1-3-propanediol), pH 9.4.

2) rinsed for 30 s in 2.0 M Tris, 0.5 M $CaCl_2$, pH 7.8

3) incubated for 20 min in 1.0 M AMPD, 0.18 M $CaCl_2$, 0.5 M KCl and 0.27 M ATP, pH 9.4.

4) rinsed three times for 30 s each in 68 mM $CaCl_2$.

5) exchanged for 3 min in 84 mM $CoCl_2$.

6) rinsed three times for 45 s each in 1.0 M AMPD in 40% v/v acetone.

7) exchanged for 2 min in 1% v/v ammonium sulphide.

8) rinsed for 3 min in H_2O

9) dried and mounted in DPX.

3.2.3.2 NADH Tetrazolium Reductase Activity (Dubowitz & Brooke 1973)

At room temperature, sections were:

1) incubated for 30 min in a solution containing 1.2 mM NBT, 1.0 mM NADH, 0.2 M Tris buffer, pH 7.4.

2) extracted with 30%, 60%, 90%, 60%, 30% acetone.

3) rinsed in H_2O for 2 - 5 min.

4) dried and mounted in DPX.

3.2.2.3 α-Glycerophosphate Dehydrogenase Activity (Dubowitz & Brooke 1973)

At room temperature, sections were:

1) incubated for 1 h in a solution containing 9.3 mM α-glycerophosphate, 1.2 mM NBT, 6.1 mM menadione in 0.2 M Tris-HCl buffer, pH 7.4.

2) extracted with 30%, 60%, 90%, 60%, 30% acetone.

3) rinsed in H_2O for 2 - 5 min.

4) dried and mounted in DPX.

3.2.4 Measurement of Fiber Diameter in the Global Region of Toad Inferior Rectus

Sections stained with mATPase were used to determine the distribution and diameters of tonic and twitch fibers in the inferior rectus EOM. The stained sections were viewed under a light microscope (BX50, Olympus). A colour video camera (TK-1280E, JVC) enabled the image to be displayed on a colour video monitor and captured by a PixelBuffer frame grabber (Perceptics) for storage on a Power Macintosh computer. The image analysis software package *IPLab Spectrum* was used to write a script (see Appendix A) which measured the minimum elliptical diameter of each fiber in the specified region of interest.

Since the inferior rectus muscle was most easily isolated, it was chosen for fiber diameter measurements and subsequent contractile activation studies. The fibers of approximately two-thirds of the global region in each muscle section were

measured. The results of each randomly selected field (n = 16) from six inferior rectus muscles were pooled, and the frequencies of fibers in nine size ranges were calculated (see Figure 3.4). Results are presented as the mean percent (± SE) of fibers occurring in each diameter range.

3.3 Results

Histochemical Staining

The staining pattern of fibers described below appeared to be consistent across the six EOMs. Thus, although photos of different EOMs are presented, these are representative of all the EOMs.

After sectioning and staining, the divided nature of EOMs could be easily discerned by differences in fiber diameter and staining patterns between regions. Staining for NADH-TR was greater in the orbital region than in the global region, especially around the perimeter of the orbital region (Figure 3.1a). Staining for α-GPDH was also greater in the orbital region than in the global region, and most intense in the inner orbital area (Figure 3.1b). The orbital region is comprised of small diameter fibers (diameter range approximately 10 – 20 μm) while the global region has fibers with a wider range of diameters (range 7 – 125 μm).

Staining of *Bufo marinus* EOM for mATPase activity showed two distinct classes of muscle fibers (Figure 3.2a). Tonic fibers were identified as those that

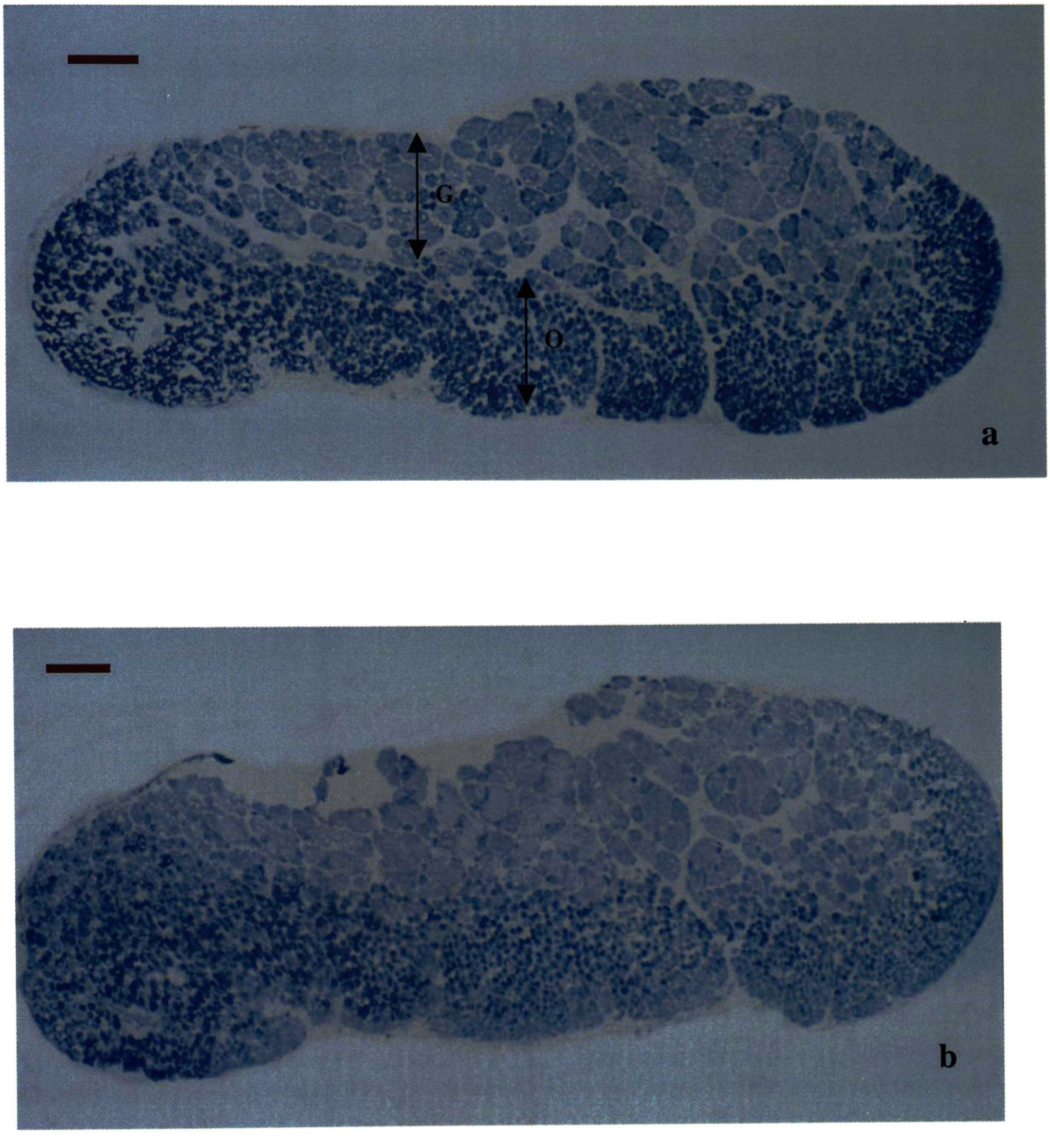

Figure 3.1: Representative transverse sections of *Bufo marinus* medial rectus muscle stained with (a) NADH-TR and (b) α-GPDH. O = orbital region; G = global region. Scale bars = 0.2 mm.

did not stain for mATPase at alkaline pH. This same population of fibers stained lightly (Figure 3.2b), or not at all (Figure 3.3a) for α-GPDH and showed a low-level diffuse darkening for NADH-TR (Figure 3.2c). Tonic fibers were distributed randomly throughout the global layer.

Of the fibers that stained darkly for mATPase, one population stained strongly for α-GPDH and NADH-TR. The strong NADH-TR staining intensity and the fact that these fibers were predominantly of small diameter suggest this population is analogous to the dark-SIFs of mammalian EOM. These fibers were termed 'twitch dark'. Another group of fibers of larger diameter showed moderate staining for both NADH-TR and α-GPDH. These appear to be analogous to the intermediate- or pale-SIFs and were termed 'twitch light'.

Fiber Diameters

Tonic fibers in the global region of the inferior rectus ranged from 11 to 80 μm in diameter, with most between 20 and 50 μm. The mean diameter (± SE) of tonic fibers was 35.1 ± 1.1 (n = 125). The twitch fibers had a wider range of diameters (from 7 to 125 μm). The frequency of tonic fibers within any size group was always less than twitch fibers and overall the tonic fibers made up 19% of all fibers measured in the global region (Figure 3.4).

Figure 3.2: Serial transverse sections showing the global region of the inferior oblique muscle of *Bufo marinus* stained for (a) mATPase, pH 9.4, (b) α-GPDH and (c) NADH-TR. Large arrows point to a tonic fiber, small arrows to twitch dark fiber and arrow heads to a twitch light fiber. These arrows identify the same fibers in each section. Scale bars = 50 μm.

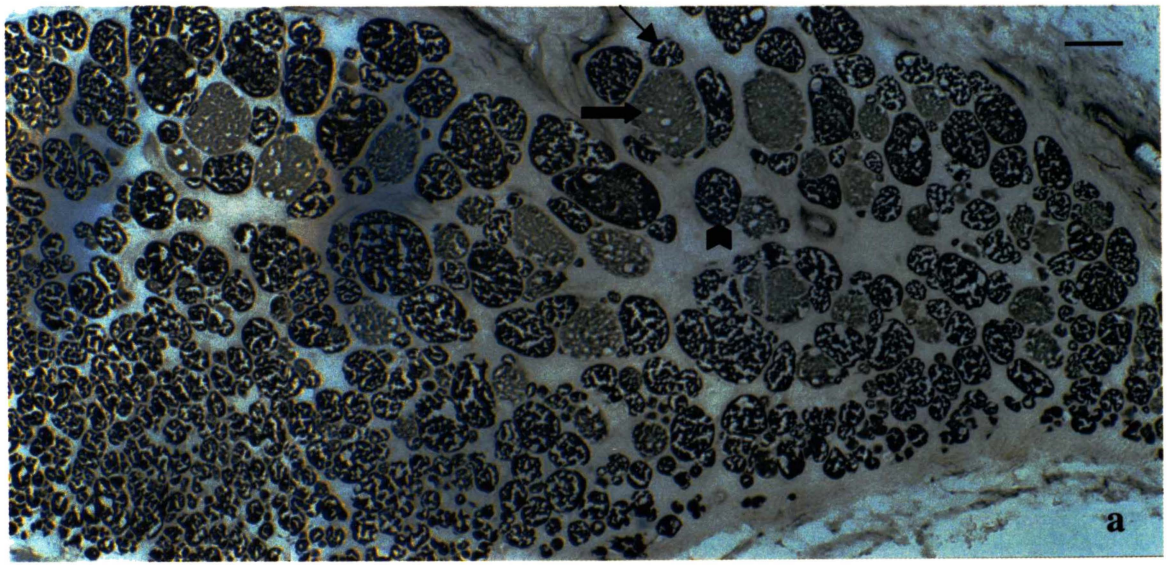
a

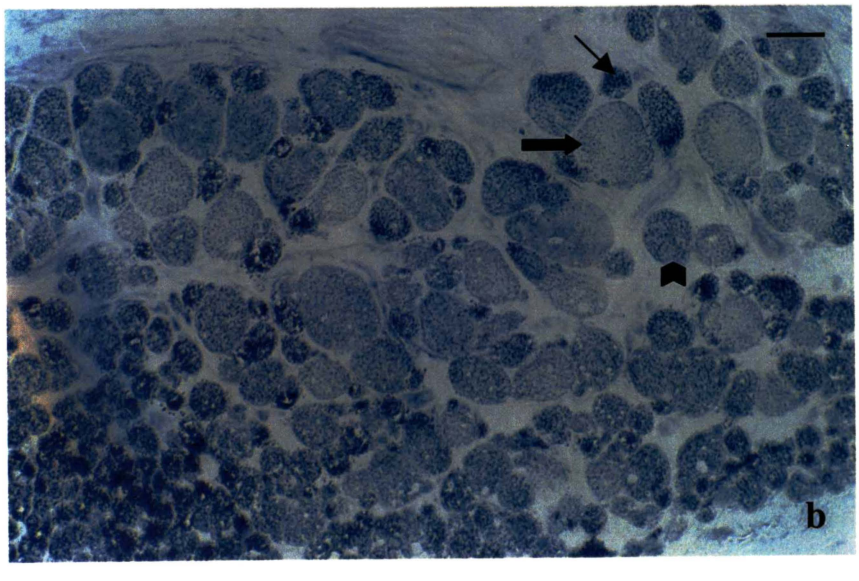
b

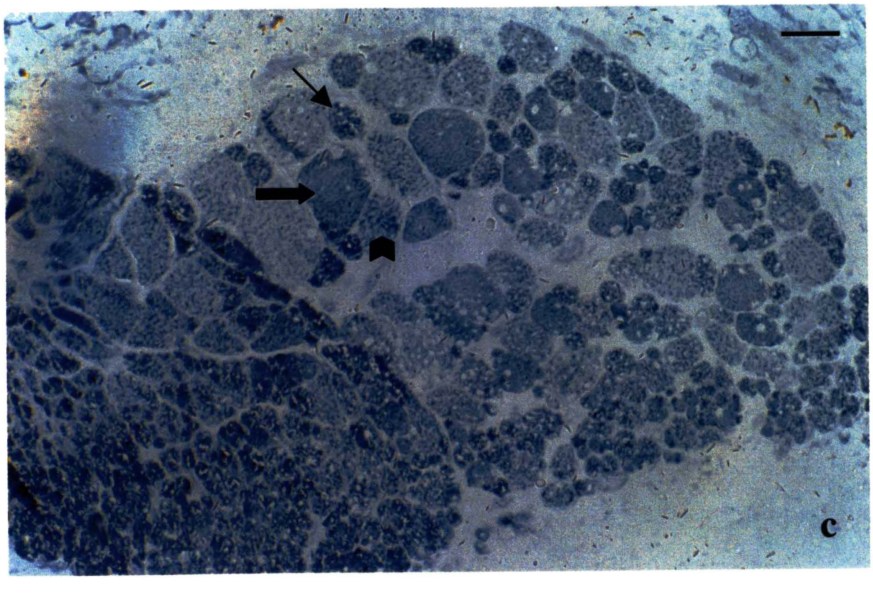
c

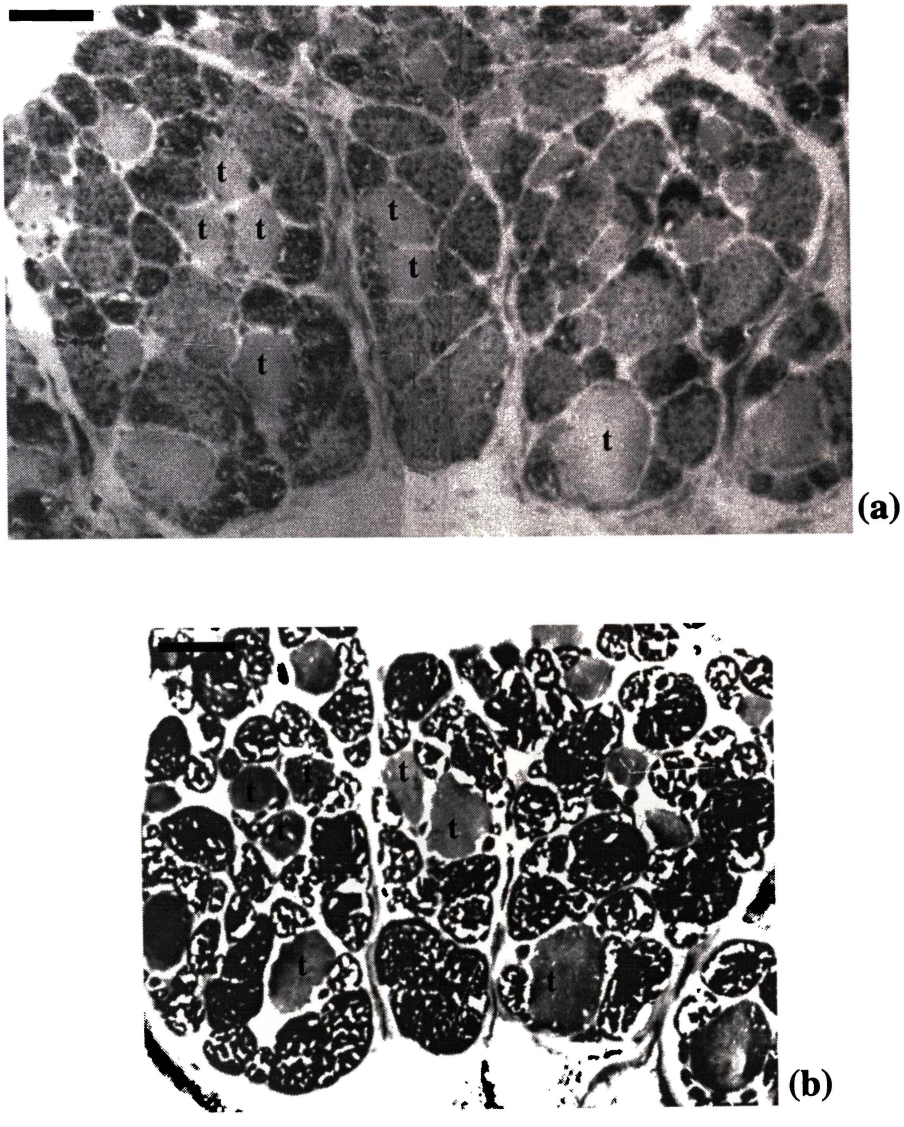

Figure 3.3: Serial transverse sections from the global region of *Bufo marinus* superior rectus muscle stained with (a) α-GPDH and (b) mATPase, pH 9.4. The tonic fibers (t) in (a), identified by using the mATPase stain (b), have not stained at all. Scale bars = 100 μm.

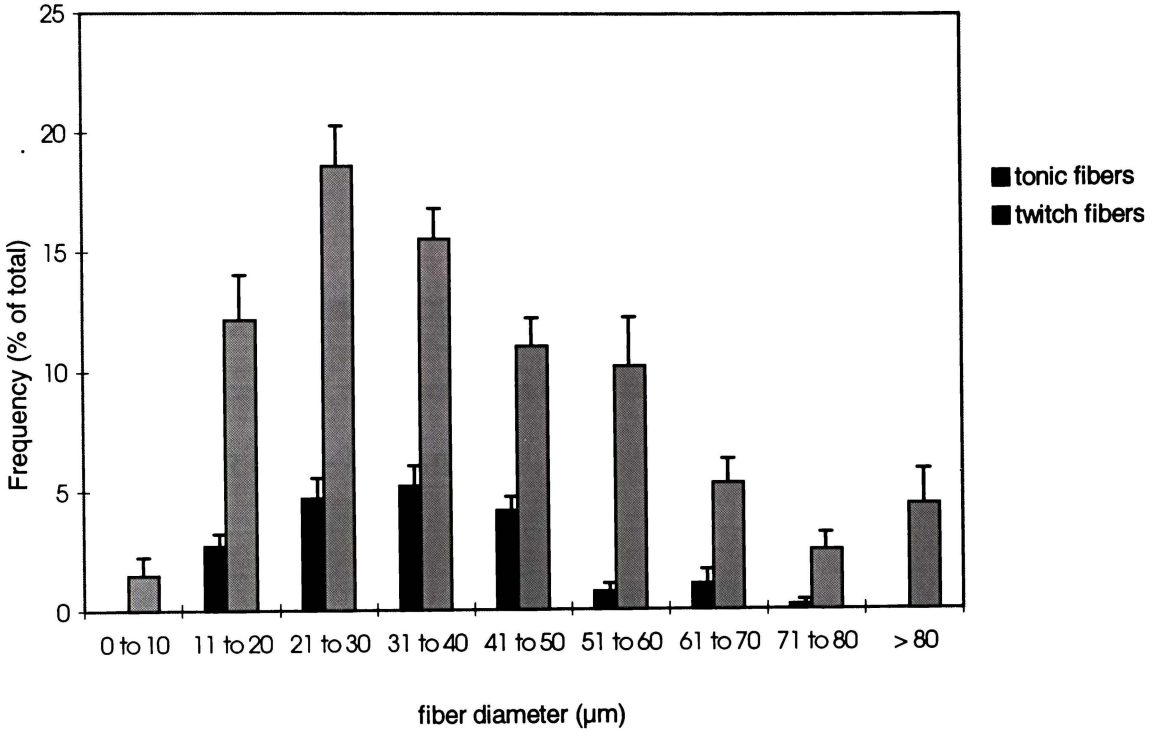

Figure 3.4: Frequency of twitch and tonic fibers as defined by mATPase staining in the global region of *Bufo marinus* inferior rectus muscle (mean ± SE, n = 6 toads).

3.4 Discussion

This study is the first to investigate fiber types in anuran EOM using the combined approach of detecting mATPase and metabolic enzyme activities within fibers. The results suggest that there are at least three types of fiber in anuran global EOM. The fibers that did not stain for mATPase at alkaline pH are the MIFs. Consistent with mammalian EOM these fibers showed little or no staining for α-GPDH and NADH-TR. The fibers that stained darkly for mATPase and moderately for α-GPDH and NADH-TR are likely composed of pale- and intermediate-SIFs. The small diameter fibers that stained darkly for mATPase, α-GPDH and NADH-TR are the dark-SIFs.

The results found here are not consistent with those of Nowogrodzka-Zagorska (1974). She studied two species of *Bufo* and observed that on the 'external' side of the muscle (orbital) the two classes of red fiber (thick and thin) and tonic fibers prevailed whereas the global region contained mainly white and pink fibers. Thus, no/few tonic fibers were identified in the global region. The small diameters (8-16.4 μm) of tonic fibers she identified suggest they were orbital-MIFs. It is possible that the population of white fibers she identified in the global region included tonic fibers. She identified these 'white' fibers as having the largest diameter, sparse mitochondria and myofibrils without a definite symmetry. Since tonic (global-MIF) fibers also have sparse mitochondria and, judging from the results of this study can occur at large diameters, then they could easily have been confused with the 'white' fibers. In addition, the unsymmetrical myofibrils she mentioned that were characteristic of her white fibers could have been

confused with the *felderstruktur* pattern of tonic myofibrils in cross-section. Since her techniques were limited to observing mainly the internal structure of the fiber, they are limited in their ability to distinguish between fiber types which may have more subtle differences that can be resolved using a combination of enzymatic techniques. Furthermore, although she states that methylene blue and azure stain mitochondria and SR, no mention of the extent of SR is given for the fiber types identified. The extent of SR appears to be a key characteristic of tonic fibers, where it is scarce, and therefore this would be an important property to identify.

NADH-TR staining of tonic fibers resulted in a light diffuse staining pattern rather than no staining as would be expected. The reason for this is unknown, however, similar results have been reported in the hindlimb skeletal muscles of four anurans. Putman and Bennet (1983) used SDH to show oxidative capacity of fibers and found that presumed tonic fibers stained lightly for mATPase and α-GPDH and lightly to moderately for SDH. They described the SDH-stained tonic fibers as having a fine-grained appearance rather than the usual coarse-grained pattern seen with SDH staining of fast fibers. Similarly, Mendiola *et al.* (1991) observed that the hindlimb muscles (gastrocnemius) of *Bufo calamita* and *Rana perezi* contained tonic fibers that showed a fine-grained appearance upon SDH staining while FOG and FG fibers had coarse-grained and light appearances, respectively.

A potential problem encountered in this study was the presence of 'holes' in the fibers of sections stained for mATPase activity. 'Holes' in sections are usually

due to freeze artifact, which is the formation of ice crystals during muscle excision and freezing (Fink & Costill 1995). However, the holes were not present in sections stained for α–GPDH or NADH-TR. This suggests that they were probably related to the multi-step staining sequence used in the mATPase staining procedure. One concern was that the holes would affect the diameter of the fibers in the mATPase-stained sections. Comparison, using image analysis, of the fiber diameters obtained from mATPase-stained sections with those of α–GPDH- and NADH-TR-stained sections showed that the 'holes' did not alter the fiber diameters.

Another problem with histochemical staining procedures such as those for NADH-TR and α-GPDH is the difficulty in visually resolving staining intensity (e.g. very high versus high). Thus, from the combination of stains used in this study, it is difficult to know whether the fiber population classified as 'twitch light' is made up of two distinct fiber types corresponding to pale- and intermediate-SIFs of mammalian muscle.

The results from this study, and the work of Nowogrodzka-Zagorska (1974) and Kilarski & Bigaj (1969), suggest that the diameter range of fibers in anuran EOM is larger than in mammals. Nowogrodzka-Zagorska (1974) found the diameter range of EOM fibers in five anurans to be 8 to 76 μm while Kilarski & Bigaj (1969) found fiber diameters in *Rana temporaria* L. to range from 10 to 65 μm. In this study fiber diameters ranged from 7 μm to 125 μm. In contrast, Mayr (1971) found diameters of fibers in both layers of rat EOM to fall between 5 and

40 μm. Similarly, Vita *et al.* (1980) found fibers in rat EOMs to be less than 45 μm in diameter.

Also unlike fibers in mammalian EOM, it appears that in the cane toad the dark-SIFs have a high glycolytic capability in addition to a high oxidative capacity. This finding is similar to that of anuran and lizard hindlimb muscle in which three fiber types are generally found: FOG, FG and tonic. Like the dark-SIFs of *Bufo marinus* EOM, the FOG fibers of anurans and lizards stain darkly for both glycolytic and oxidative enzymes (Gleeson *et al.* 1980, Putnam & Bennett 1983, Mendiola *et al.* 1991). The similar staining pattern of fibers within different anuran muscles and the contrasting results with mammalian EOM suggests that there are distinct physiological differences between the muscles of anura and mammals.

The percentage of tonic fibers in the global layer found in this study (19%) is higher than that found in mammalian EOM. The percentage of tonic fibers in global EOM is reported to be 10% in mammalian muscle (Spencer & Porter 1988). However, as Dean (1996) points out, discrepancies still remain with some workers giving 10 to 20% tonic fibers in each layer. A detailed analysis of fiber types in the orbital layer was outside the scope of this study.

Similarities with mammalian EOM include the diameter of global-MIFs. In *Bufo marinus*, tonic fibers had a mean diameter of 35.1 μm. This is similar to the size of tonic MIFs in mammalian EOM, which have a mean diameter of 35.7 μm (Spencer & Porter 1988). In addition, the characteristic C-shaped orbital layer of

mammalian rectus muscles (Spencer & Porter 1988) was also observed in the rectus muscles of *Bufo marinus*.

In this study, three distinct fiber types were identified in global EOM of *Bufo marinus*. In order to assist the selection of global MIFs (tonic fibers) from the inferior rectus muscle for use in contractile activation studies, the diameter, frequency and distribution of the histochemically-defined tonic fibers was explored. It was found that both twitch (light and dark) and tonic fibers occurred over a wide diameter range with tonic fibers occurring at a relatively low frequency in each size range compared to the twitch fibers. In addition, tonic fibers were distributed at random in the global region. Therefore, the tonic fibers cannot be identified by their sole, or majority, occurrence at a particular diameter or location within the global region. However, the chance of obtaining a tonic fiber will increase by choosing fibers between 21 and 50 μm, and especially between 42 and 50 μm.

CHAPTER 4: CONTRACTILE PROPERTIES OF SINGLE PERMEABILIZED FIBERS FROM GLOBAL EOM

4.1 Introduction

Studies utilising whole muscles can gain information regarding the contraction and relaxation time, maximum twitch and tetanic tension and maximum force per cross-sectional area produced by the muscle. However, since most muscles, especially EOMs, are composed of several fiber types, studies with whole muscles do not yield information on individual fibers. By studying single fibers, the contributions of individual fiber types to whole muscle physiology can be ascertained. Single fibers can be dissected from the muscle and used in an intact or permeabilized state. In permeabilized (skinned) single fiber preparations, the sarcolemma is removed so that the bathing medium can have a direct effect on the myofibrillar apparatus. The free calcium concentration can thus be manipulated without interference from intracellular stores.

Skinned single fiber preparations allow contractile properties such as shortening tension and velocity to be measured after manipulation of regulatory proteins and/or changes in sarcoplasmic ionic composition. The thick and thin filaments that make up the myofibril consist of both contractile and structural proteins. Since studies using permeabilized single fibers most commonly relate to the function of the contractile proteins, the following summary focuses on these proteins. The parallel overlap of the thick and thin filaments form regular repeats

called sarcomeres. The thick filament is primarily made up of myosin, a protein composed of two heavy chains and four light chains. The thin filament includes actin and associated proteins troponin and tropomyosin. Troponin is a complex of three polypeptide chains: TnC, TnI and TnT. There is one troponin complex and one tropomyosin molecule for every seven actin monomers (Harrington 1981). At these regular intervals along the thin filament, the TnI subunit binds to actin, TnT binds to tropomyosin and TnC binds calcium ions. In mammals, fast-twitch and slow-twitch muscles have distinct troponin C isoforms that differ in their capacity to bind Ca^{2+} (Wilkinson 1980). While both isoforms have two high-affinity Ca^{2+} binding sites, fast-twitch TnC has two low-affinity binding sites and slow-twitch TnC has only one. In resting muscle, Ca^{2+} is sequestered in the SR by an active transport system and the high-affinity Ca^{2+} binding sites on TnC are occupied by Ca^{2+} while the low-affinity ones are empty. Release of Ca^{2+} from the cisternae of the SR raises the level of sarcoplasmic Ca^{2+} and the low-affinity Ca^{2+} binding sites become occupied. This causes a conformational change in TnC that is then transmitted to other components of the troponin complex and then to tropomyosin. The position of tropomyosin then shifts enabling actin to interact with myosin.

Muscle contraction results from the cyclic interaction of myosin and actin. In relaxed muscle, myosin cross-bridges (S1 heads) interact with actin weakly or not at all. ADP and P_i, the hydrolysis products of ATP, are bound to myosin. When stimulated to contract, the S1 heads reach out from the thick filament and attach to actin on the thin filaments. The release of P_i is associated with the cocking of the S1 head or the power stroke that pulls the thin filaments toward the center of the sarcomere. ADP is then released and the subsequent binding of ATP reverses the

conformational change in S1 and results in the rapid release of S1 from actin. The ATPase associated with the myosin head is responsible for splitting ATP into ADP and P_i. The enzyme creatine kinase catalyses the rephosphorylation of ADP to ATP as soon as it is formed using a phosphate group from phosphocreatine (PCr). Although ATP bound to myosin is rapidly hydrolyzed, ADP and P_i are slow to leave.

Calcium regulates the interaction between actin and myosin. In skeletal muscle the binding of Ca^{2+} to troponin results in the movement of tropomyosin that allows myosin binding to actin. Therefore, the number of cross-bridges bound to actin and the consequent tension, varies with the concentration of Ca^{2+} bathing the filaments. In resting (relaxed) muscle, Ca^{2+} levels are about 0.1 μM and rise to 10 μM at the height of contraction (Ashley & Campbell 1979, Ashley 1984). The development of tension in skeletal muscles is a highly cooperative process in that tension rises rapidly with small increases in free [Ca^{2+}] above the threshold for mechanical activation (see Moss 1992 for review). In single fiber experiments the calcium chelator, EGTA, is most often used to buffer and thereby regulate free Ca^{2+} concentrations.

One of the limiting factors with single fiber work is the dependence on diffusion of critical ions and molecules from the bathing medium into the inner myofibrils. This is particularly true for ATP, the molecule that supplies the necessary energy for muscles to contract. To minimize this limitation, PCr is added to all activating solutions in order to promote regeneration of ATP. In addition, fibers are placed in a pre-activate solution with decreased EGTA buffering capacity prior to the

activation solution. By reducing the amount of chelator present, calcium diffusion into the myofibril network is optimized.

The tension response of skinned fiber preparations to submaximal and maximal calcium levels differs depending on the fiber type. For example, it has been routinely observed that the slope of the force-pCa curves obtained from slow-twitch fibers is less than the slope observed in fast-twitch fibers (e.g. Stephenson & Forrest 1980). The degree of slope is proportional to the amount of cooperativity among subunits of the thick and thin filaments (Cornish-Bowden & Koshland Jr. 1975). These interactions may include: cooperative binding of Ca^{2+} to troponin (Bremel *et al.* 1973), cooperative interactions between thin filament units (Moss *et al.* 1985, Brandt *et al.* 1987, Metzger & Moss 1991), cooperative binding of myosin heads to the thin filament and synergistic interactions between myosin head binding and Ca^{2+} binding (Grabarek *et al.* 1983, Guth & Potter 1987, Millar & Homsher 1990, Swartz & Moss 1992).

There have been only two other studies to look at the contractile properties of single EOM fibers. Lynch *et al.* (1994) examined the Ca^{2+}- and Sr^{2+}-activated contractile characteristics of single fibers from the rabbit superior rectus while Campbell (1997) similarly studied both the superior and inferior rectus muscles. Like Ca^{2+}, Sr^{2+} also binds to TnC but with lower affinity. Skinned fibers can be differentiated on the basis of their binding response and sensitivity to these two divalent ions and allocated into discrete fiber type groups (Wilson & Stephenson 1990; Lynch *et al.* 1991). Lynch *et al.* (1994) grouped superior rectus fibers into

populations I, II, III, IV and 'mixed' on the basis of their physiological response to these ions. The values obtained for Hill coefficients, (nCa and nSr), differential sensitivity to Ca^{2+} and Sr^{2+} ($pCa_{50} - pSr_{50}$), the pCa or pSr corresponding to 10% relative force (contraction threshold: pCa_{10}, pSr_{10}) were all used to group the fibers. They found fibers that could be allocated into population types I, II and III, analogous to the histochemically defined groups of type I (slow-twitch), IIA and IIB (fast-twitch), respectively. Population IV fibers displayed properties intermediate to those of typical slow-twitch and fast-twitch fibers. They also found a high proportion of fibers that exhibited mixed fast- and slow-twitch contractile characteristics. Using the same methodology, Campbell (1997) found all 26 superior rectus fibers examined to be type II and all but one of the 31 inferior rectus fibers examined to be type II. The remaining fiber fell into the type I category.

There are a number of drawbacks in using this technique for the grouping of EOM fibers. Firstly, this method may not be sensitive enough to detect differences in fibers expressing more than one myosin isoform. Bortolotto *et al.* (1997) compared the ability of the Ca^{2+}/Sr^{2+} contractile activation method with that of myosin isoform composition to classify fiber types. They found that when only one set of myosin isoforms was present both methods were in full agreement. However, in fibers that co-expressed different myosin isoforms there was only partial agreement between the two methods. That is, fibers with mixed myosin isoforms could not always be detected using the contractile activation response to Ca^{2+} and Sr^{2+}. Secondly, this method uses a predefined classification system. This

may restrict an observer's perception of fiber complexity, resulting in an over-simplification of the real situation.

The primary aim of the work in this chapter was to determine the contractile properties of fibers within the global region of EOM with emphasis on the tonic fibers or MIFs. Early in this work it became clear that determining the type of fiber whose Ca^{2+}-activation response was being measured was not going to be as straightforward a task as initially thought. Tension curve responses could not be relied upon solely as differences here could, in part, be due to problems within the fiber too small to be observed with the experimental microscope. As contractile experiments rely on the integrity of myofibrillar proteins, any damage at this level would flaw results. Clearly, a way of distinguishing the fibers prior to the difficult task of T-clipping and fixing, would be useful. It has been known for some time that fiber appearance (dark, pale, clear) under the light microscope can be correlated with lipid and (mitochondrial) enzyme content (Lannergren & Smith, 1966). Indeed, Martyn *et al.* (1993) were able to identify twitch and tonic fibers of amphibian cruralis muscle simply by their appearance under the light microscope. Those that appeared 'clear' were tonic fibers, while those that appeared 'dark' were twitch fibers. With this in mind, it was thought that perhaps tonic (global-MIF) fibers and twitch (global-SIF) fibers could be identified prior to T-clipping simply by appearance (i.e. 'clear' and 'dark', respectively). This possibility was investigated by performing TEM on single fibers that had been isolated and identified by their appearance under the light microscope. The Ca^{2+}-activation response of single permeabilized muscle fibers from global EOM was then investigated, with emphasis on obtaining data from tonic fibers. In addition to fiber

appearance, characteristics such as force responses, fiber diameter and maximum tension were used to group fibers. The force-pCa relationships, Hill coefficients at high and low [Ca^{2+}], pCa_{50} and pCa_{10} values were then determined for each group of fibers. The MLC profiles of individual fibers used in the single fiber experiments were used to confirm the grouping of twitch and tonic fibers and these are presented in Chapter 5.

4.2 Materials and Methods

4.2.1 Use and Care of CaneToads

For information regarding source, care and ethical use of cane toads, see Chapter 2: Section 2.2.1.

4.2.2 TEM of Single Muscle Fibers

After preparation of the inferior rectus muscle for skinning, and isolation of single fibers from the global region (details regarding these techniques are described in detail in Section 4.2.3, below), the fibers were subjectively identified as 'clear' or 'dark' under the stereomicroscope. They were then transferred from the 25% gycerol-relax solution into 4% glutaraldehyde, 0.1 M sodium cacodylate, pH 7.5 fixative for 20 to 30 min. The fibers were then transferred to 0.1 M sodium cacodylate, 0.1 M sodium chloride buffer, pH 7.5 and kept for up to one week at 4 °C prior to dehydration and embedding.

To prepare single fibers for dehydration and embedding, a mould was assembled using cut sections of 8 mm I.D. and 5.6 mm I.D. BEEM™ embedding capsules (Figure 4.1). A cylinder was cut from the larger capsule and a rectangular window (1.5 mm by 2 mm) was cut in the lid of a smaller capsule. This lid was inserted into one end of the cylinder. In a drop of cacodylate buffer, the T-clipped fiber was aligned in the lid of a larger capsule. The cylinder with small lid was placed over the fiber so that only the fiber was present in the window and the T-clips were secured between the small and large lids.

Unless stated otherwise, all solutions used for dehydration and embedding were the same as those given in Chapter 2. The samples were processed for TEM using a modification of the method outlined in that chapter. The drop of cacodylate buffer overlying the fiber was removed and 0.5% osmium tetroxide added for 5 min. The fiber was then washed three times with H_2O. Uranyl acetate (4%) was added for 20 min and the fiber dehydrated in 75%, 95% and then three changes of 100% ethanol. A 50/50% (v/v) mixture of Spurr's resin : ethanol was added and left for 10 min. This was replaced with 100% Spurr's resin for 30 min followed by two further changes of Spurr's resin for $1^1/_2$ and 2 h. Finally, the blocks were set overnight in an oven at 70 °C. When dry, the BEEM™ capsules were removed and the T-clips trimmed off. Fibers prepared in this manner were used for longitudinal sections. For transverse sections, the area where the fiber was embedded was cut free, carefully aligned in a silicon rubber mould and Spurr's resin added. The block was set overnight in an oven at 70 °C.

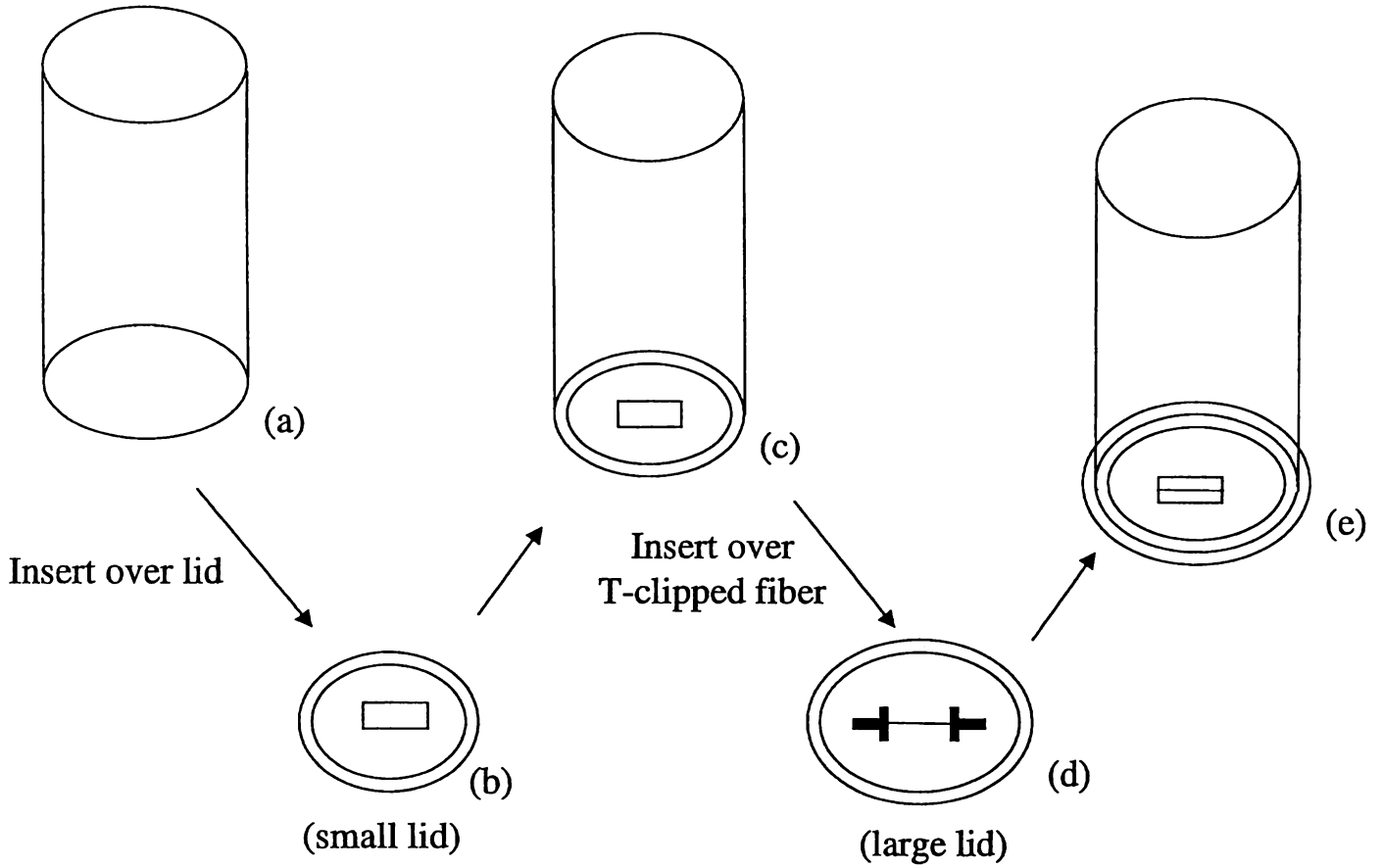

Figure 4.1: Assembly of embedding mould for TEM of single fibers. The end was cut out of a large capsule (a) and a rectangular window cut out of a small lid (b). The combined mould (c) was place over the T-clipped fiber lying in the lid of a large capsule (d), to produce the final mould (e) with fiber secured, via T-clips, between the small and large lids.

4.2.3 Single Fiber Contractile Activation Experiments

4.2.3.1 Experimental Solutions

Chemicals were obtained from Sigma or United States Biologics (USB) and all solutions were made with distilled water and stored at 5 °C unless stated otherwise.

The composition of relaxing, pre-activating and activating solutions was determined by using the computer program, '*Solution*', of Homsher and Millar (1989). This program allows the user to calculate free Ca^{2+} concentrations as well as concentrations of major ligands at specified temperatures and pHs. Each solution contained: 25 mM imidazole,10 mM EGTA, 1mM free Mg^{2+}, 5 mM free MgATP, 5 mM PCr, 150 mM ionic strength at pH 7.1 and 10 °C. The only exception to this was the pre-activate solution that had a reduced EGTA buffering capacity with 0.2 mM EGTA. The ionic strength of the solutions was maintained by altering the concentration of KCl. The relaxing and pre-activating solutions contained a free Ca^{2+} concentration of pCa 9.0 (where pCa = -log $[Ca^{2+}]$) while maximally activating solutions had pCa values of 4.8 or 4.6. Activating solutions ranged from pCa 7.2 to 4.6. All these solutions were stored at –20 °C. Refer to Table B.2 of Appendix B for a complete listing of these solutions.

4.2.3.2 Muscle Preparation

A double strength skinning stock solution of 140 mM KCL, 16 mM $MgAc_2$, 10 mM K_2EGTA and 12 mM imidazole was prepared using the stocks listed in Table B.1 of Appendix B. The following protease inhibitors were added to this solution: 0.1 mM PMSF (phenylmethyl sulfonyl flouride), 0.1 mg/ml soyabean trypsin inhibitor, 8 μg/ml leupeptin. The pH was adjusted to 6.5 at room temperature (6.8 at 0 °C) with 1 M KOH. Using this stock, a single strength skinning solution containing 0.5% (w/v) Brij-35 (polyoxyethylene lauryl ether, BDH) was prepared without inclusion of ATP (rigor skinning solution). The inferior rectus muscle was exposed and bathed in this rigor solution in order to prevent over-shortening and hence irreversible damage to the muscle. Upon dissection, the muscle was placed into single strength relax skinning solution containing 0.5% Brij-35 and 7 mM ATP. The solutions and procedures for skinning and glycerinating are outlined in Table 4.1 below. Muscles were stored at –20 °C in 50% glycerol-relax solution overnight.

Table 4.1: Solutions used for skinning EOMs. The solutions are expressed in ratios of parts.

Solution	Glycerol	Double strength skinning stock solution	H_20	Duration of gentle agitation on ice
0.5% Brij skin – rigor	0	0.5 (no ATP)	0.5	(bathed *in situ*)
0.5% Brij skin - relax	0	0.5 (+ ATP)	0.5	1-2 h
Skin rinse	0	0.5 (+ ATP)	0.5	5 min
25% Glycerol-relax	0.25	0.5 (+ ATP)	0.25	30 min
50% Glycerol-relax	0.5	0.5 (+ ATP)	0	1 h

4.2.3.3 Experimental Protocol

The muscle bundle was placed global side up in a petri dish containing cold glycerol-relax solution (25 mM imidazole, 55.9 mM KCl, 6.6 mM $MgAc_2$, 10 mM K-EGTA and 5.5 mM NaATP, 25% v/v glycerol, pH 6.9). The base of the petri dish was lined with a silicone rubber sealant (734 Flowable Sealant, Dow Corning, USA) to ease manipulation of fibers and to create a surface which pins could penetrate. Dissection was performed with fine forceps under a trans-illuminating stereomicroscope at 10X to 50X magnification. The fibers were kept cool (10 °C) by a Peltier cooling device. Most fibers were used the day following skinning and

glycerination. On occasion, when the calcium activation response was high, fibers were used again the following day.

Individual fibers were pulled free from one end of the muscle bundle and fiber appearance (clear or dark) was noted. T-shaped tabs made from aluminium foil were attached to each end of the fiber (T-clipping) (Figure 4.2). The fiber was mounted via the T-clips onto a portable apparatus and transferred to a perspex trough containing cold rigor solution (25 mM imidazole, 99.7 mM KCl, 1.5 mM $MgAc_2$, 10 mM K-EGTA, pH 6.9). The portable apparatus consisted of two horizontally placed hooks attached to each end of a U-shaped perspex arm. The distance between the hooks could be adjusted to accommodate a range of fiber lengths. A stream of high-density rigor fixative containing 4% (v/v) glutaraldehyde and 25% (v/v) glycerol was directed over each end of the fiber for 30 s (Figure 4.3). Two dyes were incorporated into this solution in order to see its path clearly and hence ensure the middle section of the fiber escaped exposure to fixative. These dyes, methylene blue and sodium fluorescein, coloured the rigor fixative solution a deep green. The use of sodium fluorescein allowed fiber fixation to be monitored using flourescent microscopy. Glycerol gave the fixative a higher density than the rigor solution and caused it to sink to the bottom of the perspex trough. During fixing, the fiber was viewed with a stereomicroscope.

Following fixing, the fiber was transferred back to the petri dish containing glycerol-relax solution and the T-clips were cut off each end of the fiber. The fiber was T-clipped again over the fixed portion of the fiber. The length of unfixed fiber between T-clips was typically between 400 and 800 μm. Using a polished glass

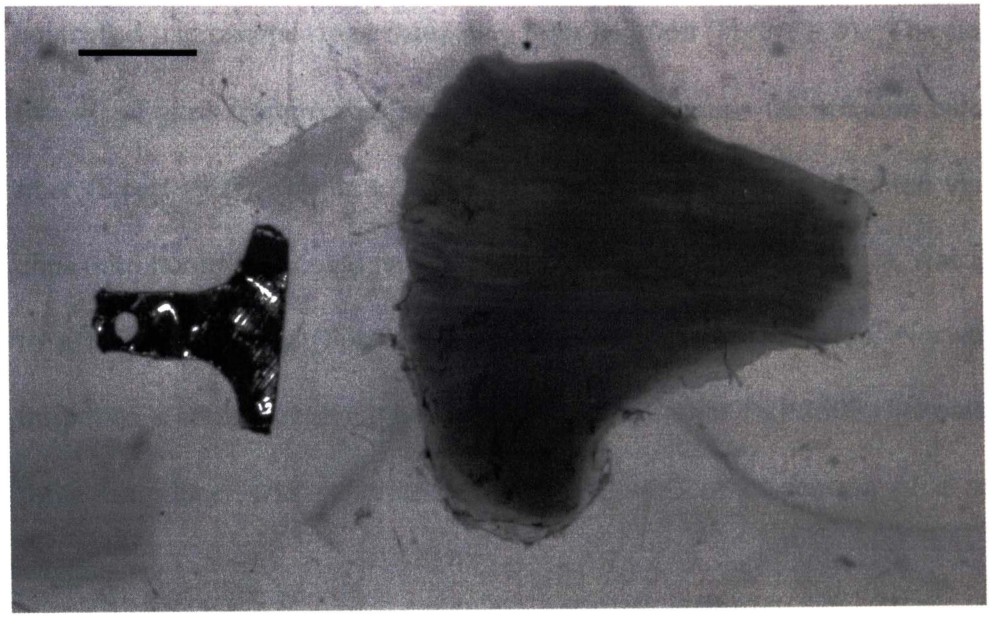

Figure 4.2: T-clip (left) and inferior rectus muscle of *Bufo marinus*. Scale bar = 1 mm.

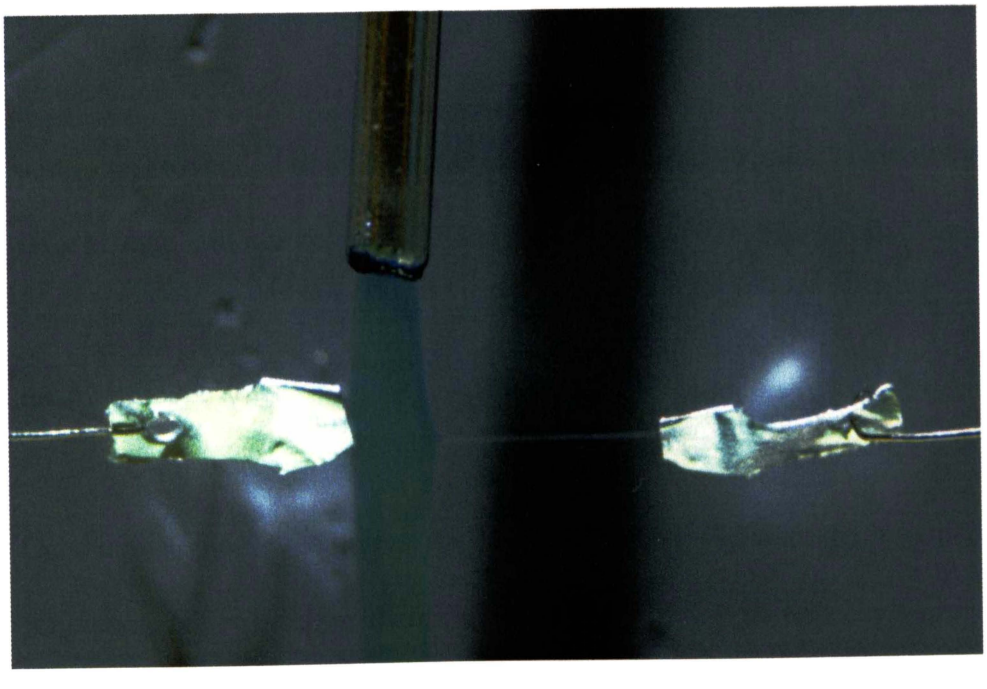

Figure 4.3: Fixing fiber ends with a stream of rigor fixative containing 4% (v/v) glutaradehyde, 25% (v/v) glycerol and two dyes.

rod, the fiber was swiftly transferred to a 40 µl glass trough on a temperature-controlled microscope stage containing relax solution (Figure 4.4). The stage held five 40 µl glass troughs that could be rotated to change the solution bathing the fiber (Sleep 1990). Using a stereomicroscope, the fiber was mounted via the T-clips onto hooks that could be independently manipulated. One hook was attached to a force transducer (SensoNor sensor element AE801, Horten, Norway) with output to a strain gauge amplifier and a chart recorder (SS-250F, Sekonic). The force transducer was calibrated regularly by vertical suspension of a series of weights.

A thermocouple (Type T, 0.13 mm wire, Omega) was attached snuggly to the right hook so that it was immersed in the solution bathing the fiber. Temperature of the bathing solution was maintained at 10 °C ± 1 °C with a microprocessor temperature controller (MCR-100 series, Shinko Technos Co. Ltd). This controller responded to a rise in the temperature of the bathing solution by turning on a heating coil immersed in a flask of liquid nitrogen. The hot coil caused cold nitrogen gas to be released from the flask via a rubber tube to the copper base of the microscope stage.

Once mounted onto the hooks, the fiber could be viewed with the light microscope (Optiphot, Nikon). Fiber diameter and sarcomere length were measured using a 40X objective lens (40X, DIC, 0.55 N.A., LWD, Nikon) and ocular micrometer. Hook separation was adjusted so that the fiber was just taut. This usually gave a sarcomere length of between 2.2 and 2.4 µm, the length found to give maximum force generation. This optimum sarcomere length was determined for single fibers

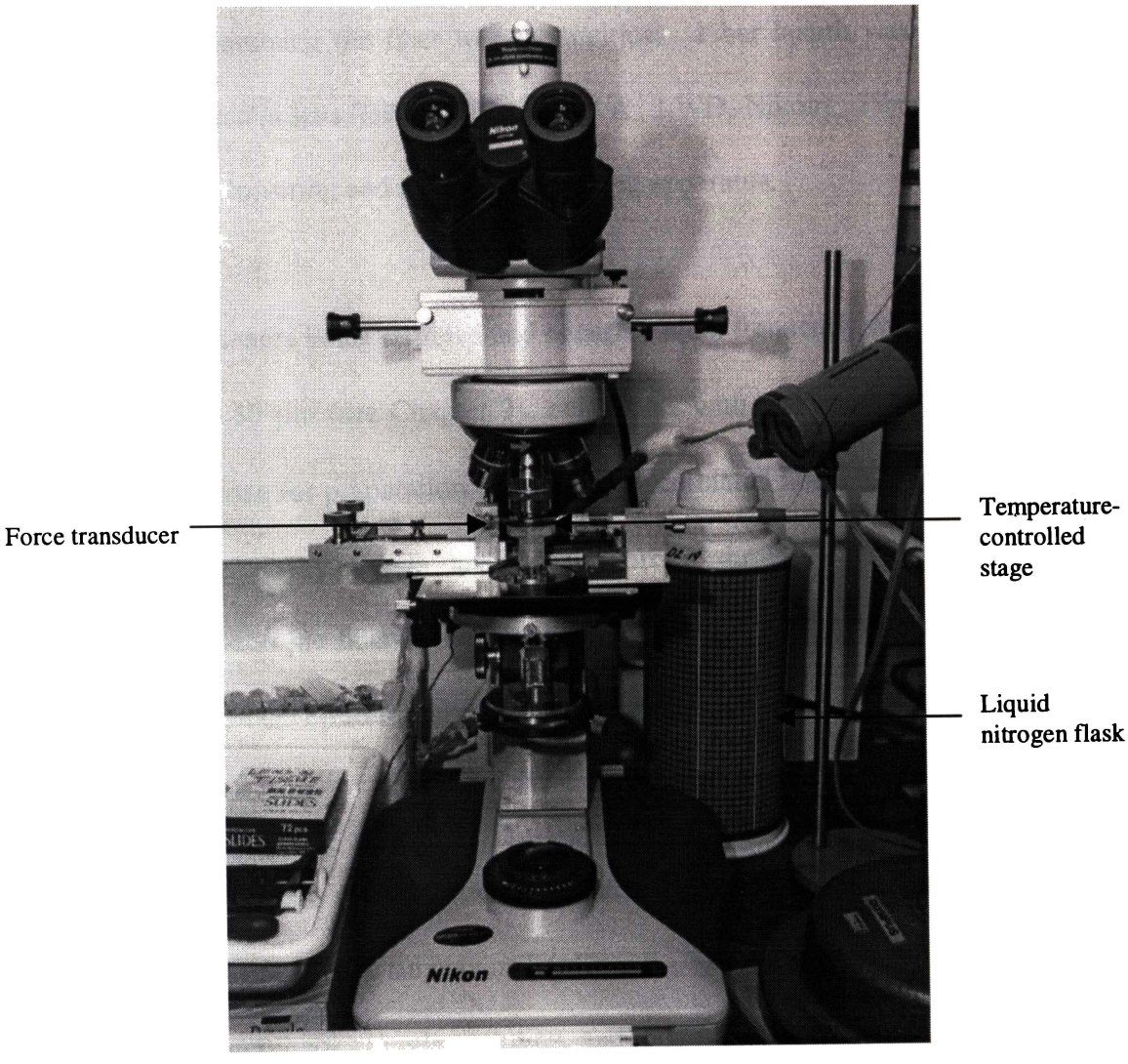

Figure 4.4: Single fiber experimental apparatus.

by measuring the force response to maximally activating [Ca^{2+}] at a range of (randomly selected) sarcomere lengths. Fiber diameter was measured at three points along the length of the fiber and the average taken. The cross-sectional area was calculated assuming the fiber to be cylindrical. Fiber length was measured using a 10X objective lens (EPlan 10X, 0.25 N.A., LWD, Nikon). Fiber solutions were changed by lowering and rotating the bathing apparatus.

Since tonic fibers were being targeted and occurred most frequently with diameters between 20 and 50 μm (see Chapter 3), only fibers with diameters in this range were initially chosen for preparation. However, glycerinated fibers less than 40 μm in diameter were very fragile and usually broke during transfer from the stereomicroscope to the fiber-fixing apparatus. Since tonic fibers occur up to 80 μm in diameter, fibers up to this size were subsequently used.

Force-pCa relationships were determined by recording peak isometric force during maximal (pCa 4.6/4.8) and submaximal (pCa 7.2 – 5.0) Ca^{2+} activation. Fibers were mounted onto hooks in relax solution, and then subjected to a 'full activation' (pCa 4.8/4.6). This was followed by relax solution and a random order of pCa solutions, each preceeded by pre-activate and followed by relax solutions. Tension decline throughout the experiment was measured as the difference between the first and last full activation and was expressed as a percentage of the first activation. It was assumed that maximum force decreased linearly with activations. Force measurements were normalized for cross-sectional area and expressed as P_r, the ratio of peak tension at a given pCa (P_n) to peak tension obtained at pCa 4.6/4.8

(P_o). Force-pCa data were fitted to separate Hill plots {pCa vs log [P_r/(1-P_r)]} for responses at high ($P_r > 0.5$) and low ($P_r < 0.5$) calcium concentrations. Hill coefficients (n) were obtained from the slope of linear regressions of these data (termed n_1 for responses at high [Ca^{2+}] and n_2 for responses at low [Ca^{2+}]). The value for the free Ca^{2+} concentration eliciting one-half maximal activation (pCa_{50}) was calculated as the mean abscissal intercept of the Hill plot regression lines for high and low calcium concentrations. On occasion, there were not enough points derived from force-pCa experiments to obtain Hill plot regression lines for both high and low calcium concentrations. In these cases, when only a single Hill plot was available for a fiber, the abscissal intercept of that plot was used to determine the pCa_{50} value. The Ca^{2+} activation threshold was determined to be the pCa that produced 10% maximal tension (pCa_{10}) and was calculated from the Hill plot regression line at low calcium concentrations. The pCa index was calculated as the sum of the molar concentrations of calcium that each fiber was subjected to over the course of an experiment. Thus, the pCa index is equal to the total cumulative concentration of free Ca^{2+} that the fiber received.

All fibers were included in these analyses regardless of percent decline in maximum tension since it was found that n_1, n_2 and pCa_{50} values did not vary with decline in maximum tension (see Results section). Student's t-test was used for pairwise comparison of means from pooled data, with differences being considered significant at the $P < 0.05$ level. All values for the parameters above are given as the mean ± SE of the mean. Results from experiments using two different batches of pCa solutions are presented and, when appropriate, the results from fibers used with each of these batches are presented separately. This is because the pCa_{50}

values, of a single fiber population, resulting from each batch were significantly different.

After force-pCa measurements were obtained, T-clips were removed from each end of the fiber which was then placed into 15 µl of SDS-sample buffer (composition in Chapter 5: Methods and Materials) and frozen at –70 °C for later electrophoretic analysis (see Chapter 5).

4.3 RESULTS

4.3.1 Ultrastructure of 'Light' and 'Dark' Fibers

In transverse section, all of the four fibers identified as 'dark' had discrete myofibrils and large lipid droplets (Figure 4.5a). Two of the four fibers identified as 'clear' had discrete myofibrils (Figure 4.5b) while two had ill-defined myofibrils (Figure 4.5c). Few, if any lipid droplets were evident in these fibers. In longitudinal section, all three fibers identified as 'dark' showed a definite M-line (Figure 4.5d). This was also true of the three fibers identified as 'clear' (Figure 4.5e).

From these results it would appear that all seven fibers identified as dark were twitch fibers or SIFs. Of those identified as clear, two of the seven fibers prepared for TEM were tonic or MIFs. On the basis of these results, clear fibers were preferentially used for contractile experiments.

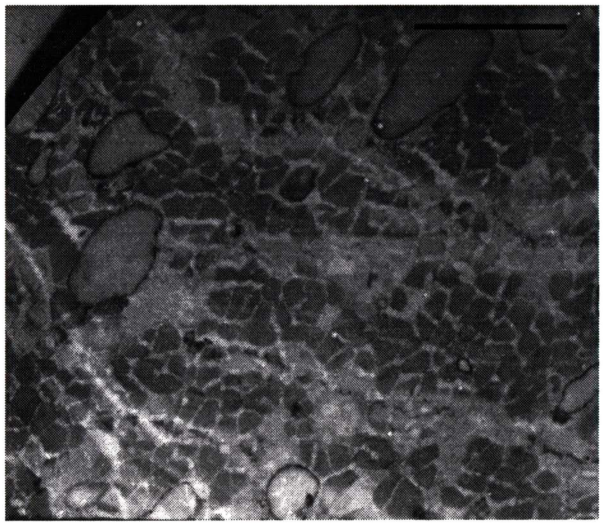

(a)

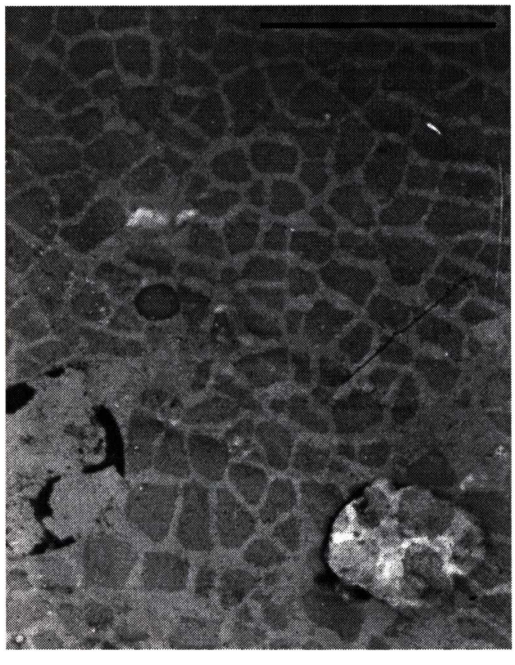

(b)

(c)

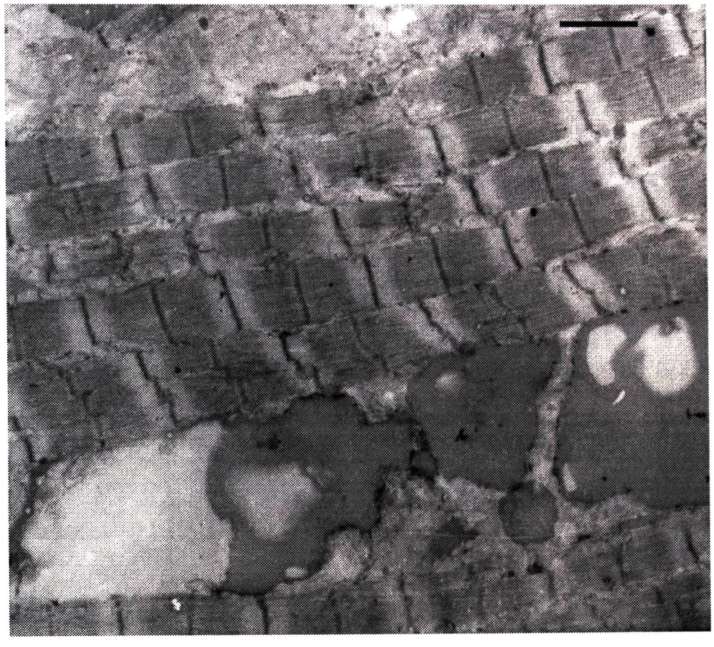

(d)

(e)

Figure 4.5: Representative micrographs of 'dark' (a) and 'clear' (b and c) fibers cut transversely, and 'dark' (d) and 'clear' (e) fibers cut longitudinally. Scale bars = 5 μm for (a) to (c) and 1 μm for (d) and (e).

4.3.2 Maximim Force Responses

Three distinctly different groups of fibers were identified by virtue of their responses to maximal and initial activation (pCa 4.6/4.8). The group of fibers that showed a fast but low tension response was termed 'twitch dark' (Figure 4.6a). These fibers took 8.0 ± 3.3 s (n = 6) to reach 90% maximal activation (Figure 4.7) and reached a low maximal force of 129.2 ± 7.5 μN (n = 6). Another group had a similar response time (9.1 ± 9.6 s; n = 10) but showed a higher maximal force of 598.9 ± 42.8 μN (n = 50) and were termed 'twitch light' (Figures 4.6b and 4.7). The third group of fibers developed tension slowly and was called tonic. These fibers took significantly longer (P = 0.04) to reach 90% full activation (29.5 ± 8.7 s; n = 10) and had low maximum force levels of 179.9 ± 16.5 μN (n = 10) (Figures 4.6c and 4.7).

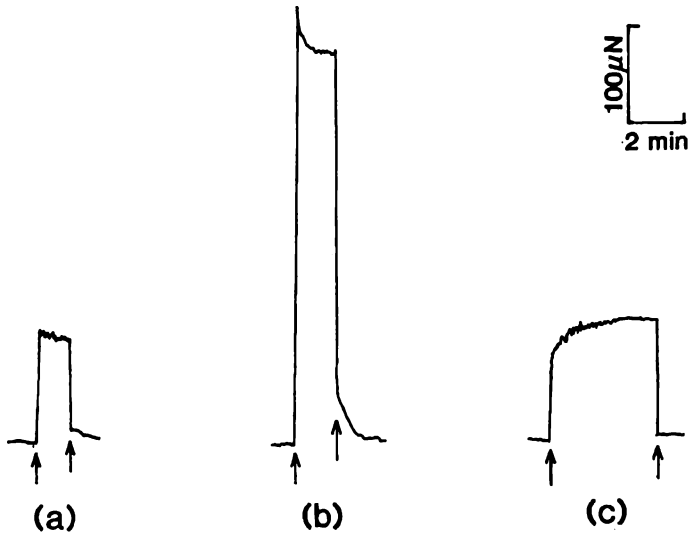

Figure 4.6: Representative force responses obtained upon initial and maximal activation from (a) twitch dark, (b) twitch light and (c) tonic fibers. The first arrow indicates the moment when the fiber was transferred from pre-activating to activating solution, while the second arrow indicates transfer from activating to relaxing solution.

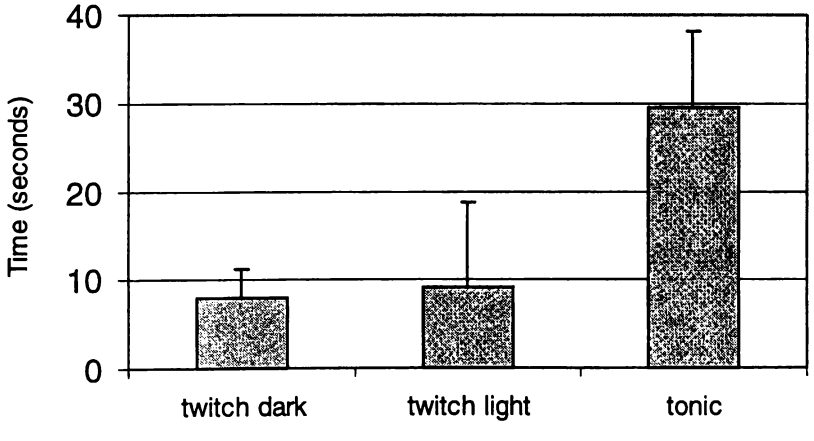

Figure 4.7: Time to 90% maximum force for twitch dark (n = 6), twitch light (n = 10) and tonic (n = 10) fibers. Values are means ± SE.

4.3.3 Maximum Normalized Tension

The mean maximum normalized tension for each group of fibers is shown in Figure 4.8. Twitch light fibers showed a significantly higher mean tension (140.2 ± 9.2 kN/m^2; n = 50) than both twitch dark (60.0 ± 2.4 kN/m^2; n = 6) ($P < 0.001$) and tonic fibers (97.5 ± 6.3 kN/m^2; n = 10) ($P < 0.001$). Twitch dark fibers showed significantly lower mean tension than tonic fibers ($P < 0.001$).

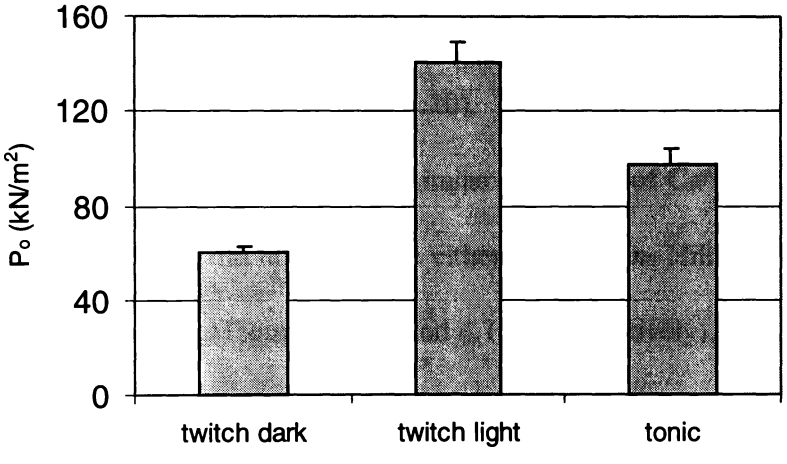

Figure 4.8: Maximum normalized tension, P_o (kN/m^2), for twitch dark (n = 6), twitch light (n = 50) and tonic (n = 10) fibers. Values are means ± SE.

4.3.4 Force-pCa Curves

The mean force-pCa curves for twitch dark, twitch light and tonic fibers are presented in Figure 4.9. Each graph shows data collected from a single pCa batch. Each fiber population showed a sigmoidal curve. At low [Ca^{2+}], the curve was steeper for the twitch dark and twitch light fibers than for the tonic fibers.

4.3.5 Decline in Maximum Tension

The maximum tension attained by both tonic and twitch light fibers declined with increasing exposure to Ca^{2+} (Figure 4.10). This decline was greater for tonic fibers than for twitch fibers subjected to a similar challenge of Ca^{2+}. The percent decline in maximum tension did not influence either the n_1 or n_2 Hill coefficients for twitch light and tonic fibers (Figures 4.11a and 4.11b, respectively).

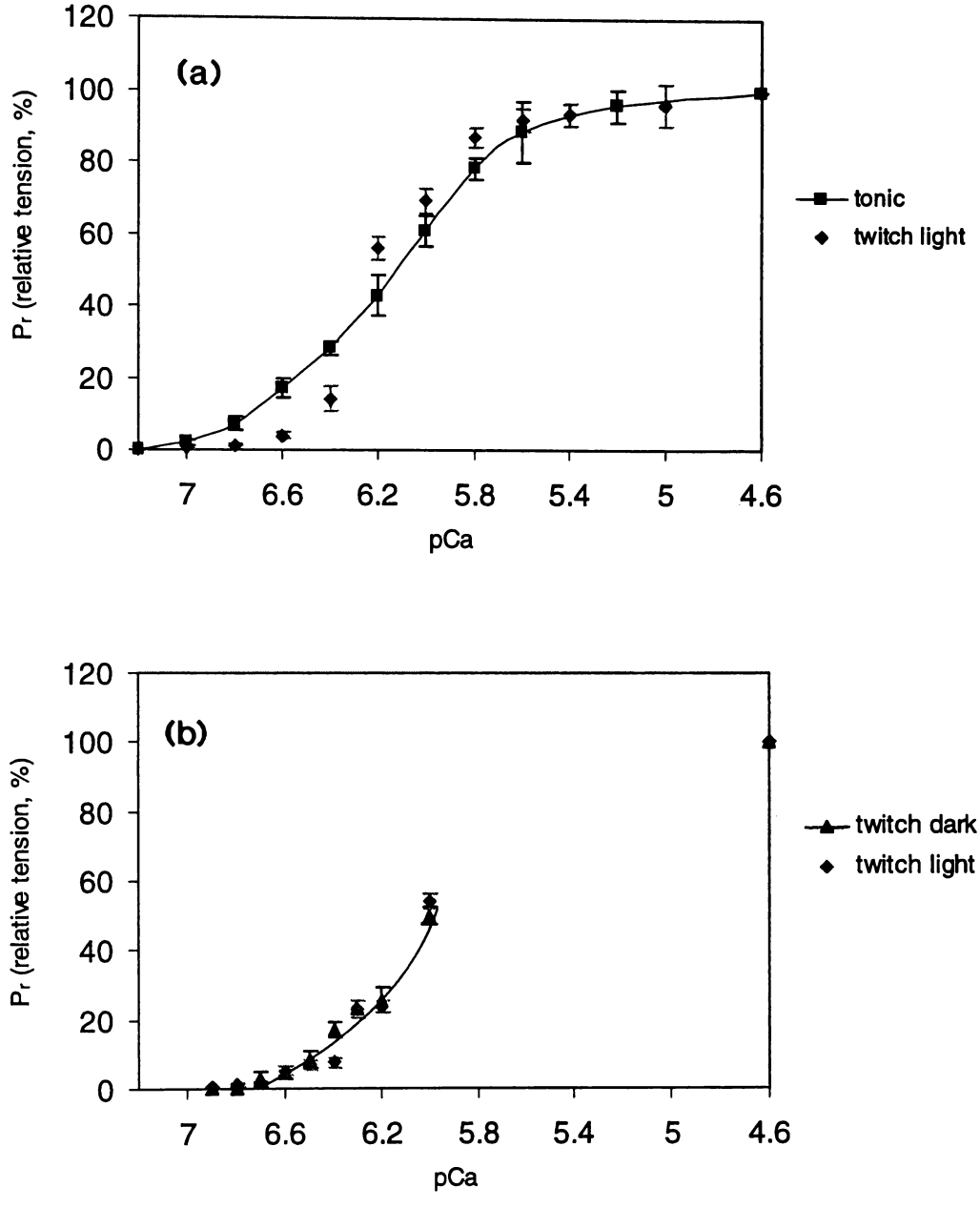

Figure 4.9: Force-pCa curves for (a) twitch light (n = 10) and tonic (n = 7) fibers and (b) twitch light (n = 20) and twitch dark (n = 5) fibers. Each graph shows data collected from a single pCa batch. Each point represents the mean ± SE of measurements on 3 to 20 fibers. Standard error bars are not shown if the standard error is smaller than the symbol.

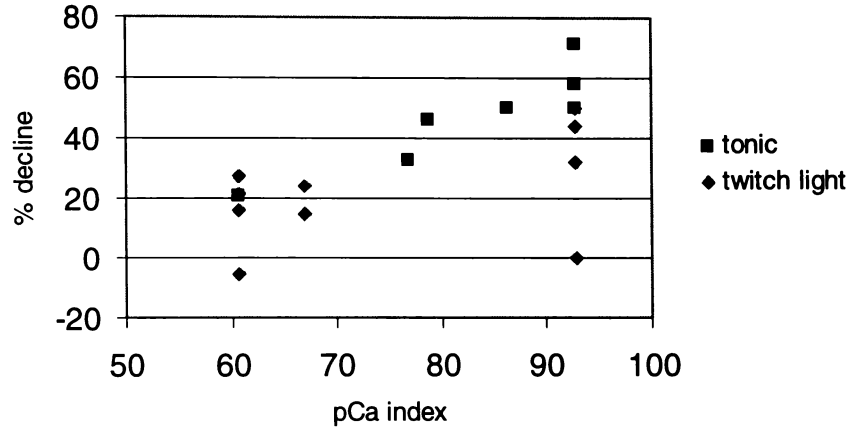

Figure 4.10: Decline in maximum tension with pCa index (see text for details).

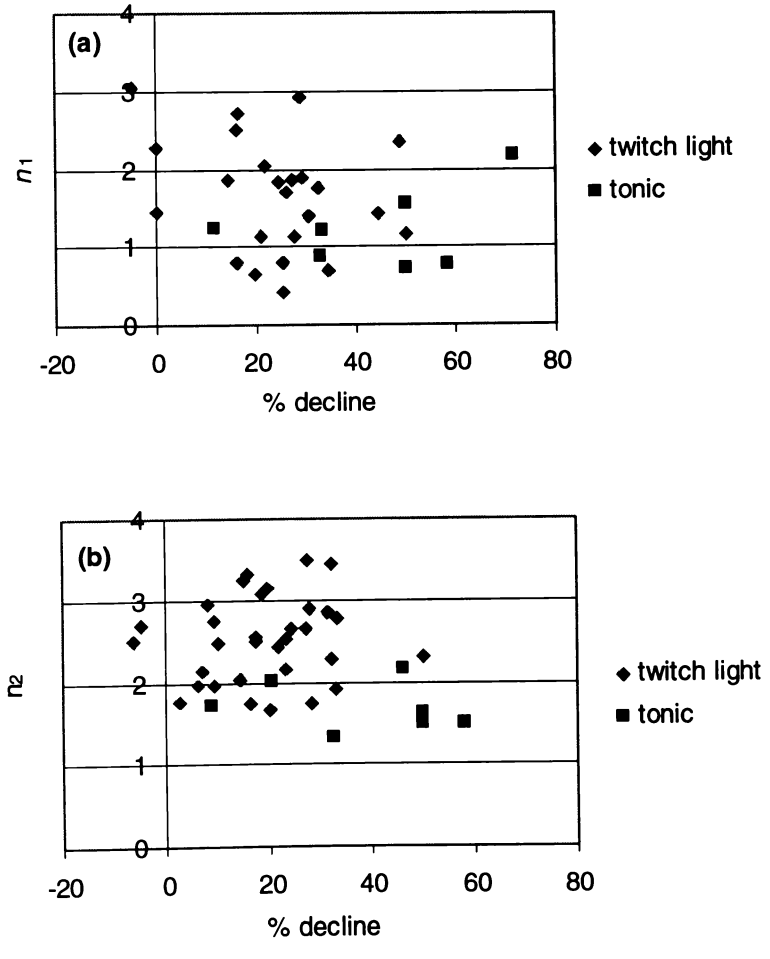

Figure 4.11: Decline in maximum tension versus Hill coefficients, (a) n_1 and (b) n_2 for twitch light and tonic fibers.

4.3.6 Hill Coefficients

The Hill coefficients obtained for each group of fibers are presented in Figure 4.12. The Hill coefficient, n_2, for tonic fibers is significantly lower (P = 0.005) than for twitch light fibers. There was no significant difference between n_1 values for tonic and twitch light fibers. There was a significant difference (P = 0.02) between the n_1 and n_2 values for twitch light fibers, however, this was not the case with tonic fibers. There was no significant difference between n_2 values of twitch dark and twitch light fibers. Data for twitch dark fibers were obtained using only pCa Batch One and are presented separately to the data obtained using Batch Two. A Hill coefficient for twitch dark and twitch light fibers at high [Ca^{2+}] was not obtained from the first pCa batch due to a lack of activations in this range.

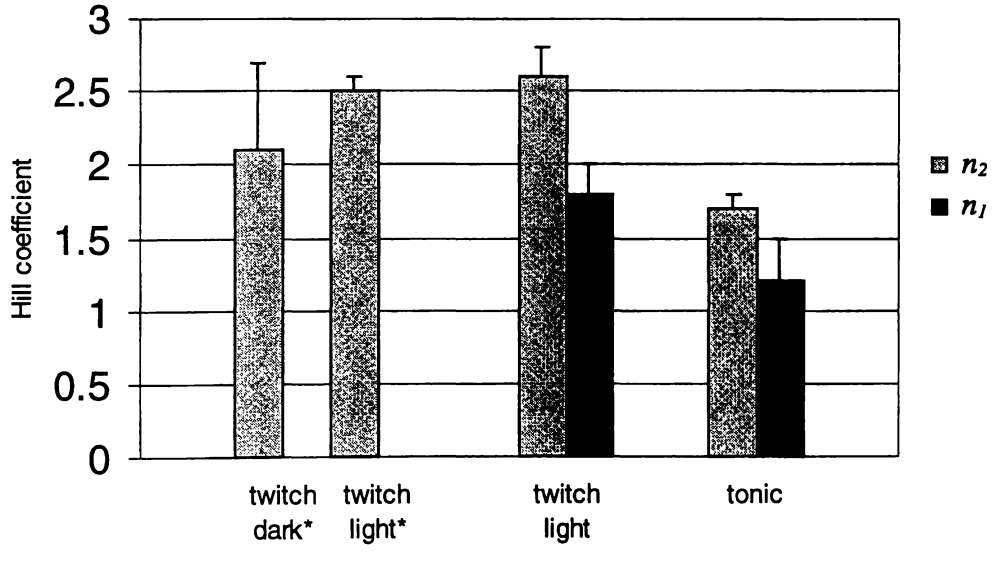

Figure 4.12: Hill coefficients, n_1 and n_2, obtained for EOM fiber types. Results from two pCa batches are shown: *Batch One: twitch dark (n = 4) and twitch light (n = 20) fibers; Batch Two: twitch light (n = 8) and tonic (n = 6) fibers. Values are means ± SE.

Hill coefficients were also obtained by pooling force-pCa data within each group of fibers. For each pCa, P_r values from fibers were averaged and these data used to obtain Hill plots. (The resulting force-pCa curves are presented in Figure 4.9). The values obtained by this method were not significantly different to those obtained by averaging *n* values from individual fibers. Table 4.2 compares the values obtained using each method.

Table 4.2. : Comparison of Hill coefficients obtained by 1) calculating *n* value(s) for individual fibers and taking the mean for that fiber group, and 2) combining force-pCa data for each fiber group, obtaining Hill plots and then calculating the Hill coefficient(s). Data are from two batches of pCa solutions. The number of fibers is given in parenthesis.

	n_1		n_2	
	1) mean ± SE	2) From pCa curve	1) mean ± SE	2) From pCa curve
Twitch dark				
Batch One	-	-	2.1 ± 0.6 (4)	2.2 (5)
Twitch light				
Batch One	-	-	2.5 ± 0.1 (20)	2.8 (20)
Batch Two	1.8 ± 0.2 (10)	1.6 (10)	2.6 ± 0.2 (8)	2.90 (10)
Tonic				
Batch Two	1.2 ± 0.3 (5)	1.4 (7)	1.7 ± 0.1 (6)	1.8 (7)

4.3.7 Sensitivity to Ca^{2+}: pCa_{50}

The pCa_{50} values obtained for twitch light fibers using different pCa batches were significantly different (P = 0.01). However, within a pCa batch, the pCa_{50} values did not differ between fiber groups. The pCa_{50} values obtained for twitch dark and twitch light fibers using pCa Batch One did not significantly differ, and nor did those of twitch light and tonic fibers obtained using pCa Batch Two (Figure 4.13).

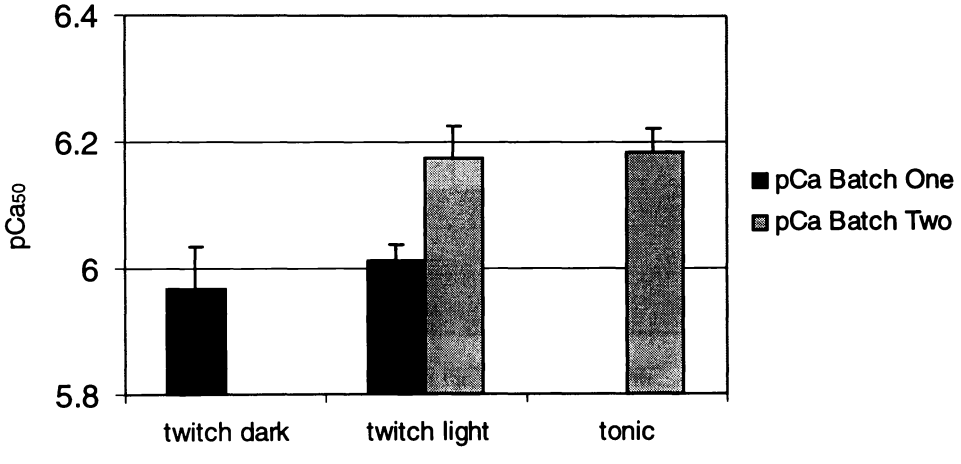

Figure 4.13: pCa_{50} values for twitch dark (n = 4), twitch light (n = 10, 20) and tonic (n = 7) fibers. Results from two pCa batches are shown. Values are means ± SE.

4.3.8 Ca^{2+} Threshold for Activation: pCa_{10}

There was no significant difference in pCa_{10} values between pCa batches for twitch light fibers. Tonic fibers had a significantly higher (P = 0.002) pCa_{10} value (lower calcium concentration) than twitch light fibers (Figure 4.14). pCa_{10} values for twitch dark and twitch light fibers did not differ significantly.

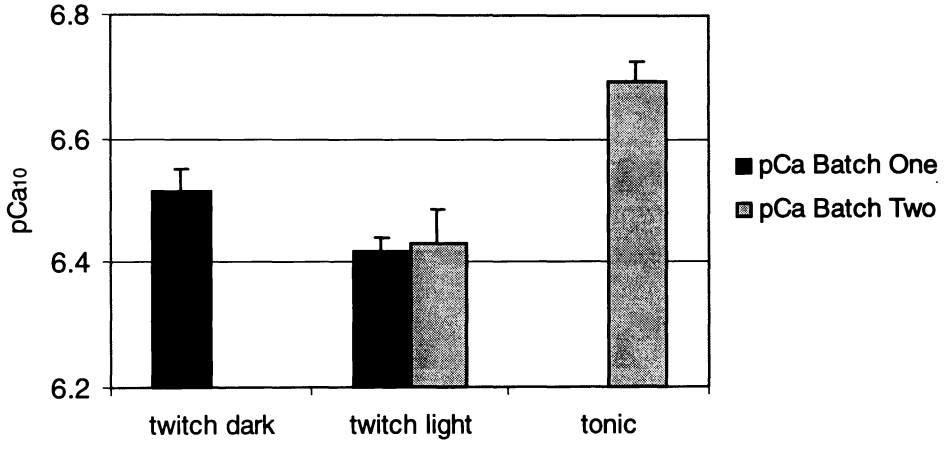

Figure 4.14: pCa_{10} values for twitch dark (n = 4), twitch light (n = 20, 8) and tonic (n = 7) fibers. Results from two pCa batches are shown. Values are means ± SE.

A summary of the contractile properties for each fiber group is presented in Table 4.3.

Table 4.3: Summary of tension-pCa relations for tonic, twitch light and twitch dark fiber populations of EOM. Values are means ± SE. The number of fibers is given in parenthesis. For n_1, n_2, pCa_{50} and pCa_{10} values, *italicised numbers* indicate data obtained using pCa Batch One, non-italicised numbers indicate data obtained using pCa Batch Two.

	n_1	n_2	pCa_{50}	pCa_{10}	Po(μN)	Po(kN/m^2)	time to 90% maximum. tension (s)
Twitch dark	—	*2.1 ±0.6* *(4)*	*5.97 ± 0.07* *(4)*	*6.52 ±0.03* *(4)*	129.2 ± 7.5[a,b] (6)	60.0 ± 2.4[a,b] (6)	8.0 ± 3.3[a] (6)
Twitch light	– 1.8 ± 0.2 (10)	*2.5 ±0.1* *(20)* 2.6 ± 0.2[a] (8)	*6.01 ±0.03* *(20)* 6.18 ± 0.05 (10)	*6.42 ±.02* *(20)* 6.43 ± .06[a] (8)	598.9 ± 42.8[a] (50)	140.2 ± 9.2[a] (50)	9.1 ± 9.6[a] (10)
Tonic	1.2 ± 0.3 (5)	1.7 ± 0.1 (6)	6.18 ± 0.04 (7)	6.69 ± 0.03 (7)	179.9 ± 16.5 (10)	97.5 ± 6.3 (10)	29.5 ± 8.7 (10)

[a] significantly different from tonic fiber
[b] significantly different from twitch light fiber

4.4 Discussion

4.4.1 Appearance

Under the light microscope fibers could be identified by their appearance as dark and clear. The ultrastructure of dark fibers in longitudinal and transverse section was consistently that of twitch fibers (see Chapter 2). These fibers were also easily distinguishable by their small diameter and are most probably the dark-SIFs of global EOM. The fibers identified as clear did not belong to a single fiber population judging by the inconsistent ultrastructural results. Five of the seven fibers identified as clear had twitch fiber morphology. They also had a relatively large myofibrillar diameter suggesting that they are more analogous to the pale-SIFs of mammalian EOM rather than the intermediate-SIFs. The other two fibers had a morphology consistent with that of tonic fibers. Thus the appearances of MIFs and pale-SIFs are easily confused and although all tonic fibers are likely to appear as clear, it seems that not all clear fibers are tonic fibers.

Single fiber TEM showed that the dark appearance of fibers was due to large accumulations of lipid. Although whole muscle TEM revealed fibers with high mitochondrial content and lipid droplets, the lipid was never as abundant as in the single fibers prepared for TEM. Therefore, the skinning procedure is assumed to be responsible for this increase.

Chemical skinning is known to cause several changes in extra-myofibrillar components of muscle fibers. For example, Eastwood *et al.* (1979) showed that

after 30 min in a skinning solution (170 mM Mg, 2.5 mM ATP, 5 mM EGTA, 170 mM potassium propionate, 10 mM imidazole, pH 7.0), the mitochondria of single rabbit psoas fibers were swollen compared to control fibers. Thus it appears that even skinning solutions without glycerol and a detergent can affect fiber organelles. Additional skinning chemicals such as glycerol make the sarcolemma leaky (Eastwood *et al.* 1979) by disrupting the membrane components (SR, T-tubule system and mitochondria) through a combination of solubilization and osmotic shock (Bagshaw 1994). This technique is usually combined with the use of non-ionic detergents such as Brij-35 and –85 that largely destroy the SR and other membranous compartments (Julian 1971, Moss *et al.* 1976, Stephenson & Williams 1983).

The fibers in this study were chemically skinned using aqueous glycerol (50% v/v) and the detergent Brij-35 (0.5% w/v). It is possible that, as a result of the skinning procedure, the membranes of the mitochondria in twitch dark fibers were disrupted and the amphipathic molecules of the lipid bilayer reorganized in such as way as to form the large lipid accumulations observed under TEM. Due to the substantial numbers of mitochondria in twitch dark fibers, large aggregates of lipid were formed. The large size of these aggregates may have prevented them from leaching out of the fiber despite the leaky sarcolemma, thereby trapping them between the myofibrils.

4.4.2 Maximum Force Responses and Decline in Maximum Force

Tonic fibers were distinguished, in the first instance, from twitch fibers by their slow development of force in response to maximal Ca^{2+}-activation. This could be due to differences in the rate of cross-bridge cycling between fiber types. The myosin heads of tonic fibers could associate and dissociate from actin at a slower rate than those of the twitch fibers. This would most likely be due to different isoforms of myosin proteins.

The maintenance of maximum force by single fiber preparations is due to steady-state cross-bridge cycling. Single fibers from other muscles (e.g. semitendinosis, iliofibularis) generally maintain a maximum tension until placed in relax solution (Donaldson & Kerrick 1975, Moisescu & Thieleczek 1979). The rapid decline in maximum tension seen in twitch fibers in this study is most likely due to a lack of structural integrity in these fibers. Although not as obvious, damage to tonic fibers is also likely to have occurred judging by the significant positive correlation between decline in maximum tension and pCa index. Indeed, repeated activations (nine to thirteen) of all fiber types would often cause myofilaments to break and as a result, 'bunching' of the fibers at one end would occur.

Instability of the permeabilized single fiber preparation is a recognized drawback of this technique and several methods have been used to minimize it. These include activating for as brief a period as possible, using submaximal Ca^{2+}-activation levels and cycling the fiber between states of isometric force development and isovelocity shortenings at near maximal velocity (V_{max}) (Sweeney *et al.* 1987). While the first

method could be used with the twitch fibers which reached maximum force rapidly, it could not be used to advantage with the tonic fibers as they were slow to reach maximum force. The second method could not be used as it was necessary to measure maximum Ca^{2+}-activation in order to calculate relative force values. The third method uses a computerized fiber mechanics system that was not available to this study. However, steps were taken to maximize fiber performance. For example, experiments were carried out at 10 °C rather than higher temperatures. This reduces fiber deterioration since an increase in fiber force has been observed at higher temperatures (Kasuga & Umazume 1990, Stienen *et al.* 1996). In addition, fibers were used the day following skinning. Although glycerol acts as an antifreeze enabling the muscle to be stored at –20 °C, storage for more than a month may lead to loss of function. It has been found that small soluble proteins such as troponin subunits can leach out of skinned preparations after one to three months in storage (Nakayama *et al.* 1983). The results of my study suggest that in future studies using permeabilized single tonic fibers, the number and level of Ca^{2+}-activations should be kept to a minimum in order to preserve the structural integrity of the fiber.

4.4.3 Maximum Normalized Tension

Both the twitch dark and tonic fibers had relatively low maximum normalized tension values when compared to the twitch light fibers of EOM. Twitch light fibers appeared to produce maximum normalized tension values comparable to, or greater than, that of twitch fibers in frog limb muscle (Julian 1971, Martyn *et al.* 1993). With regard to whole muscle, Luff (1981) found that inferior rectus

muscles of the mouse had a much lower normalized maximum force than limb skeletal muscles such as extensor digitorum longus and soleus. He could not explain this "anomaly" and suggested that it was due to damaged and non-contracting fibers. This occurred in spite of taking great care to remove damaged fibers prior to the experiment and carefully examining the preparation after the experiment. An alternative explanation may be that the tonic and twitch dark fibers are responsible for the lower maximum normalized tension of EOM compared to limb muscles. In this study, the tonic fiber population was found to comprise about 19% of the inferior rectus muscle in global EOM of *Bufo marinus.* If the percentage of twitch dark fibers (i.e. dark-SIFs) in global EOM of *Bufo marinus* is similar to that found in mammalian muscle, they could comprise 33% of the global layer. Thus, together these two fiber populations could constitute about 50% of global EOM and account for the observations of Luff (1981) and Frueh *et al.* (1994). Frueh *et al.* (1994) found maximum normalized tension values for rabbit superior rectus to be approximately one third of the values of Luff (1981).

Although the mean diameter of twitch dark fibers was similar to that of the tonics (51.8 ± 1.5 μm and 48.0 ± 2.4 μm, respectively), the mean maximum normalized tension is significantly lower for the twitch dark fibers than the tonic fibers. This is probably due to the higher quantities of mitochondria, lipid and SR (i.e. comparatively less contractile machinery).

Maximum normalized tension values obtained in this study are similar to those obtained by the other two investigators who have worked with single EOM fibers. Lynch *et al.* (1994) and Campbell (1997) corrected their maximum normalized

tension values for the swelling effect of skinning on the fiber (up to 30% by area). Lynch *et al.* (1994) found the maximum force of single fibers from the rabbit superior rectus ranged from 120 to 220 kN/m ^{2}. Campbell (1997) found population II fibers (analogous to fast-twitch fibers) of the inferior rectus to have maximum force of 162.2 kN/m ^{2}. When corrected for swelling by 30%, the mean maximum normalized tension for twitch light (fast-twitch) fibers found in this study was 200 ± 12 kN/m^2. It is more difficult to compare the maximum normalized tension of tonic fibers in EOM with that of tonic fibers in limb skeletal muscle as, to the author's knowledge, information on the latter in *Bufo marinus* is not readily available. Martyn *et al.* (1993) studied force-pCa responses of both *Rana pipiens* and *Bufo marinus* but reported only the values obtained for *Rana pipiens.* However, if the values obtained from permeabilized fibers for these amphibia are assumed similar, then the maximum normalized tension of tonic fibers in EOM appears similar to tonic fibers of limb muscle. Martyn *et al.* (1993) found skinned tonic fibers from the cruralis muscle of *Rana pipiens* to have a mean maximum normalized tension of 89 kN/m^2 under conditions of: [EDTA]= 9 mM, IS = 120, pH = 7, sarcomere length = 2.4 μm. In this study tonic fibers from EOM had a maximum normalized tension of 97.5 ± 6.3 kN/m^2 ([EDTA] = 10 mM, IS = 150 mM, pH 7.1, sarcomere length = 2.2 - 2.4 μm).

4.4.4 Force pCa-Relationships

The twitch light fibers showed a force-pCa relationship similar to that seen in other skeletal muscles with the curve being steeper at low than at high [Ca^{2+}]. The steepness of the curve at low [Ca^{2+}] has generally been interpreted as the presence

of a high degree of cooperativity within and between the thick and thin filaments and between Ca^{2+} binding to the thin filament. These cooperative mechanisms allow a full transition between rest and activity within a relatively small change in free calcium ion concentrations. Fast-twitch fibers generally have steeper force-pCa relationships than slow-twitch fibers (Stephenson & Forrest 1980). Studies comparing the force-pCa response of slow-tonic and twitch fibers in limb skeletal muscle have obtained results similar to those presented here. For example, Reiser *et al.* (1996) found that the fiber population from the chicken pectoralis red strip muscle, which had the same force-pCa response as slow-tonic fibers from the anterior latissimus dorsi muscle, had a lower n_2 value than fast fibers from the same muscle. Similarly, the Hill coefficients obtained from tonic fibers of the frog cruralis were lower than those of twitch fibers of the same muscle, at each condition studied (Martyn *et al.* 1993). The reason for these observations may be due to different Ca^{2+} binding properties mediated by fiber-type specific isoforms of thin filament regulatory proteins. However, when Moss *et al.* (1991) substituted slow TnC into skinned psoas fibers containing endogenous fast TnC, the steepness of the tension-pCa relationship was unaltered. This suggested that TnC isoforms were not involved but it does not eliminate the possibility that the steepness of the relationship is related to the other subunits of troponin, TnI or TnT. Another possibility is that the fiber types differ in their response to the strong binding of myosin cross-bridges, however, more research is necessary in this area. The use of NEM-S1, a strong-binding derivative of myosin S1 that does not bear tension or hydrolyze ATP, may prove to be a valuable tool in resolving this issue.

The finding that the population of fibers classified as tonic had a significantly lower threshold of activation (pCa_{10}) than the twitch fibers is in keeping with the results of others. Reiser *et al.* (1996) found the threshold (pCa_{th}) of fast (twitch) fibers from the chicken pectoralis major muscle to be 6.4 while for the slow (tonic) fibers it was 7.0. (They estimated threshold pCa values by inspection of the tension-pCa curves.) Although not reported, similar results were obtained by Martyn *et al.* (1993) working with twitch and slow-tonic muscle fibers of the frog cruralis. Regardless of ionic strength, sarcomere length and pH, inspection of their tension-pCa curves show the tonic fibers to have a lower threshold of activation.

It is difficult to compare the force-pCa findings of this study with those of Lynch *et al.* (1994) and Campbell (1997) because they sampled fibers from the whole muscle, not just the global region. The fact that they were dealing with fibers with diameters as low as 12.5 μm suggests that orbital fibers were among those sampled as very few global fibers occur at that diameter. The population of fibers that Lynch *et al.* (1994) found to show 'mixed' properties is likely to be the orbital-MIFs as these fibers show morphological (Pachter 1982), histochemical (Pachter 1984), electrical (Jacoby *et al.* 1989a) and myosin (Jacoby *et al.* 1989b) variation along their length. However, it is possible that the fibers they grouped as population I (slow-twitch) are the same as the fibers identified in this study as tonic. The Hill coefficient, n_{Ca}, they found for this population (1.6) was lower than those found in the other fiber populations (range of 2.12 to 3.7). In addition, the threshold of activation for the population I fibers was lower (pCa 6.41) than for the population II, III and IV (*cf* pCa 6.15, 6.25, 6.10, respectively) fibers. Lynch *et al.* (1994) acknowledged the possibility that the population I fibers could be tonic

fibers by concluding that either tonic fibers have contractile activation characteristics similar to those of other slow-twitch fibers from mammalian skeletal muscle, or that EOM contain a small proportion of classical slow-twitch fibers.

4.4.5 Problems Encountered

There were a number of problems encountered in this work due to the nature of EOM tissue. Firstly, the muscle has a high content of connective tissue (Asmussen & Gaunitz 1981; Campbell 1997) which had to be thoroughly dissected away in order for the skinning and glycerinating solutions to penetrate enough to allow the fibers to be teased uninjured from the muscle. Secondly, the small size of the muscle fibers made them extremely difficult to handle at times. For example, it was found that glycerinated fibers of approximately 40 μm or less would break on transfer to the fixing trough. This breakage was caused by the surface tension created between the fiber and the portable apparatus on which it was mounted. Taking into account the swelling known to occur in glycerinated single fibers, no fibers less than approximately 36 μm could be used in experiments. This made it difficult to obtain measurements on the tonic fibers which were found to occur most frequently at diameters between 30 to 40 μm (Refer to Figure 3.4, Chapter 3). Fortunately, approximately 22% of the tonic fiber population occur in the diameter range of 40 – 50 μm and it was fibers in this range that were most commonly teased out and used for experiments (i.e. mean diameter of glycerinated tonic fibers used was 48 ± 2.4 μm, or about 43 μm prior to glycerination). In addition, the twitch dark fibers appeared even more susceptible to breakage

although this population had a mean diameter similar to the tonic fibers (51.8 ± 1.5 μm). This was possibly due to the lower content of myofibrillar protein that may act to give the fiber strength. Since the twitch dark fibers occurred within a narrower diameter range than the other two fiber populations, it was difficult to obtain many twitch dark fibers for measurements.

4.4.6 Summary

In this study, the Ca^{2+}-activation response of single EOM fibers was investigated. Although fiber appearance proved to be of limited value in differentiating tonic fibers, the force response to maximally activating [Ca^{2+}] allowed these fibers to be identified from the twitch fibers. Tonic fibers developed force slowly and reached low force levels. Twitch fibers rapidly responded to maximally activating [Ca^{2+}]. Fiber appearance, diameter and maximum force levels all proved useful in distinguishing two groups of twitch fiber, that is the twitch dark from the twitch light fibers. Significant differences in the force-pCa relationship between tonic and twitch fibers were seen at low [Ca^{2+}]. Thus, the tonic fibers had a markedly lower n_2 Hill coefficient than the twitch light fibers. However, sensitivity to calcium (i.e. pCa_{50} values) did not differ between fiber groups.

It is perhaps not surprising to find fibers so different in their contractile properties to one another within a muscle of such diverse capabilities. Since expression of different myofibrillar protein isoforms is a major determinant of contractile properties, comparison of the myosin isoforms of the fibers for which Ca^{2+}-activation characteristics were known might confirm their grouping. The following

chapter presents the MLC profiles of single fibers and confirms the grouping of fibers in this chapter.

CHAPTER 5: MYOSIN LIGHT CHAIN PROFILES OF SINGLE FIBERS FROM GLOBAL EOM

5.1 Introduction

Myosin makes up 43% by weight of myofibrillar proteins and consists of two heavy chains (MHC) (MW 200 kDa each) and four light chains (MLC) (approximately 20 kDa each) (Lowey & Risby 1971). The two heavy chains intertwine to form the rod portion of the myosin molecule. The two heads are formed at one end by the coiling of each myosin chain. Digestion of this protein with chymotrypsin yields the head region, termed S1, and the tail, termed S2. Each myosin head contains a regulatory light chain (MLC2) and an essential (alkali) light chain (either MLC1 or MLC3). The light chains are associated with the neck region of S1, with the regulatory light chain further towards the tail region than the essential light chain (Rayment *et al.* 1993). This location has prompted suggestions that the light chains impart mechanical rigidity to the neck region of the myosin head (Rayment *et al.* 1993). Hofmann *et al.* (1990) showed that MLC2 reversibly altered the Ca^{2+} sensitivities of tension generation, fiber stiffness, and maximum velocity of shortening, leading them to conclude that this light chain may modulate contraction via an influence on the conformation of the S1-S2 hinge region. Consistent with this conclusion are results of studies showing that the orientation of regulatory light chains in skinned muscle fibers changes depending on whether the fiber is in a relaxed, rigor or active state (Allen *et al.* 1996, Ling *et al.* 1996). Furthermore, three types of motion of the myosin

heads have been identified in working muscle fibers, all involving the tilting of the myosin heads with respect to the fiber axis (Irving & Piazzesi 1997)

The proteins that make up the myofibril can be studied using electrophoretic techniques under denaturing conditions (see Barany *et al.* 1995 for review). Polyacrylamide gel electrophoresis in the presence of sodium dodecyl sulphate (SDS) is the method most routinely used. SDS binds to the denatured polypeptide chains thereby giving them a similar negative charge per unit length. The polypeptides are 'pulled' by their electrical charge through the acrylamide matrix toward the anode. The extent to which the polypeptides travel is dictated by the amount of cross-linking of the matrix and the concentration of acrylamide.

As with many of the myofibrillar proteins, myosin exists in multiple isoforms (see Pette & Staron 1990 for review). These isoforms vary in their amino acid sequence and can occur not only within the same organism but also within the same muscle fiber. The speed of contraction of a muscle is correlated with the presence of specific isoforms of most of the myofibrillar contractile proteins. This is especially true for the myosin heavy chains (MHCs) which have been studied extensively in adult mammalian skeletal muscle (Reiser *et al.* 1985; Pette & Staron 1990). MHC expression in EOM has been studied in developing (Brueckner *et al.* 1996, Brueckner & Porter 1998) and adult (Wieczorek *et al.* 1985, Sartore *et al.* 1987, Jacoby *et al.* 1989b, Rushbrook *et al.* 1994) mammals. Among the findings of these studies were: that some developmental isoforms are retained into adulthood, that an EOM-specific MHC is expressed in addition to

the α-cardiac MHC isoform, and that there is heterogeneous protein expression along the length of individual fibers.

Different isoforms of MLCs also occur between and within muscle fibers (Schachat *et al.* 1980, Lowey 1994). Mammalian muscles that primarily contain fast-twitch fibers, such as psoas and extensor digitorum longus, are known to have three MLCs of molecular weight 25, 18 and 16 (± 5%) kD. The nomenclature most often used to identify these proteins is MLC1f, MLC2f and MLC3f, respectively. They occur in a stoichiometric ratio of approximately 1:2:1 (Lowey & Risby 1971). Fast-twitch muscles from Amphibia, Avia and mammals all show this pattern.

Muscles known to be primarily slow-twitch in nature are more variable across species. Many slow-twitch muscles have two myosin light chains of approximately 27 and 20 kD, with the low molecular weight isoform of the essential light chain, MLC3, absent (Pate *et al.* 1992). In the case of the soleus muscles from rat, rabbit, cat and guinea pig, MLC3 is lacking but the MLC1 band can be resolved into two components, both of reduced mobility when compared to MLC1f (see Lowey 1994 for review). These two bands are referred to as MLC1s and MLC2s or MLC1's and MLC1s. In Amphibia, some slow-twitch fibers also lack the low molecular weight isoform of the essential light chain, MLC3 (Lannergren 1987). Using denaturing and non-denaturing gel electrophoresis, Lannergren (1987) examined the myosin heavy and light chains of individual fibers from *Xenopus laevis* for which isotonic contractile properties had been examined. He showed that the division of amphibian muscle fibers into fast-

twitch, slow-twitch and slow-tonic categories was perhaps an over-simplification. Although fiber 'types' 1, 2, 3 and 4 (fast-twitch, slow-twitch, slow-twitch intermediate and slow-tonic) do exist, so do transitional forms both with respect to mechanical performance and myosin composition.

The myosin light chains of slow-tonic fibers of avian muscle (e.g. anterior latissumus dorsi) resolve into two bands of reduced mobility. These MLCs have molecular weights of approximately 27 and 20 kD and are termed MLC1s and MLC2s, respectively. Slow-tonic fibers of amphibian limb muscle contain MLC1 and MLC2 but lack MLC3 (Focant & Reznic 1980, Pliszka & Strzelecka-Golaszewska 1981). Pliszka and Strzelecka-Golaszewska (1981) found that myosin light chains from the frog sartorius (fast-twitch muscle) had the same electrophoretic mobilities as myosin from the cruralis muscle which is composed of 50% slow-tonic fibers. They attributed the small amount of MLC3 present in preparations from the cruralis bundle to the fast fibers that also comprise this muscle. Therefore, the slow-tonic fibers of amphibia appeared to contain isoforms with electrophoretic mobilities equal to MLC1f and MLC2f. Focant and Reznic (1980) also found that MLC1 of slow-tonic muscle had the same electrophoretic mobility as MLC1 from fast muscle. However, they observed that MLC2 from tonic fibers had a faster migration than MLC2 from fast fibers.

The myosin light chains have been correlated with contractile properties. Lowey *et al.* (1993) found that skeletal muscle light chains were essential for physiological speeds of shortening. They prepared MHCs that were free of both the regulatory and essential light chains and, using a motility assay, determined

whether these light chains were necessary for movement. They found that removal of these light chains from myosin reduced the velocity of actin filament movement ten-fold without significantly decreasing the ATPase activity. Although evidence as to whether the myosin light chains play a significant role in determining contractile properties of fibers is conflicting, it is generally accepted that light chain isoform content is an important determinant of V_{max} (Moss *et al.* 1982, Moss *et al.* 1995). Sweeney *et al.* (1988) used two types of permeabilized fast-twitch fibers from rabbit psoas and tibialis anterior muscle both with identical MHCs but different ratios of the alkali light chains. They were able to demonstrate that a difference in the velocity of unloaded shortening was correlated with a shift in the MLC1f : MLC3f ratio. Greaser *et al.* (1988) found that V_{max} increased with the relative MLC3 content of single adult rabbit plantaris muscle fibers grouped as having intermediate- and high-velocities. In another study, MLC3 was exchanged for MLC1 in chemically skinned single fibers from rat psoas muscles (Moss *et al.* 1990). These fibers exhibited an average increase in V_{max} of 42%. These investigators have suggested that the type of MHC(s) present in a fiber determines whether the V_{max} range will be slow or fast, but variation of V_{max} within the fast velocity range can be explained by the relative proportions of the different alkali light chains present.

There have been four studies reporting on the MLC content of EOM (Figure 5.1). These have used tissue derived from mammalian species and have used whole muscle or regions of EOM. Reichmann and Srihari (1983) performed two dimensional electrophoresis on myosin purified from rabbit EOMs and compared the results to those obtained from psoas (fast) and soleus (slow) limb muscle

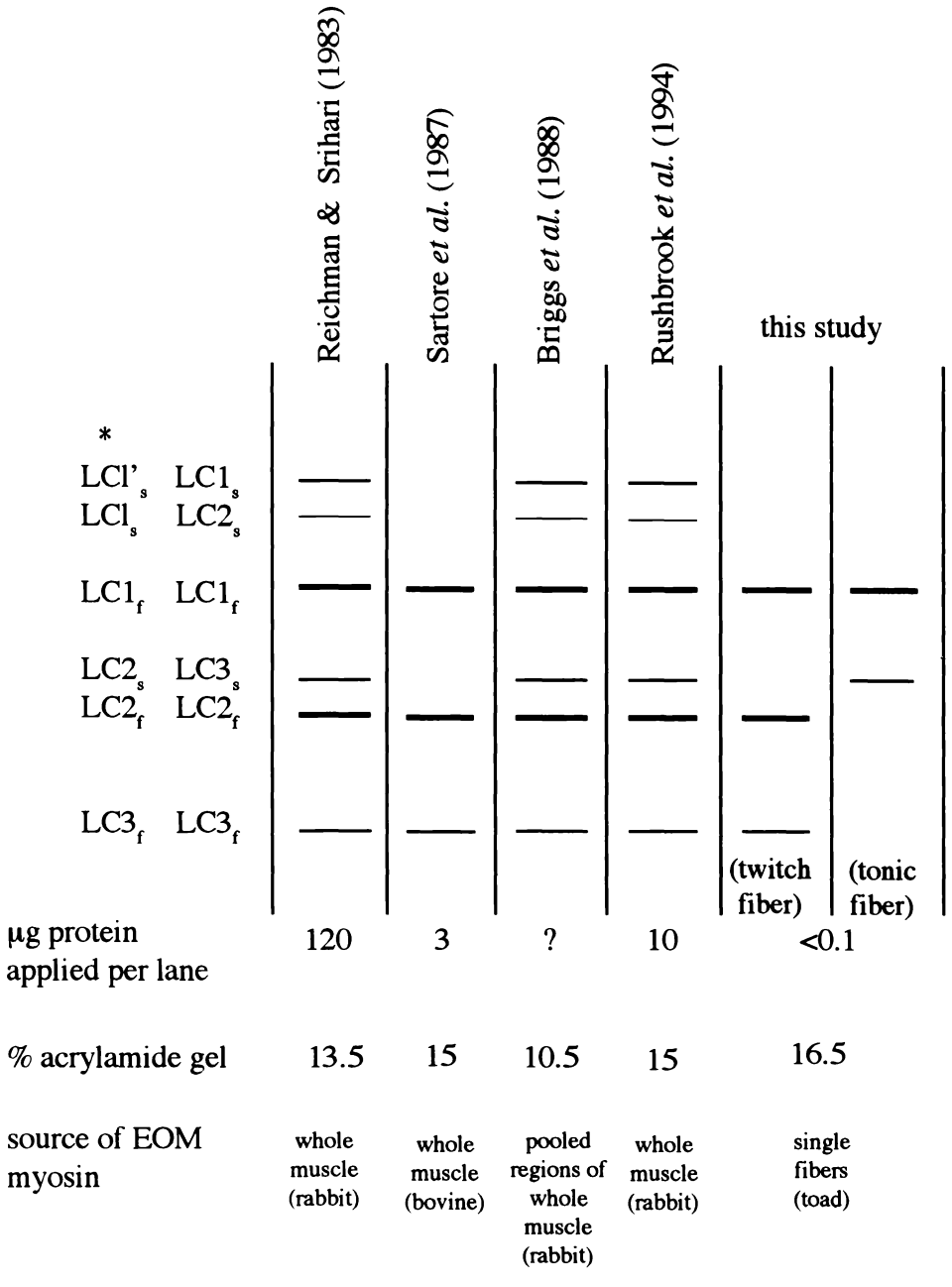

* Terminology of Reichman & Srihari (1983)

Figure 5.1: Schematic diagram showing MLC profiles of EOM as found in five studies, including the present study.

myosins. They found EOM contained MLCs of both slow and fast skeletal muscles, with the latter being predominant. They termed the six myosin light chains found in EOM LC1's, LC1s, LC1f, LC2s, LC2f and LC3f, in order of increasing electrophoretic mobility. The results of Briggs *et al.* (1988) are similar to those of Reichmann & Srihari (1983). They found both slow and fast myosin light chains in rabbit EOM with approximately 90% being the fast muscle isoforms. They used different terminology to Reichmann & Srihari (1983) and termed the six bands LC1s, LC2s, LC1f, LC3s, LC2f and LC3f. Similarly, Rushbrook *et al.* (1994) found fast and slow myosins in rabbit EOM and used the same terminology as Briggs *et al.* (1988) to identify them. In contrast to these three studies, Sartore *et al.* (1987) found only LC1f, LC2f and LC3f in bovine EOM using both one- and two-dimensional PAGE. When discussing the MLC bands of mammalian muscle the terminology of Reichmann & Srihari (1983) is most commonly used. This terminology will also be used in the present study to identify the light chain bands of myosin in *Bufo marinus* EOM fibers.

The studies of Reichmann & Srihari (1983), Sartore *et al.* (1987) and Rushbrook *et al.* (1994) all used myosin from whole EOM. Briggs *et al.* (1988) used myosins in different regions of the muscle that were known to contain high amounts of either twitch (SIFs) or tonic (MIFs) fibers. The thesis of Campbell (1997) contains work on SDS-PAGE of light chains from single EOM fibers of the rabbit superior rectus. However, no conclusions were made, possibly because no MLC3 band was observed in fibers that would be expected to have it. The single fiber segments from superior rectus muscles of the rabbit, all classified as Population II (fast-twitch) based on their contractile characteristics, showed two bands

corresponding to MLC1 and MLC2. Since MLC3 would be expected to be present in Population II fibers, it appears the staining method used was not sensitive enough.

The present study is the first to investigate the MLC content of amphibian EOM fibers and, to my knowledge, the first to observe the MLC content of single EOM fibers. The aim of this work was to determine the MLC profile of single EOM fibers for which force-pCa measurements had been obtained. In so doing, differences in the calcium activation response of fibers could be correlated with their MLC profile, thus confirming the fiber groupings of Chapter 4.

5.2 Materials and Methods

Unless stated otherwise, all chemicals were obtained from Sigma and milli-Q grade water was used to make up solutions.

5.2.1 Extraction and Purification of Myosin Light Chains

In order to confirm the identity of MLC bands on the gels of single fibers, myosin from *Bufo marinus* EOM was extracted, purified and resolved on SDS-PAGE. Myosin from rabbit psoas was prepared and used in the same manner to provide a standard for comparison of toad EOM myosin light chains.

A modification of the extraction methods of Crockford and Johnston (1995) and Ball and Johnston (1996) was used to purify myosin from *Bufo marinus* EOM and rabbit psoas. Two toads were euthanased (see Chapter 2, Section 2.2.1 for details) and the four inferior rectus muscles removed. The total wet weight of the four muscles was 0.0282 g. Approximately 1g of rabbit psoas muscle that had previously been frozen at –70 °C was similarly prepared.

The muscle samples were homogenized (at 0 - 4 °C) using a Polytron blender for 10 s in 20 volumes of the following isolation solution: 10 mM Tris-HCl, 100 mM NaCl, 5 mM EDTA, 0.5% Triton X-100, pH 7 at 20 °C. The homogenate was centrifuged at 1500 g for 5 min and the supernatant discarded. The pellet was homogenised again and resuspended in 20 volumes of ice-cold isolation buffer without the Triton X-100 and EDTA. After centrifugation, the final myofibril pellet was resuspended two more times in isolation buffer. Myosin was prepared from the myofibril pellet by extraction for 10 min (0 °C) in the following solution: 7.5 mM ATP, 675 mM KCl, 7.5 mM $MgCl_2$, 1 mM DTT, pH 6.4 at 4 °C. The crude myosin solution was centrifuged at 8500 g for 20 min and the supernatant mixed with 12 volumes of ice-cold water. Myosin was precipitated overnight at 5 °C. Crude myosin was collected by centrifuging at 12000 g for 15 min and the pellet resuspended in 1ml of 20 mM Tris, pH 8 (on ice).

FPLC (Pharmacia) was used to further purify the myosin light chains. One ml of MLC extract in 20 mM Tris/HCl, pH 8, was loaded onto a Mono-Q anion exchange column with a bed volume of 15 ml, equilibrated with 20 mM Tris-HCl, pH 8. Myosin was eluted using a linear gradient of NaCl (0 M to 1 M). Fractions

(0.5 ml) were collected and eluant from the column was monitored by absorbance at 280 nm. The program used on the FPLC is given in Appendix C. Samples were concentrated by freeze drying (rabbit psoas samples) or vacuum evaporation (toad EOM).

5.2.2 Preparation of Whole EOM Extract

A toad was euthanased (as outlined in Chapter 2, Section 2.2.1: Use and Care of Cane Toads) and the two inferior rectus muscles were dissected out and placed into 0.9% NaCl prior to being plunged into liquid nitrogen. With a mortar partially immersed in liquid nitrogen the muscles were ground to a find powder. The powder was suspended in 500 µl of sample buffer (4% SDS, 12% glycerol (w/v), 50 mM Tris, 2% mercaptoethanol (v/v), 0.01% Serva blue G, pH 6.8) and the solution heated for 4 min at 95 °C. The tubes were spun for 5 min on a bench top centrifuge (Beckman Microfuge E) and the supernatant removed and aliquoted into 20 and 50 µl lots and frozen at –70 °C.

5.2.3 SDS-PAGE of Single Fiber Proteins

After force-pCa measurements were obtained (as outlined in Chapter 4, Section 4.2.3.3: Experimental Protocol) the entire fiber was placed into 15 µl of sample buffer (see above) and frozen at –70 °C.

Gels of high polyacrylamide concentration were used for optimal resolution of the low molecular weight myosin proteins. The highly sensitive technique of silver

staining was used in order to detect proteins in amounts as low as 2 - 5 ng (Rabilloud 1992). Two SDS-PAGE methods were used, both of which were modifications of Laemmli (1970). Initially, the Tris-Tricine method of Schagger and von Jagow (1987) was used with the following solutions:

Sample buffer	4% SDS, 12% (w/v) glycerol, 50 mM Tris, 2% (v/v) mercaptoethanol, 0.01% Serva blue G, pH 6.8.
Gel buffer stock solution	1.5 M Tris, 0.15% SDS, pH 8.45
Anode buffer	0.2 M Tris, pH 8.9
Cathode buffer	0.1M Tris, 0.1M Tricine, 0.1% SDS, pH 8.25

Vertical SDS-discontinuous PAGE was carried out using a mini-protean II dual slab cell system (BioRad) on slab gels (100 mm x 72 mm x 0.75 mm). Both the separating and stacking gels (Table 5.1) were made using a 40% acrylamide:bis 29:1, 3.3% crosslinking solution (Bio-Rad). Fifteen ml of separating gel solution was prepared by degassing for 15 min before adding 100 µl of 10% ammonium persulfate and 10 µl N,N,N',N'-tetramethylethylene-diamine (TEMED). The fiber samples were heated at 100 °C for 4 min prior to gel application. Gels were run on a Bio Rad Model 1000/500 power supply for 1 to $1^1/_2$ h at 150V and room temperature, until the indicator dye migrated off the bottom of the gel.

Table 5.1 : Composition of stacking and separating gels.

	Stacking gel 4%T/3%C	Separating gel 16.5%T/3%C
40% acrylamide/ bisacrylamide solution	1.25 ml	6.7 ml
Gel buffer	6.25 ml	8.0 ml
Glycerol	-	1.5 ml = 2.16g
H_2O	5.00 ml	-
Final volume	12.50 ml	16.2 ml

%T = total acrylmide content (w/v)
%C = ratio of bisacrylamide to acrylamide monomer (w/w)

Subsequently, 4%T, 3.3%C stacking; 16.5%T, 3.3%C separating Tris-Tricine Ready Gels (100 mm x 80 mm x 1 mm) (BioRad) were used along with the sample and running buffers outlined in the BioRad Ready Gels Application Guide (Catalog Number 161-0993). These gels were run using the same power supply for 1 h 45 min at 100V and room temperature.

Both types of gels were silver stained using a modification of Rabilloud *et al.* (1988) and Nesterenko *et al.* (1994) as outlined in Table 5.2. Gels were stained on orbital shakers in glass dishes at room temperature. After the rinse step the gels were immersed in 5% glycerol for 1 – 2 h in order to prevent cracking upon drying. Gel images were captured and optimized using a COHU High Performance CCD camera and software package (*Scion Image*). The software package *GelCompar* was used to standardize gels and compile densitometric scans. The gels were dried under vacuum at 40 °C for 2 h using a Speed Gel (SG 210D, Savant) dryer.

Table 5.2: Silver staining procedure.

Step	Solution	Duration
1) Fix	30% EtOH, 10% AcOH	20 – 30 min
2) Rinse	30% EtOH	3 x 15 min
3) Rinse	H_2O	1 x 5 min
4) Sensitize	100 µl $Na_2S_2O_3.5H_2O$ stock [a] in 60 ml H_2O	1 min
5) Rinse	H_2O	1 x 5 min
6) Impregnate	1 ml $AgNO_3$ stock [b], 100 µl HCOH in 100 ml H_2O (per gel)	30 min
7) Rinse	H_2O	1 min
8) Develop	3 g Na_2CO_3 100 µl HCOH 40 µl $Na_2S_2O_3.5H_2O$ made fresh in 100 ml H_2O (enough for 2 gels)	by sight (approx. 20 – 25 min)
9) Stop	2.5 ml of 2.3 M citric acid added directly to 50 ml developing solution	10 min
10) Rinse	H_2O	2 x 10 min

Abbreviations: AcOH: acetic acid, EtOH: ethanol, HCOH: 37% formaldehyde, $Na_2S_2O_3.5H_2O$: sodium thiosulfate pentahydrate.

[a] $Na_2S_2O_3.5H_2O$ stock = 10% in H_2O

[b] $AgNO_3$ stock = 20% in H_2O

Standards

Purified proteins (Sigma) with a range of known molecular weights were used as standards (Table 5.3).

Table 5.3: Standards that were routinely used in the gels.

Protein	MW(kDa)	Concentration used (μg/ml)
Lysozyme	14.2	0.4
Myoglobin	17.8	0.4
Trypsinogen	24	5.0
Whole Troponin[+]	18-19 (C), 25* (I)	5.0
Carbonic Anhydrase	29	4.0
Bovine Serum Albumin (BSA)	66	2.0

[+]Only TnI and TnC were apparent in the Sigma preparation.
*Apparent molecular weight of Troponin I under the electrophoretic conditions used.

The myosin light chains of individual EOM fibers were identified by 1) their migration in relation to the protein standards, 2) their co-migration with purified light chains of rabbit psoas muscle and 3) by co-migration with purified light chains of *Bufo marinus* EOM. Troponins C and I were identified on the basis of their co-migration with subunits of the troponin standard (from rabbit muscle) and their expected migration pattern (Greaser & Gergely 1971). Troponin I was not observed in gels of single fibers as it co-migrated with MLC1.

5.3 Results

Myosin extraction and subsequent purification using anion-exchange chromatography yielded EOM myosin light chains that eluted at 0.6 to 0.7 M NaCl (Figure 5.2). This main peak resolved into three bands on SDS-PAGE with the middle band appearing as a doublet (Figure 5.3, lane b). These bands had the same mobility as the bands purified from rabbit psoas myosin (Figure 5.3, lane a). This procedure clearly isolated myosin light chains from other myofibrillar proteins (compare lanes b and c).

From SDS-PAGE of single EOM fibers, two groups of fibers could be differentiated on the basis of their MLC profiles. One group showed three MLC bands (MLC1, MLC2 and MLC3) and these correlated to fibers that gave a fast response to maximal activation (see Chapter 4) and are assumed to be twitch fibers (Figure 5.3, lanes f, g and i). Another group of fibers showed only two MLC bands (MLC1 and MLC2) with no detectable MLC3 band (Figure 5.3, lane h). These fibers corresponded to those giving a slow rise to peak tension and are assumed to be tonic fibers.

MLC1 bands of single tonic and twitch fibers had similar mobility, however, MLC2 of tonic fibers tended to run more slowly than MLC2 of twitch fibers (Figure 5.3, lane h and Figure 5.4).

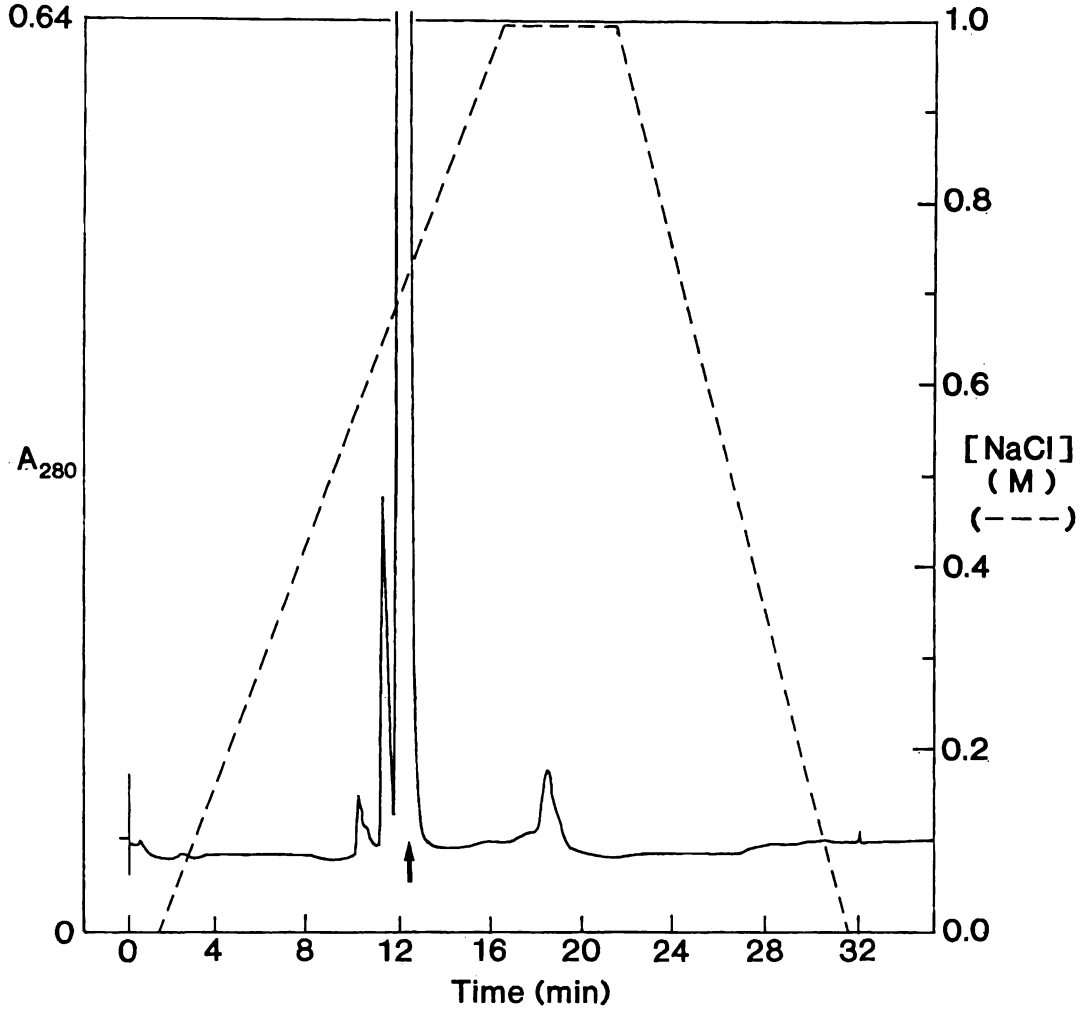

Figure 5.2. Purification of low molecular weight components of toad EOM myosin by anion exchange chromatography on a Mono-Q column. The arrow indicates the fraction that gave rise to the protein bands on gel strip (b) of Figure 5.3.

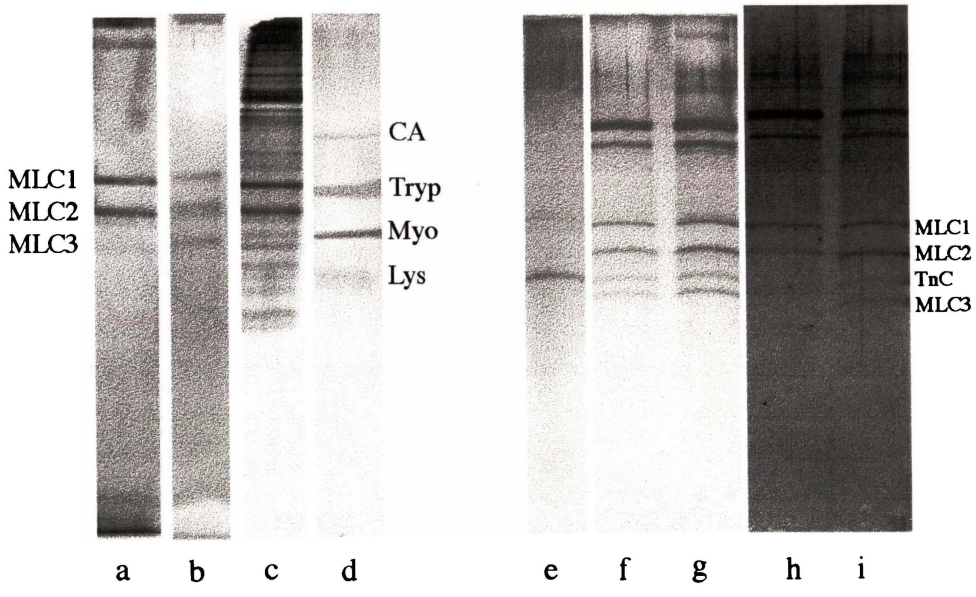

Figure 5.3: SDS-PAGE of (a) purified myosin light chains from rabbit psoas, (b) myosin light chains from toad EOM, (c) toad whole EOM extract, (d) standards, (e) troponin standard, (f) twitch dark fiber, (g) twitch light fiber, (h) tonic fiber and (i) twitch light fiber. CA = carbonic anhydrase, Tryp = trypsinogen, Myo = myoglobin, Lys = lysozyme.

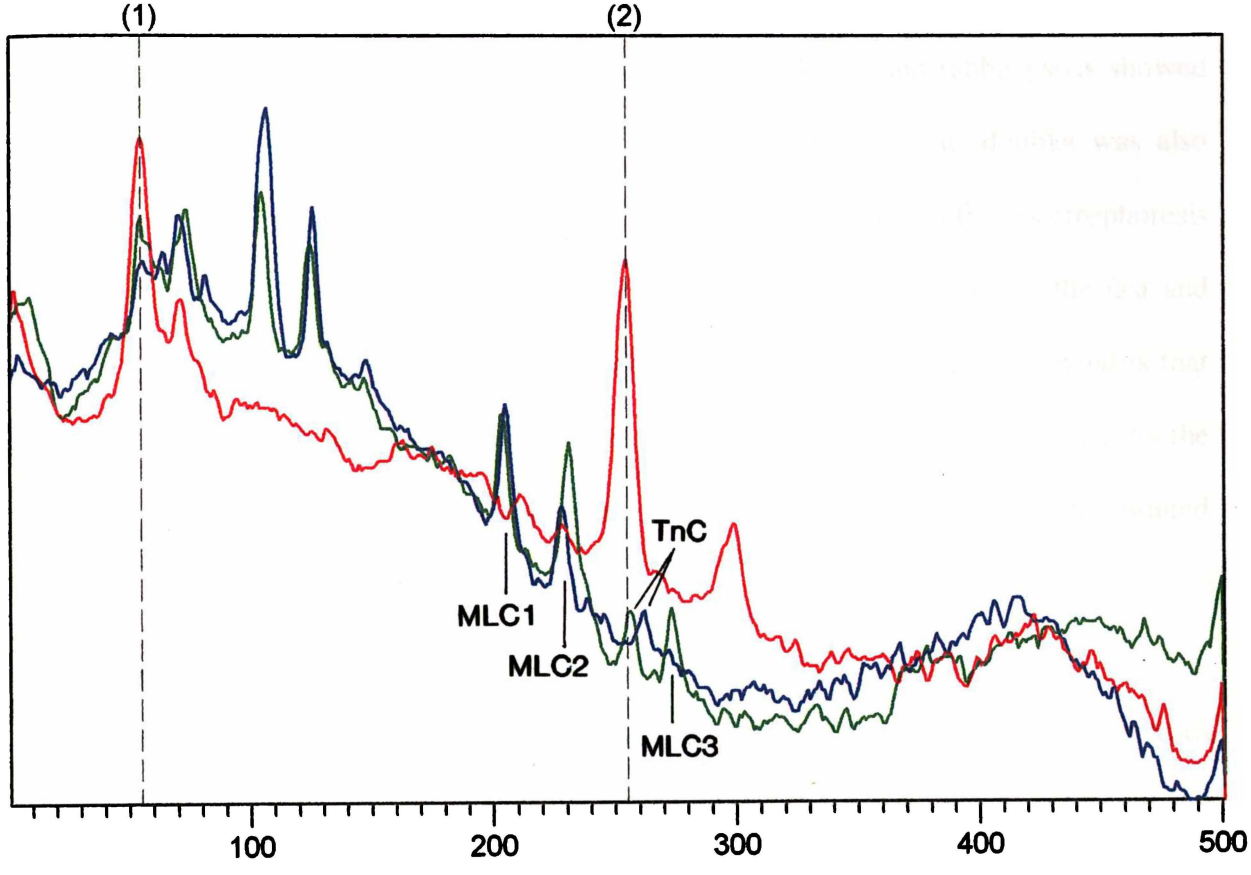

Figure 5.4. Representative densitometric scan of gel obtained from a toad EOM tonic fiber (blue line) and a twitch light fiber (green line). The peaks marked (1) and (2) correspond to BSA and myoglobin standards (red line), respectively.

5.4 Discussion

The myosin light chains purified from both toad EOM and rabbit psoas showed three major bands with MLC2 appearing as a doublet. This doublet was also observed in the MLC profiles of single EOM (twitch) fibers in two electrophoresis runs. Therefore, these bands cannot be attributed to the presence of the fast and slow MLC2 isoforms. The most likely explanation for the additional band is that a portion of the fiber proteins were not completely reduced giving rise to the additional band (Bollag & Edelstein 1991). Another reason could be that limited proteolysis of MLC2 occurred.

The co-migration of purified myosins from toad EOM and rabbit psoas indicates the presence of predominantly fast MLC isoforms in EOM as found by Reichmann and Srihari (1983), Briggs *et al.* (1988) and Rushbrook *et al.* (1994). The three myosin light chains identified in fibers that gave fast responses to initial and maximum Ca^{2+}-activation (twitch dark and twitch light fibers) are consistent with MLC1f, MLC2f and MLC3f, and have previously been observed by others (Reichmann & Srihari 1983, Sartore *et al.* 1987, Rushbrook *et al.* 1994).

Two MLC bands were found from fibers that gave a slow response to initial and maximum Ca^{2+}-activation (tonic fibers). The regulatory light chain (MLC2) of these fibers showed a reduced mobility compared to the twitch fibers and is probably the slow isoform, MLC2s. This is consistent with the findings in mammalian EOM (Reichmann & Srihari 1983, Briggs *et al.* 1988, Rushbrook *et al.* 1994). The absence of MLC2s in the purified myosin is likely to be the result

of non-detection due to its scarcity. The quantity of MLC2s purified from only 28 mg of tissue was probably insufficient to resolve on the gels since only about 20% of fibers in toad global EOM are of the tonic type (refer to Chapter 3) and probably no more than 20% of fibers in toad orbital EOM would contribute this isoform (see Table 1.2, Chapter 1).

The alkali light chain, MLC1, of tonic fibers co-migrated with those of the twitch fibers. Thus, contrary to what others have found in mammalian EOM (Reichmann & Srihari 1983, Briggs *et al.* 1988, Rushbrook *et al.* 1994), no slow MLC1 isoform (MLC1s' or MLC1s) was observed on the gels of either purified EOM or tonic fibers from *Bufo marinus*. The highest molecular weight MLC band of the tonic fibers appeared to have the same mobility as MLC1 of the twitch fibers.

This apparent lack of a slow MLC1 isoform could be due to phylogenetic variation. For example, while MLC1 of many mammalian limb muscle slow-twitch fibers is split into two bands, MLC1's and MLC1s, this does not appear to be the case with slow-twitch fibers of Amphibia. These fibers usually contain a single band, MLC1s, although at times some MLC1f appears from fibers that are transitional between fast- and slow-twitch (Lannergren 1987).

One other possibility is that MLC1's, in the SDS-PAGE system used in this study, had the same mobility as MLC1f, and that MLC1s was present in such small quantities that it did not show up on the gels. With respect to this latter point, the results of Reichmann and Srihari (1983), Briggs *et al.* (1988) and Rushbrook *et al.*

(1994) show that MLC1s occurs in much lower quantities than MLC1's. In addition, the amount of protein loaded onto a gel can be a critical factor in its detection. In this study, small quantities of protein were applied (less than 0.1 μg per lane) to the gels. Indeed, Sartore *et al.* (1987) only found MLC1f and MLC2f using one dimensional SDS-PAGE when applying about 3 ug protein per lane. Upon subsequent two-dimensional gel electrophoresis MLC3f was visible. Furthermore, Rushbrook *et al.* (1994) had difficulty visualising MLC1s using 10 μg protein per lane. Reichmann and Srihari (1983) loaded 120 μg onto their two-dimensional gels and were able to observe three slow and three fast myosin light chains.

The absence of MLC3 in EOM tonic fibers appears to be a general characteristic of tonic fibers in skeletal muscle of amphibians and avians. For example, Focant and Reznik (1980), Pliszka and Strzelecka-Golaszewska (1981) and Martyn *et al.* (1993) found that myosin of slow-tonic fibers from frog cruralis muscle were characterized on gels by having no low molecular weight band (i.e. MLC3). Reiser *et al.* (1996) found that fibers from the slow red strip of chicken pectoralis major muscle lacked MLC3 whereas the fast white fibers of this muscle had MLC1f, MLC2f and MLC3.

The results of this chapter show that differences in the force-pCa relationship of tonic and twitch fibers in *Bufo marinus* EOM are correlated with differences in the MLC profile of these fibers. Furthermore, the results confirm the grouping of twitch and tonic fibers made in Chapter 4. The speed of contraction of a muscle fiber is correlated with the presence of specific isoforms of most of the

myofibrillar contractile proteins. Therefore, it was perhaps not surprising that the MLC profile of the tonic fibers, which gave a characteristic slow response to maximally activating [Ca^{2+}], differs from the two twitch fibers, which gave a fast response (Chapter 4, Section 4.3.2).

CHAPTER 6: CONCLUSION

Although the morphological complexity of EOM is well appreciated, an in depth knowledge of the physiology of the individual fibers has been lacking. This study aimed to examine the fiber types in toad EOM and elucidate some of the contractile properties of these fibers, especially the tonic fibers. To achieve this aim a variety of approaches were ultimately used, including ultrastructural, histochemical and protein isoform analyses. This multi-faceted approach was necessary in order to identify and fully characterize the fibers used in the contractile activation experiments.

Three groups of fibers were found in global EOM. The tonic fibers showed marked differences from the twitch light and twitch dark fibers at the ultrastructural, histochemical, contractile and MLC isoform levels. Tonic fibers had a significantly lower Hill co-efficient than twitch light fibers at low calcium concentrations suggesting that the cooperative interaction between thick and thin filament subunits differs in these fibers. Differences between the twitch light and twitch dark fibers were confined mainly to morphology (i.e. number of mitochondria and fiber diameter) and metabolism (activity of oxidative and glycolytic enzymes).

It is hoped that others endeavoring to undertake contractile experiments on these fibers can use the information gained here. For example, the finding that permeabilized tonic fibers developed maximum force slowly and appeared to hold a constant force can be used to more easily identify these fibers without the need

to determine MLC profiles. There are many avenues that future work could take using permeabilized single fiber preparations of EOM fibers. For example, the maximum shortening velocity (V_{max}) of tonic fibers could be compared to the twitch fibers. Barany (1967) found that the ATPase activity of myosin is correlated to the speed of muscle shortening. Thus, given the histochemical result (mATPase activity) of this study and the slow rate of maximum, initial force development, a much slower response in the tonic fibers would be expected. In addition, information regarding the cross-bridge interaction cycle could be obtained using tension transients, where a fiber is subjected to a rapid length change and the recovery of tension is monitored. Other studies could focus on manipulating sarcoplasmic constituents such as ATP, ADP, P_i and Mg^{2+} in permeabilized fibers. Differences in other protein isoforms could also be explored further. For example, although some unique MHCs have been isolated from EOM, to the author's knowledge, analyses of MHC isoforms in single fibers has yet to be carried out to confirm the MHC content of each fiber type. Other myofibrillar proteins could also be examined. TnT isoforms in EOM have been investigated by Briggs *et al.* (1988) who found that the MIFs expressed the slow troponin T isoform (TnT2s) while the SIFs contained mainly TnT3f. Further work could be carried out on the other troponin subunits. Results in this study show that TnC from tonic and twitch fibers differs and this could be investigated more thoroughly.

The results of this study can be used to supplement what is known in the area of motor unit recruitment. Dean (1996) has constructed a model to simulate motor unit recruitment in EOM in order to help understand how oculomotor control

signals might be organized. He found a U-shaped recruitment pattern when unit strength was plotted as a function of unit threshold. The earliest recruited units were relatively strong whereas those recruited subsequently became progressively weaker until a minimum value was reached. Units were then recruited in order of increasing strength. Thus the pattern differs somewhat to that usually observed in spinal muscles in which units are recruited in order of increasing strength (Binder & Mendell 1990).

Findings from a variety of different studies need to be considered when proposing a recruitment order of EOM motoneurons. Browne (1976) studied the contractile properties of slow fibers (presumed MIFs) in sheep EOM and found them to be very resistant to fatigue. Shall and Goldberg (1992), using intra- and extra-cellular techniques to study single motor units of the abducens nucleus and lateral rectus in the cat, found similar results. The non-twitch units (MIFs) were the most fatigue resistant, in addition to having the lowest maximum tetanic tension range of the five motor unit types identified. Matyuskin (1962, 1963) working on the decerebrate rabbit, found that MIFs were tonically active in that they were innervated by low threshold motoneurons (those that fire even when the eye is pointing in the 'off-direction' for that muscle). In considering these results, and those of his own, Dean (1996) has put forth a recruitment order beginning with relatively strong units composed of MIFs, particularly orbital MIFs, then the weak units of the orbital and global dark-SIFs (trough) and finally the stronger units consisting of global intermediate- and pale-SIFs.

Robinson (1978) suggested a recruitment order based more on the metabolic demands placed on the fiber and on the need for ripple-free contraction to produce

fine control. He proposed the following recruitment order: orbital-SIFs and global dark-SIFs, orbital-MIFs, global-MIFs, global intermediate-SIFs and global pale-SIFs. He based this argument on the fact that those fibers recruited the earliest would be the most fatigue resistant and therefore have an appearance and histochemical characteristics of oxidative metabolism. Also, the non-twitch contractile nature of the global-MIFs would ensure smooth contractions of the first recruited units that generally have low frequency firing rates.

The Ca^{2+}-activation studies on single permeabilized fibers showed that the tonic (global-MIFs) fibers had significantly greater maximum tension levels than twitch dark (dark-SIFs) fibers. This observation, combined with the reported fatigue resistance of these fibers (Browne 1976, Shall & Goldberg 1992) would tend to support the recruitment of global-MIFs first, followed by the dark-SIFs in the trough of the 'U'. However, the subject is complicated by many unknown parameters such as motor unit size and the presence of polyneuronal innervation (MIFs).

Since few muscles are composed of a single fiber type, studies utilizing single fibers are valuable in gaining a clearer understanding of whole muscle physiology. This is especially true for EOM because of its complex assortment of fiber types. This study has shown that differences in EOM fibers extend to the level of the proteins comprising the contractile apparatus and the interaction of these proteins during muscle activation. Future studies in EOM research can hopefully build on the work presented here and gain more insight on the physiology of the individual fibers, especially the tonic fibers, that make up these remarkable muscles.

REFERENCES

Allen, T. St. C., Ling, N., Irving, M. and Goldman, Y.E. (1996) Orientation changes in myosin regulatory light chains following photorelease of ATP in skinned muscle fibers. *Biophysical Journal* 70: 1847-1862.

Alvarado, J.A. and van Horn, C. (1975) Muscle cell types of the cat inferior oblique. In: *Basic Mechanisms of Ocular Motility and Their Clinical Implications*. Eds: G. Lennerstrand and P. Bach-y-Rita, Pergamon Press, Oxford. pp. 15-45.

Ashley, C.C. (1984) Calcium in muscle. In*: Calcium in Biological Systems*, Ed: T. Spiro, Wiley, New York.

Ashley, C.C. and Campbell, A.K. (1979) *The Detection and Measurement of Free Ca^{2+} in Cells*, Elsevier/North-Holland, New York.

Assmussen, G. and Gaunitz, U. (1981) Mechanical properties of the isolated inferior oblique muscle of the rabbit. *Pflugers Archives. European Journal of Physiology* 392: 183-190.

Bagshaw, C.R. (1993) *Muscle Contraction* (second edition), Chapman & Hall, Melbourne.

Ball, D. and Johnston, I.A. (1996) Molecular mechanisms underlying the plasticity of muscle contractile properties with temperature acclimation in the marine fish *Myosocephalus scorpius. The Journal of Experimental Biology* 199: 1363-1373.

Barany, M. (1967) ATPase activity of myosin correlated with speed of muscle shortening. *Journal of General Physiology* 50: 197-217.

Barany, K., Barany, M. and Giometti, C.S. (1995) Review: Polyacrylamide gel electrophoretic methods in the separation of structural muscle proteins. *Journal of Chromatography* A 698: 301-332.

Barnard, R.J., Edgerton, V.R., Furukawa, T. and Peter, J.B. (1971) Histochemical, biochemical and contractile properties of red, white, and intermediate fibers. *American Journal of Physiology* 220: 410-414.

Bates, W.H. (1920) *Perfect Sight Without Glasses*, Henry Holt & Co., New York.

Benjamin, H. (1974) *Better Sight Without Glasses,* Thorsons, Wellingborough.

Binder, M.D. and Mendell, L.M. (Eds) (1990) *The Segmental Motor System*, Oxford University Press, New York.

Bollag, D.M. and Edelstein, S.J. (1991) *Protein Methods*, John Wiley & Sons Inc. New York.

Bortolotto, S.K., Stephenson, D.G. and Stephenson, G.M.M. (1997) A comparison of myosin expression and contractile activation characteristics in single soleus muscle fibres of the rat. *Proceedings of the Australian Physiological and Pharmacological Society* 28(2): 83P.

Bottinelli, R., Schiaffino, S. and Reggiani, C. (1991) Force-velocity relations and myosin heavy chain compositions of skinned fibres from rat skeletal muscle. *Journal of Physiology (Lond)* 437: 655-672.

Brandt, P.W., Diamond, M.S. and Rutchik, J.S. (1987) Co-operative interactions between troponin-tropomyosin units extend the length of the thin filament in skeletal muscle. *Journal of Molecular Biology* 195: 885-896.

Bremel, R.D., Murray, J.M. and Weber, A. (1973) Manifestations of cooperative behaviour in regulated actin filament during actin-activated ATP hydrolysis in presence of calcium. *Cold Spring Harbor Symposium on Quantitative Biology* 37: 267-275.

Briggs, M.M., Jacoby, J., Davidowitz, J. and Schachat, F.H. (1988) Expression of a novel combination of fast and slow troponin T isoforms in rabbit extraocular muscles. *Journal of Muscle Research and Cell Motility* 9: 241-247.

Brooke M.H. and Kaiser K.K. (1970) Three "myosin adenosine triphosphatase" systems: the nature of their pH lability and sulfhydryl dependence. *Journal of Histochemistry and Cytochemistry* 18: 670-672.

Browne, J.S. (1976) The contractile properties of slow muscle fibres in sheep extraocular muscle. *Journal of Physiology (Lond)* 254: 535-550.

Brueckner, J.K. and Porter, J.D. (1998) Visual system maldevelopment disrupts extraocular muscle-specific myosin expression. *Journal of Applied Physiology* 85(2): 584-592.

Brueckner, J.K., Itkis, O. and Porter, J.D. (1996) Spatial and temporal patterns of myosin heavy chain expression in developing rat extraocular muscle. *Journal of Muscle Research and Cell Motility* 17: 297-312.

Campbell, S. (1997) *Contractile activation characteristics of mammalian extraocular muscle fibres.* Ph.D. thesis, University of Melbourne.

Cheng-Minoda, K., Davidowitz, J., Liebowitz, A. and Breinin, G.M. (1968) Fine structure of extraocular muscle in rabbit. *Journal of Cellular Biology* 39: 193-197.

Chiarandini, D.J. and Davidowitz, J. (1979) Structure and function of extraocular muscle fibers. In: *Current Topics In Eye Research, Vol. 1*, Eds: J.A. Zadunaisky and H. Davison, Academic Press Inc., New York. pp. 91-142.

Chiarandini, D.J. and Stefani, E. (1979) Electrophysiologcial identification of two types of fibres in rat extraocular muscles. *Journal of Physiology (Lond)* 290: 453-465.

Close, R.I. (1972) Dynamic properties of mammalian skeletal muscles. *Physiology Reviews* 52: 129-197.

Cooper, J.A. (1994) Capping Proteins., In: *Guidebook to the Cytoskeletal and Motor Proteins*. Eds: T. Kreis and R. Vale, Sambrook and Tooze, Oxford University Press, Oxford. pp. 34-35.

Cords, E. (1924) Zur Frage des M. retractor bulbi der Sauger. *Zeitschrift fuer Anatomie Und Entwicklungsgeschichte* 71: 240-260.

Cornish-Bowden, A. and Koshland Jr., D.E. (1975) Diagnostic uses of the Hill (Logit and Nernst) plots. *Journal of Molecular Biology* 95: 201-212.

Critchley, D.R. (1994) α– Actinins In: *Guidebook to the Cytoskeletal and Motor Proteins*, Eds: T. Kreis and R. Vale, Sambrook and Tooze, Oxford University Press, Oxford. pp. 22-23.

Crockford, T. and Johnston, I.A. (1995) Isolation of unstable myosins and the analysis of light chains by capillary electrophoresis. *Analytical Biochemistry* 231: 20-26.

Davidowitz, J., Chiarandini, D.J., Philips, G. and Breinin, G.M. (1982) Morphological variation along multiply innervated fibers of rat extraocular muscles. In: *Functional Basis of Ocular Motility Disorders*, Eds: G. Lennerstrand, D.S. Zee and E.L. Keller, Pergamon Press, Oxford. pp. 17-26.

Dean, P. (1996) Motor unit recruitment in a distributed model of extraocular muscle. *Journal of Neurophysiology* 76(2): 727-742.

Dietert, S.E. (1965) The demonstration of different types of muscle fibers in human extraocular muscle by electron microscopy and cholinesterase staining. *Investigative Ophthalmology* 4(1): 51-63.

Donaldson, S.K.B. and Kerrick, W.G.L. (1975) Characterization of the effects of Mg^{2+}on Ca^{2+}- and Sr^{2+}-activated tension generation of skinned skeletal muscle fibers. *Journal of General Physiology* 66: 427-444.

Dubowitz, V. and Brooke, M.H. (1973) Muscle biopsy: a modern approach – Volume 2. In: *Major Problems in Neurology*, Ed: J.N. Walton, Saunders, London.

Eastwood, A.B., Wood, D.S., Bock, K.L. and Sorenson, M.M. (1979) Chemically skinned mammalian skeletal muscle. I. The structure of skinned rabbit psoas. *Tissue & Cell* 11(3): 553-566.

Engel, E.K. (1962) The essentiality of histo- and cytochemical studies of skeletal muscle in the investigation of neuromuscular disease. *Neurology* 12: 778-784.

Fink, W.J. and Costill, D.L. (1995) Skeletal muscle structure and function. In: *Physiological Assessment of Human Fitness*, Eds: P.J. Maud and C. Foster, Human Kinetics, Champaign, IL.

Focant, B. and Reznik, M. (1980) Comparison of the sarcoplasmic and myofibrillar proteins of twitch and tonic fibres of frog muscle (*Rana esculenta*) *European Journal of Cell Biology* 21:195-199.

Frueh, B.R., Hayes, A., Lynch, G.S. and Williams, D.A. (1994) Contractile properties and temperature sensitivity of the extraocular muscles, the levator and superior rectus, of the rabbit. *Journal of Physiology (Lond)* 475.2: 327-336.

Galler, S., Schmitt, T.L. and Pette, D. (1994) Stretch activation, unloaded shortening velocity, and myosin heavy chain isoforms of rat skeletal muscle fibres. *Journal of Physiology (Lond)* 478.3: 513-521.

Gauthier, G.F. (1969) On the relationship of ultrastructural and cytochemical features to color in mammalian skeletal muscle. *Zeitschrift fuer Zellforschung und Mikroskopische Anatomie* 95: 462-482.

Ginsborg, B.L. (1960) Some properties of avian skeletal muscle fibers with multiple neuromuscular junctions. *Journal of Physiology (Lond)* 154: 581-598.

Gleeson, T., Putnam, R.W. and Bennett, A.F. (1980) Histochemical, enzymatic, and contractile properties of skeletal muscle fibers in the lizard *Dipsosaurus dorsalis*. *The Journal of Experimental Zoology* 214: 293-302.

Goldberg, S.J. and Shall, M.S. (1997) Lateral rectus whole muscle and motor unit contractile measures with the extraocular muscles intact. *Journal of Neuroscience Methods* 78: 47-50.

Grabarek, Z., Grabarek, J., Leavis, P.C. and Gergely, J. (1983) Cooperative binding to the Ca^{2+}-specific sites of troponin C in regulated actin and actomyosin. *Journal of Biological Chemistry* 258: 14098-14102.

Greaser, M.L. and Gergely, J. (1971) Reconstitution of troponin activity from three protein components. *The Journal of Biological Chemistry* 246(13): 4226-4233.

Greaser, M.L., Moss, R.L. and Reiser, P.J. (1988) Variations in contractile properties of rabbit single muscle fibres in relation to troponin T isoforms and myosin light chains. *Journal of Physiology* 406: 85-98.

Guth, K. and Potter, J.D. (1987) Effect of rigor and cycling cross-bridges on the structure of troponin C and the Ca^{2+} affinity of the Ca^{2+}-specific regulatory sites in skinned rabbit psoas fibers. *Journal of Biological Chemistry* 262: 13627-13635.

Harker D.W. (1972) The structure and innervation of sheep superior rectus and levator palpebrae extraocular muscles I. Extrafusal muscle fibers. *Investigative Ophthalmology* 11(12): 956-969.

Harrington, W.F. (1981) Muscle contraction, *Carolina Biology Reader 114*, Scientific Publications Division, Burlington, N.C.

Hess, A. (1961a) The structure of slow and fast extrafusal muscle fibers in the extraocular muscles and their nerve endings in guinea pigs. *Journal of Cellular and Comparative Physiology* 58: 63-80.

Hess, A. (1961b) Structural differences of fast and slow extrafusal muscle fibers and their nerve endings in chickens. *Journal of Physiology (Lond)* 157: 211.

Hess, A. and Pilar, G. (1963) Slow fibers in the extraocular muscles of the cat. *Journal of Physiology (Lond)* 169: 780-798.

Hofmann, P.A., Metzger, J.M., Greaser, M.L. and Moss, R.L. (1990) Effects of partial extraction of light chain 2 on the Ca^{2+} sensitivities of isometric tension, stiffness, and velocity of shortening in skinned skeletal muscle fibers. *Journal of General Physiology* 95: 477-498.

Hoh, J.F.Y., Hughes, S., Hugh, G. and Pozgaj, I. (1989) Three hierarchies in skeletal muscle fibre classification: allotype, isotype, and phenotype In: *Cellular and Molecular Biology of Muscle Development.* Eds: L.H. Kedes and F.E. Stockdale, Alan R. Liss, New York. pp. 15-26.

Homsher, E. and Millar, N.C. (1989) *Solution – Muscle Solution Calculation Program.* [Computer program], System requirements: IBM PC.

Irving, M. and Piazzesi, G. (1997) Motions of myosin heads that drive muscle contraction. *News in Physiological Sciences* 12: 249-254.

Isomura G. (1981) Comparative anatomy of the extrinsic ocular muscles in vertebrates. *Anatomischer Anzeiger* 150: 498-515.

Jacoby, J., Chiarandini, D.J. and Stefani, E. (1989a) Electrical properties and innervation of fibers in the orbital layer of rat extraocular muscles. *Journal of Neurophysiology* 61(1): 116-125.

Jacoby, J., Ko, K., Weiss, C. and Rushbrook, J.I. (1989b) Systematic variation in myosin expression along extraocular muscle fibres of the adult rat. *Journal of Muscle Research and Cell Motility* 11: 25-40.

Julian, F.J. (1971) The effect of calcium on the force-velocity relation of briefly glycerinated frog muscle fibers. *Journal of Physiology* 218: 117-145.

Kaminiski, H.J., Mass, E., Spiegel, P. and Ruff, R.L. (1990) Why are eye muscles frequently involved in myasthenia gravis? *Neurology* 40: 1663-1669.

Kato, T. (1938) Uber histologische Untersuchungen der Augenmuskeln von Menschen und Saugetieren. *Okajimas Folia Anatomica Japonica* 16: 131-145.

Kilarski W. and Bigaj J. (1969) Organization and fine structure of extraocular muscles in *Carassius* and *Rana*. *Zeitschrift fuer Zellforschung und Mikroskopische Anatomie* 94: 194-204.

Kuffler, S.W. and Vaughan Williams, E.M. (1953) Small-nerve junctional potentials. The distribution of small motor nerves to frog skeletal muscle, and the membrane characteristics of the fibres they innervate. *Journal of Physiology (Lond)* 121: 289-317.

Laemmli, U.K. (1970) Cleavage of structural proteins during the assembly of the head of bacteriophage T4. *Nature* 227: 680-685.

Lannergren, J. (1987) Contractile properties and myosin isoenzymes of various kinds of *Xenopus* twitch muscle fibres. *Journal of Muscle Research and Cell Motility* 8: 260-273.

Lannergren, J. and Smith, R.S. (1966) Types of muscle fibres in toad skeletal muscle. *Acta Physiologica Scandinavica* 68: 263-274.

Ling, N., Shrimpton, C., Sleep, J., Kendrick-Jones, J. and Irving, M. (1996) Fluorescent probes of the orientation of myosin regulatory light chains in relaxed, rigor and contracting muscle. *Biophysical Journal* 70: 1836-1846.

Lowey, S. (1994) The structure of vertebrate muscle myosin. In: *Myology: basic and clinical.* (Second edition), Eds: A.G. Engel and C. Franzini-Armstrong, McGraw-Hill, New York, pp. 489-492.

Lowey, S. and Risby, D. (1971) Light chains from fast and slow muscle myosins. *Nature* 234: 81-85.

Lowey, S., Waller, G.S. and Trybus, K.M. (1993) Skeletal muscle myosin light chains are essential for physiological speeds of shortening. *Nature* 365: 454-456.

Luff, A.R. (1981) Dynamic properties of the inferior rectus, extensor digitorum longus, diaphragm and soleus muscle of the mouse. *Journal of Physiology (Lond)* 313: 161-171.

Luff, A.R. and Proske, U. (1979) Properties of motor units of the frog iliofibularis muscle. *American Journal of Physiology* 236: C35-C40.

Lynch, G.S., Stephenson, D.G. and Williams, D.A. (1991) Endurance exercise effects on the contractile properties of single skinned skeletal muscle fibres of young rats. *Pflugers Archives* 418: 161-167.

Lynch, G.S., Frueh, B.R. and Williams, D.A. (1994) Contractile properties of single skinned fibres from the extraocular muscles, the levator and superior rectus, of the rabbit. *Journal of Physiology (Lond)* 475.2: 337-346.

Martyn, D.A, Coby, R., Huntsman, L.L. and Gordon, A.M. (1993) Force-calcium relations in skinned twitch and slow-tonic frog muscle fibres have similar sarcomere length dependencies. *Journal of Muscle Research and Cell Motility* 14: 65-75.

Matyuskin, D.P. (1962) Phasic and tonic neuromotor units in the oculomotor apparatus of the rabbit *Sechenov Physiologyical Journal of the USSR* 47(7): 65-69.

Matyuskin, D.P. (1963) Motor innervation of tonic muscle fibres of the oculomotor system. *Federation Proceedings* 22: T728-T731.

Mayr, R. (1971) Structure and distribution of fibre types in the external eye muscles of the rat. *Tissue & Cell* 3(3): 433-462.

Mayr, R., Gottschall, J., Gruger, H. and Neuhuber, W. (1975) Internal structure of cat extraocular muscle. *Anatomy and Embryology [Germany]* 148: 25-34.

Mendiola P., De Costa J., Lozano M.T. and Agulleiro B. (1991) Histochemical determination of muscle fiber types in locomotor muscles of anuran amphibians. *Comparative Biochemistry and Physiology* 99A (3): 365-368.

Metzger, J.M. and Moss, R.L. (1991) Kinetics of a Ca^{2+}-sensitive cross-bridge state transition in skeletal muscle fibers. *Journal of General Physiology* 98: 233-248.

Millar, N.C. and Homsher, E. (1990) The effect of phosphate and calcium on force generation in glycerinated rabbit skeletal muscle fibers. *Journal of Biological Chemistry* 265(33): 20234-20240.

Miller, J.E. (1967) Cellular organization of rhesus extraocular muscle. *Investigative Ophthalmology* 6(1): 18-39.

Moisescu, D.G. and Thieleczek, R. (1979) Sarcomere length effects on the Sr^{2+} and Ca^{2+}-activation curves in skinned frog muscle fibres. *Biochimica et Biophysica Acta* 546: 64-76.

Morgan D.L. and Proske U. (1984) Vertebrate slow muscle: its structure, pattern of innervation, and mechanical properties. *Physiological Reviews* 64(1): 103-169.

Moss, R.L. (1992) Ca^{2+} regulation of mechanical properties of striated muscle. *Circulation Research* 70(5): 865-883.

Moss, R.L., Sollins, M.R. and Julian, F.J. (1976) Calcium activation produces a characteristic response to stretch in both skeletal and cardiac muscle. *Nature (Lond)* 260: 619-621.

Moss, R.L., Diffee, G.M. and Greaser, M.L. (1995) Contractile properties of skeletal muscle fibers in relation to myofibrillar protein isoforms. *Reviews in Physiology, Biochemistry and Pharmacology* 129: 1-63.

Moss, R.L., Guilian, G.G. and Greaser, M.L. (1982) Physiological effects accompanying the removal of myosin LC_2 from skinned skeletal muscle fibers. *Journal of Biological Chemistry* 257(15): 8588-8591.

Moss, R.L., Guilian, G.G. and Greaser, M.L. (1985) The effects of partial extraction of TnC upon the tension-pCa relationship in rabbit skinned skeletal muscle fibers. *Journal of General Physioloy* 86: 585-600.

Moss, R.L., Nwoye, L.O. and Greaser, M.L. (1991) Substitution of cardiac troponin-C into rabbit muscle does not alter the length dependence of Ca^{2+} sensitivity of tension. *Journal of Physiology (Lond)* 440: 273-289.

Moss, R.L., Reiser, P.J., Greaser, M.L. and Eddinger, T.J. (1990) Varied expression of myosin alkali light chains is associated with altered speed of contraction in rabbit fast twitch skeletal muscles. In: *The Dynamic State of Muscle Fibers.* Ed: D. Pette. De Gruyter, Berlin.

Nakayama, Y., Yamacuchi, M., Watanabe, K. and Sekine, T. (1983) Loss of Ca^{2+}-dependent regulation in glycerinated skeletal muscle contraction. *Japanese Journal of Physiology* 33: 559-566.

Nasledov, G.A. and Lebedinskaya, I.I. (1971) Studies of the contractile mechanism of tonic muscle fibers in the frog. *Sechenov Physiologyical Journal of the USSR* 57: 1307-1312.

Nesterenko, M.V., Tilley, M. and Upton, S.J. (1994) A simple modification of Blum's silver stain method allows for 30 minute detection of proteins in polyacrylamide gels. *Journal of Biochemical and Biophysical Methods* 28: 239-242.

Nowogrodzka-Zagorska M. (1974) The organization of extraocular muscles in Anura. *Acta Anatomica* 87: 22-44.

Pachter, B.R. (1982) Fiber composition of the superior rectus extraocular muscle of the rhesus macaque. *Journal of Morphology* 174: 237-250.

Pachter, B.R. (1984) Rat extraocular muscle 3. Histochemical variability along the length of multiply-innervated fibers of the orbital surface layer. *Histochemistry* 80: 535-538.

Pachter, B.R, Davidowitz, J. and Breinin, G.M. (1976) Light and electron microscopic serial analysis of mouse extraocular muscle: morphology, innervation and topographical organization of component fiber populations. *Tissue & Cell* 8(3): 547-560.

Padykula, H.A. and Gauthier, G.F. (1967) Morphological and cytochemical characteristics of fiber types in normal mammalian skeletal muscle In: *Exploratory Concepts in Muscluar Dystrophy and Related Disorders*, Ed: A.T. Milhorat, Excerpta Medica, New York. pp. 117-131.

Padykula H.A. and Herman E. (1955) The specificity of the histochemical method for adenosine triphosphatase. *Journal of Histochemistry and Cytochemistry* 3: 170-183.

Page, S.G. (1965) A comparison of the fine structures of frog slow and twitch muscle fibres. *Journal of Cell Biology* 26: 477-497.

Pate, E., Lin, M., Franks-skiba, K. and Cooke, R. (1992) Contraction of glycerinated rabbit slow-twitch muscle fibers as a function of MgATP concentration. *American Journal of Physiology* 262: C1039-C1046.

Peachy, L.D., Takeichi, M. and Nag, A.C. (1974) Muscle fiber types and innervation in adult cat extraocular muscles. In: *Exploratory Concepts in Muscular Dystrophy II*, Ed: A.T. Milhorat, Excerpta Medica, Amsterdam. pp. 246-257.

Perriard, J.C. (1994) Myomesin and M-protein. In: *Guidebook to the Cytoskeletal and Motor Proteins*, Eds: T. Kreis and R. Vale, Sambrook and Tooze, Oxford University Press, Oxford. pp. 58-59.

Peter, J.B., Barnard, R.J., Edgerton, V.R., Gillespie, C.A. and Stempel, K.E. (1972) Metabolic profiles of three fiber types of skeletal muscle in guinea pigs and rabbits. *Biochemistry* 11: 2627-2633.

Pette, D. (1989) Early effects of chronic low frequency stimulation on calcium-sequestering proteins and contractile properties of rabbit fast-twitch muscle. In: *Neuromuscular stimulation*, Eds: F.C. Rose and R Jones, Demos, New York. pp. 185-191.

Pette, D. and Staron, R.S. (1990) Cellular and molecular diversities of mammalian skeletal muscle fibers. In: *Review of Physiology, Biochemistry and Pharmacology* 116, Springer-Verlag, New York. pp. 1-76.

Pierobon Bormioli S., Torresan P., Sartore S., Moschini G.B. and Schiaffino S. (1979) Immunohistochemical identification of slow-tonic fibers in human extrinsic eye muscles. *Investigative Ophthalmology and Visual Science: 303-306.*

Pliszka, B. and Strzelecka-Golaszewska, H. (1981) Comparison of myosin isoenzymes from slow-tonic and fast-twitch fibers of frog muscle. *European Journal of Cell Biology* 25: 144-149.

Porter, J.D. and Baker, M.D. (1996) Muscles of a different 'color': The unusual properties of the extraocular muscles may predispose or protect them in neurogenic and myogenic disease. *Neurology* 46: 30-37.

Porter, J.D., Baker, R.S., Ragusa, R.J. and Brueckner, J.K. (1995) Extraocular muscles: basic and clinical aspects of structure and function. *Survey of Ophthalmology* 39(6): 451-484.

Porter, J.D., Burns, L.A. and May, P.J. (1989) Morphological substrate for eyelid movements: innervation and structure of primate levator palpebrae

superioris and orbicularis oculi muscles. *The Journal of Comparative Neurology* 287: 64-81.

Putnam, W. and Bennett, A. (1983) Histochemical, enzymatic, and contractile properties of skeletal muscles of three anuran amphibians. *American Journal of Physiology* 244: R558-R567.

Quackenbush, T.R. (1997) *Relearning to See,* North Atlantic Books, Berkley, California.

Rabilloud, T. (1992) A comparison between low background silver diammine and silver nitrate protein stains. *Electrophoresis* 13: 429-439.

Rabilloud, T., Carpentier, G. and Tarroux, P. (1988) Improvement and simplification of low-background silver staining of proteins by using dithionate. *Electrophoresis* 9: 288-290.

Rayment, I., Rypniewski, W.R., Schmidt-Base, K., Smith, R., Tomchick, D.R., Benning, M.M., Winkelmann, D.A., Wesenberg, G. and Holden, H.M. (1993) Three-dimensional structure of myosin subfragment-1: a molecular motor. *Science* 261: 50-58.

Reichmann, H. and Srihari, T. (1983) Enzyme activities, histochemistry and myosin light chain pattern in extraocular muscles of rabbit. *Histochemistry* 78: 111-120.

Reiser, P.J., Moss, R.L., Giulian, G.G. and Greaser, M.L. (1985) Shortening velocity in single fibers from adult rabbit soleus muscles is correlated with mysoin heavy chain composition. *Journal of Biological Chemistry* 260: 9077-9080.

Reiser, P.J., Greaser, M.L. and Moss, R.L. (1996) Contractile properties and protein isoforms of single fibres from the chicken pectoralis red strip muscle. *Journal of Physiology* 493: 553-562.

Reynolds, E.S. (1963) The use of lead citrate at high pH as an electron-opaque stain in electron microscopy. *Journal of Cell Biology* 17: 208.

Robinson, D.A. (1978) The functional behavior of the peripheral ocular motor apparatus: a review. In: *Disorders of Ocular Motility*, Ed: G. Kommerell, J.F. Bergman, Munich. pp. 43-61.

Rushbrook, J.I., Weiss, C., Ko, K., Feuerman, M.H., Carleton, S., Ing, A. and Jacoby, J. (1994) Identification of alpha-cardiac myosin heavy chain mRNA and protein in extraocular muscle of the adult rabbit. *Journal of Muscle Research and Cell Motility* 15: 505-515.

Sartore, S., Mascarello, F., Rowlerson, A., Gorza, L., Ausoni, S., Vianello, M. and Schiaffino, S. (1987) Fibre types in extraocular muscles: a new myosin isoform in the fast fibres. *Journal of Muscle Research and Cell Motility* 8: 161-172.

Schachat, F.H., Bronson, D.D. and McDonald, O.B. (1980) Two kinds of slow skeletal muscle fibers which differ in their myosin light chain complements. *FEBS Letters* 122(1): 80-82.

Schagger, H. and von Jagow, G. (1987) Tricine-sodium dodecyl sulfate-polyacrylamide gel electrophoreseis for the separation of proteins in the range from 1 to 100kDa. *Analytical Biochemistry* 166: 368-379.

Seidel, J.C. (1967) Studies on myosin from red and white skeletal muscles of the rabbit. II. Inactivation of myosin from red muscles under mild alkaline conditions. *Journal of Biological Chemistry* 242: 5623-5629.

Shall, M.S. and Goldberg, S.J. (1992) Extraocular motor units: type classification and motoneuron stimulation frequency-muscle unit force relationships. *Brain Research* 587: 291-300.

Shall, M.S. and Goldberg, S.J. (1995) Lateral rectus EMG and contractile responses elicited by cat abducens motoneurons. *Muscle & Nerve* 18: 948-955.

Siebeck, R. and Kruger, P. (1955) Die histologische Struktur der auberen Augenmuskeln als Ausdruck ihrer Funktion, *von Graefes Arch. Ophth.* 156: 637.

Simoneau, J.A., Kaufmann, M., Hartner, K.T. and Pette, D. (1989) Relations between chronic stimulation-induced changes in contractile properties and the Ca^{2+}-sequestering system of rat and rabbit fast-twitch muscles. *Pflugers Archives* 414: 629-633.

Sleep, J. (1990) Temperature control and exchange of the bathing solution for skinned muscle fibres. *Journal of Physiology* 423: 7P.

Spencer, R.F. and Porter, J.D. (1988) Structural organization of the extraocular muscles. In: *Neuroanatomy of the Oculomotor System*, Ed: Buttner-Ennever, Elsevier Science Publishers BV (Biomedical Division). pp. 33-79.

Spurr, A.R. (1969) A low-viscosity epoxy resin embedding medium for electron microscopy. *Journal of Ultrastructure Research* 26: 31.

Sreter, F.A., Seidel, J.C. and Gergely, J. (1966) Studies on myosin from red and white skeletal muscles of the rabbit. I. Adenosine triphosphatase activity. *Journal of Biological Chemistry* 241: 5772-5776.

Stephenson, D.G. and Forrest, Q.G. (1980) Different isometric force – $[Ca^{2+}]$ relationships in slow and fast twitch skinned muscle fibres of the rat. *Biochimica et Biophysica Acta* 589: 358-362.

Stephenson, D.G. and Williams, D.A. (1983) Slow amphibian muscle fibres become less sensitive to Ca^{2+} with increasing sarcomere length. *Pflugers Archives* 397: 248-250.

Stienen, G.J.M., Kiers, J.L., Bottinelli, R. and Reggiani, C. (1996) Myofibrillar ATPase activity in skinned human skeletal muscle fibres: fibre type and temperature dependence. *Journal of Physiology (Lond)* 493.2: 299-307.

Swartz, D.R. and Moss, R.L. (1992) Influence of a strong-binding myosin analogue on calcium-sensitive mechanical properties of skinned skeletal muscle fibers. *Journal of Biological Chemistry* 267(28): 20497-20506.

Sweeney, H.L., Corteselli, S.A. and Kushmerick, M.J. (1987) Measurement of permeabilized skeletal muscle fibers during continuous activation. *American Journal of Physiology* 252: C575-C580.

Sweeney, H.L., Kushmerick, M.J., Mabuchi, K., Sreter, F.A. and Gergely, J. (1988) Myosin alkali light chain and heavy chain variations correlate with altered shortening velocity of isolated skeletal muscle fibers. *The Journal of Biological Chemistry* 263(18): 9034-9039.

Turner, D.C., Wallimann, T. and Eppenberger, H.M. (1973) A protein that binds specifically to the M-line of skeletal muscle is identified as the muscle form of creatine kinase. *Proceedings of the National Academy of Sciences (USA)* 70: 702-705.

Uehara Y., Campbell G.R. and Burnstock G. (1976) *Muscle and its Innervation: An atlas of Fine Structure.* Edward Arnold, London.

Vita, G.F., Mastaglia, F.L. and Johnson, M.A. (1980) A histochemical study of fibre types in rat extraocular muscles. *Neuropathology and Applied Neurobiology* 6: 449-463.

Webster, D. and Webster, M. (1974) *Comparative Vertebrate Morphology.* Academic Press, New York, pp 126.

Wieczork, D.F., Periasamy, M., Butler-Browne, G.S., Whalen, R.G. and Nadal-Ginard, B. (1985) Co-expression of multiple myosin heavy chain genes, in addition to a tissue-specific one, in extraocular musculature. *Journal of Cell Biology* 101: 618-629.

Wilkinson, J.M. (1980) Troponin C from rabbit slow skeletal and cardiac muscle is the product of a single gene. *European Journal of Biochemistry* 103: 179-188.

Wilson, G.J. and Stephenson, D.G. (1990) Calcium and strontium activation characteristics of skeletal muscle fibres from the small marsupial *Sminthopsis macroura*. *Journal of Muscle Research and Cell Motility* 10: 12-24.

APPENDIX A

IPLab Spectrum (Signal Analytics Corporation) is a scientific imaging software for the Macintosh. Outlined below is the script created using *IPLab Spectrum* (version 3.1) to measure minimum elliptical diameter of tonic and twitch muscle fibers in sections stained for mATPase activity.

SCRIPT	NOTES
Set XY Units	assign predefined units to image
Segmentation	colour tonic fibers green (intensity thresholding)
Alert	
Modify Segments	fill holes in tonics with green
Pause	
Modify Segments	erode (separate segments that are touching)
Modify Segments	dilate (thicken boundary line)
Set Measurements	minor axis
Measurement Options	measure green segments
Measure Segments	
Segmentation	colour twitch fibers yellow
Alert	
Modify Segments	fill holes in twitch with yellow
Pause	
Modify Segments	erode
Modify Segments	dilate
Set Measurements	minor axis
Measurement Options	measure yellow segments
Measure Segments	
END	

APPENDIX B

Table B.1: Stock solutions used in the preparation of the inferior rectus muscle for skinning and the pCa solutions listed in Table B.2.

Solution*	Concentration (M)	pH
KCl	2.0	7.1
$MgAc_2$	1.0	7.3
K_2EGTA	0.05	7.3
Imidazole	1.0	6.9
KCaEGTA	0.1	7.1
NaATP	0.1	7.2
NaPCr	0.1	7.0

* 2mM sodium azide was added to the stock solutions.

Table B.2: Composition of solutions used in single fiber experiments.

Concentrations in mM

	IS	pH	Temp.	Imidazole	KCl	$MgAc_2$	K-EGTA	KCaEGTA	Na-ATP	Na-PCr
Relax (pCa 9.0)	150mM	7.1	10	25	55.93	6.6	10	0	5.545	5
Pre-activate	150mM	7.1	10	25	85.65	6.11	0.2	0	5.565	5
Activate:										
pCa 4.6	150mM	7.1	10	25	26.21	6.3	0	10.028	5.611	15
pCa 4.8	150mM	7.1	10	25	26.31	6.3	0	9.961	5.589	15
pCa 5.0	150mM	7.1	10	25	26.37	6.3	0.114	9.886	5.576	15
pCa 5.2	150mM	7.1	10	25	26.4	6.3	0.212	9.788	5.568	15
pCa 5.4	150mM	7.1	10	25	26.423	6.31	0.352	9.648	5.562	15
pCa 5.6	150mM	7.1	10	25	26.43	6.32	0.559	9.441	5.559	15
pCa 5.8	150mM	7.1	10	25	26.431	6.34	0.866	9.134	5.557	15
pCa6.0	150mM	7.1	10	25	26.42	6.36	1.311	8.689	5.555	15
pCa 6.2	150mM	7.1	10	25	26.41	6.39	1.932	8.068	5.554	15
PCa 6.3	150mM	7.1	10	25	26.40	6.41	2.317	7.683	5.554	15
pCa 6.4	150mM	7.1	10	25	26.38	6.43	2.753	7.247	5.554	15
PCa 6.5	150mM	7.1	10	25	26.36	6.46	3.236	6.764	5.554	15
pCa 6.6	150mM	7.1	10	25	26.35	6.48	3.759	6.241	5.553	15
PCa 6.7	150mM	7.1	10	25	26.33	6.51	4.313	5.687	5.554	15
pCa 6.8	150mM	7.1	10	25	26.31	6.54	4.884	5.116	5.553	15
PCa 6.9	150mM	7.1	10	25	26.29	6.57	5.458	4.542	5.554	15
pCa 7.0	150mM	7.1	10	25	26.27	6.6	6.021	3.979	5.553	15
pCa 7.1	150mM	7.1	10	25	26.25	6.623	6.558	3.442	5.553	15
pCa 7.2	150mM	7.1	10	25	26.24	6.65	7.057	2.943	5.553	15
pCa 7.4	150mM	7.1	10	25	26.21	6.69	7.917	2.083	5.553	15
pCa 7.6	150mM	7.1	10	25	26.18	6.73	8.58	1.42	5.553	15
pCa 7.8	150mM	7.1	10	25	26.17	6.75	9.052	0.948	5.553	15
pCa 8.0	150mM	7.1	10	25	26.16	6.77	9.38	0.62	5.553	15

Total volume of each solution = 10 ml

Volume to add in µl

	IS	pH	Temp.	Imidazole	KCl	$MgAc_2$	K-EGTA	KCaEGTA	Na-ATP	Na-PCr	Total Volume
Relax (pCa 9)	150mM	7.1	10C	250	280	66	2000	0	555	500	3652
Pre-activate	150mM	7.1	10C	250	428	61	40	0	556	500	2195
Activate:											
pCa4.6	150mM	7.1	10C	250	131	63	0	1003	561	1500	3508
pCa 4.8	150mM	7.1	10C	250	132	63	0	996	559	1500	3500
pCa 5.0	150mM	7.1	10C	250	132	63	22	989	558	1500	3514
pCa 5.2	150mM	7.1	10C	250	132	63	42	979	557	1500	3503
pCa 5.4	150mM	7.1	10C	250	132	63	70	965	556	1500	3536
pCa 5.6	150mM	7.1	10C	250	132	63	112	944	556	1500	3557
pCa 5.8	150mM	7.1	10C	250	132	63	174	913	556	1500	3588
pCa 6.0	150mM	7.1	10C	250	132	64	262	869	556	1500	3633
pCa 6.2	150mM	7.1	10C	250	132	64	386	807	555	1500	3694
PCa 6.3	150mM	7.1	10C	250	132	64	464	768	555	1500	3733
pCa 6.4	150mM	7.1	10C	250	132	64	550	725	555	1500	3776
PCa 6.5	150mM	7.1	10C	250	132	65	648	676	555	1500	3826
pCa 6.6	150mM	7.1	10C	250	132	65	752	624	555	1500	3878
PCa 6.7	150mM	7.1	10C	250	132	65	862	569	555	1500	3933
pCa 6.8	150mM	7.1	10C	250	132	65	976	512	555	1500	3990
PCa 6.9	150mM	7.1	10C	250	132	66	1092	454	555	1500	4049
pCa 7.0	150mM	7.1	10C	250	132	66	1204	398	555	1500	4105
PCa 7.1	150mM	7.1	10C	250	132	66	1312	344	555	1500	4159
pCa 7.2	150mM	7.1	10C	250	131	67	1412	294	555	1500	4209
pCa 7.4	150mM	7.1	10C	250	131	67	1584	208	555	1500	4295
pCa 7.6	150mM	7.1	10C	250	131	67	1716	142	555	1500	4361
pCa 7.8	150mM	7.1	10C	250	131	68	1810	95	555	1500	4409
pCa 8.0	150mM	7.1	10C	250	131	68	1876	62	555	1500	4442

APPENDIX C

The Liquid Chromatography Controller (LCC-500) of the FPLC apparatus was programmed as follows:

Time (min)		
0.0	CONC %B	0.0
0.0	ML/MIN	0.50
0.0	CM/MIN	0.50
0.0	VALVE POS	1.2
2.0	CONC %B	0.0
2.0	ML/MIN	0.50
2.0	CM/MIN	0.50
17.0	CONC %B	100
17.0	ML/MIN	0.50
17.0	CM/MIN	0.50
17.0	CONC %B	100
22.0	CONC %B	100
32.0	CONC %B	0.0
32.0	ML/MIN	0.00
32.0	CM/MIN	0.00